Materials Advances

ROYAL SOCIETY OF CHEMISTRY

REVIEW

View Article Online
View Journal | View Issue

Check for updates

Cite this: *Mater. Adv.*, 2025, 6, 8839

Progress in biochar derived adsorbents: preparation, modification strategies, and applications in remediation of antibiotics from wastewater

Van Doan Nguyen,[a] The Anh Luu,[a] Guo-Ping Chang-Chien[bc] and Van Giang Le *[a]

The increasing presence of antibiotic compounds in aquatic environments has become a serious concern due to their potential to promote antibiotic resistance and adversely affect ecosystems. Conventional treatment methods are often insufficient for the complete removal of these pollutants. In this context, biochar, a porous carbonaceous material derived from biomass pyrolysis, has attracted significant attention as a promising material for the remediation of antibiotics in wastewater. This review systematically highlights recent advances in the study of biochar, including its sources and synthesis techniques such as pyrolysis, gasification, hydrothermal carbonization, and mild pyrolysis. It also explores various activation and modification strategies including physical and chemical activation, electrochemical techniques, and environmentally friendly modification approaches. Furthermore, the effects of operational parameters such as pH, temperature, duration time, biochar dosage, and pollutant concentration on uptake performance are thoroughly examined. The underlying adsorption mechanisms such as electrostatic interactions, ion exchange, $\pi-\pi$ interactions, surface complexation, and capillary diffusion are analyzed in detail. In addition, quantum chemical approaches, particularly density functional theory (DFT), are discussed for their role in elucidating the fundamental interactions between antibiotics and biochar materials. Finally, this review addresses current challenges, potential risks, and emerging trends in the development of hybrid biochar materials, particularly those incorporating MOFs and MXenes for effective antibiotic pollution control.

Received 8th August 2025,
Accepted 29th September 2025

DOI: 10.1039/d5ma00872g

rsc.li/materials-advances

Open Access Article. Published on 06 10 2025. Downloaded on 2026-05-13 12:47:34.
This article is licensed under a Creative Commons Attribution-NonCommercial 3.0 Unported Licence.

1. Introduction

Biochar, also known as ''black gold'', is a solid substance abundant in carbon fabricated *via* the pyrolysis of biomass derived from sludge and agricultural and livestock wastes in low oxygen environments.[1] The name ''biochar'' refers to the combination of the prefix ''bio'' representing biomass and the suffix ''char'' originating from charcoal. Since the introduction of its name, the concept has been mentioned in many research works.[2] Alternatively, biomass is a general term for the collection of organic materials originating from living entities or a mixture of related substances.[3] In fact, plant-based biomass materials are formed by the process of photosynthesis and are commonly present in both terrestrial and aquatic plants. Among them, lignocellulosic biomass consists of three fundamental components: hemicellulose, lignin, and cellulose. Owing to its low cost, renewable ability, and carbon neutrality, this type of biomass is considered a promising option in solving energy problems. Its origin can come from natural materials or through intermediate effects.[4]

Thermal processes including incineration, pyrolysis or hydrothermal carbonization (HTC) can be utilized to fabricate biochar from biomass wastes such as manure, rice husk, sawdust or leaves.[5] Among these techniques, pyrolysis stands as the most commonly utilized method to fabricate biochar under oxygen-free and high-temperature conditions.[6–8] This method also generates by-products such as heat energy, syngas, liquid fuel, and wood vinegar (pyroligneous acid).[9,10] HTC technology represents a new method for synthesizing carbonaceous materials such as biochar, which is receiving much attention due to its environmental friendliness, reasonable cost, and relatively simple process.[11,12] During this process, the crude material is heated at high pressure and temperature

[a] *Central Institute for Natural Resources and Environmental Studies, Vietnam National University, Hanoi, Viet Nam. E-mail: levangiangcres@.vnu.edu.vn*
[b] *Center for Environmental Toxin and Emerging-Contaminant Research, Cheng Shiu University, Kaohsiung 833301, Taiwan*
[c] *Super Micro Mass Research and Technology Center, Cheng Shiu University, Taiwan*

© 2025 The Author(s). Published by the Royal Society of Chemistry

Open Access Article. Published on 06 10 2025. Downloaded on 2026-05-13 12:47:34.
This article is licensed under a Creative Commons Attribution-NonCommercial 3.0 Unported Licence.

to create hydrochar, a carbon-rich material with high calorific value, low moisture, and good combustion properties.[13,14] Hydrochar can be used for many purposes such as providing energy for gas storage,[15] soil improvement,[16] catalysis,[17] fuel cells[13] or adsorbing pollutants from water, including antibiotics[18] and heavy metals.[19]

Biochar is a widely utilized and effective material globally for removing pollutants from water, thanks to its porous structure similar to activated carbon (AC). As opposed to AC, biochar is a new, low-cost but highly efficient material. While activated carbon requires a complex activation process and high temperature, biochar is easier to produce and more energy-efficient.[2] Therefore, biochar may be employed as an initial precursor for the fabrication of AC.[20] However, due to being produced under low-energy conditions and without an activation stage, biochar usually exhibits a smaller surface area and reduced mechanical strength compared to AC. While the fabrication of AC requires chemical activation of the input material along with gas activation during pyrolysis, biochar hardly needs these steps.[21]

Biochar is considered an effective soil additive due to its ability to retain nutrients and enhance soil stability, thereby contributing to increased crop yields. In addition to its role in agriculture, biochar also brings great benefits in environmental remediation, especially in controlling soil pollution. Currently, soil pollution caused by heavy metals[22,23] and persistent organic pollutants (such as chlorinated furans (PCDFs), chlorinated biphenyls (PCBs), brominated flame retardants (BFRs), and chlorinated dioxins (PCDDs))[24–26] is a serious global problem, directly threatening human health and ecosystems. Contaminants persist in soil and water for extended periods because they are not biodegradable, causing soil quality deterioration and hindering agricultural activities. The treatment of these pollutants is often very expensive and lengthy. Nevertheless, biochar can stabilize pollutants through enhanced removal mechanisms (including electrostatic attraction, coordination, and surface complexation) and chemical precipitation (arising from the increase in soil pH as well as the addition of carbonate ash and phosphate ash).[27–29] Physicochemical attributes of biochar therefore effectively enable the remediation of metal species and antibiotic contaminants in soil, helping to reduce their mobility and potential for harm.[30–33] Thus, the utilization of biochar not only contributes to soil quality restoration but is also a sustainable solution to minimize the environmental impact caused by soil pollution.

To address the pressing need for water conservation under global environmental strain, biochar is being used as a water purifier in various agricultural and industrial applications.[29,34–36] The quality of aquatic ecosystems is continuously declining due to a growing array of pollutants stemming from human activities.[37,38] These include common contaminants like pesticides, heavy metals, pathogens, antibiotics, dyes, pharmaceuticals, and personal care products.[37,39–42] Notably, antibiotics are frequently found in aquatic environments at comparatively high levels,[43,44] making their pollution a widespread global environmental concern.[45]

Water and wastewater systems can be contaminated with antibiotics from various natural and human-related sources including medical waste, urine and feces from humans, and animals treated with antibiotics, and runoff from livestock farms.[46,47] The primary sources include hospital waste, pharmaceutical manufacturing facilities, livestock farms using antibiotics as growth promoters, and inadequately treated municipal wastewater.[48] Measured concentrations of these antibiotics in the environment often exceed safe limits, posing a risk of drug resistance and affecting the ecosystem.[48] For example, antibiotic concentrations in some polluted water sources can reach extremely high levels. A study in India detected ciprofloxacin (CIP) concentrations in streams near pharmaceutical factories as high as 296 mg L^{-1}, over 1500 times the recommended safety limit.[49] In Pakistan, CIP levels in wastewater reached 331.15 mg L^{-1} while hospital wastewater in Egypt contained amoxicillin, ampicillin, and dicloxacillin at concentrations of 99.04, 70.06, and 119.24 mg L^{-1}, respectively.[50] In Vietnam, sulfamethoxazole (SMX) levels in the To Lich, Lu, and Kim Nguu rivers were measured at 0.585, 1.09, and 0.535 mg L^{-1}, respectively.[51] The persistent presence of these antibiotics in aquatic environments promotes the emergence of antibiotic-resistant bacterial strains, posing serious risks to ecosystems and human health.[52]

As depicted in Fig. 1, multiple approaches can be employed to eliminate antibiotics from water, like solvent extraction, chemical precipitation, membrane filtration, ion exchange, sedimentation, coagulation, and both electrochemical and genetic approaches.[53–56] Among these, adsorption using natural and eco-friendly materials stands out as a promising solution owing to its user-friendliness, low expense, high performance, and environmental sustainability.[57–59] Traditional approaches like coagulation and sedimentation are inexpensive and straightforward to implement, yet they typically offer low removal efficiency and pose significant challenges in managing the generated sludge. In contrast, advanced oxidation processes can break down pollutants that resist conventional treatment methods. However, they demand substantial chemical inputs, leading to higher operational costs

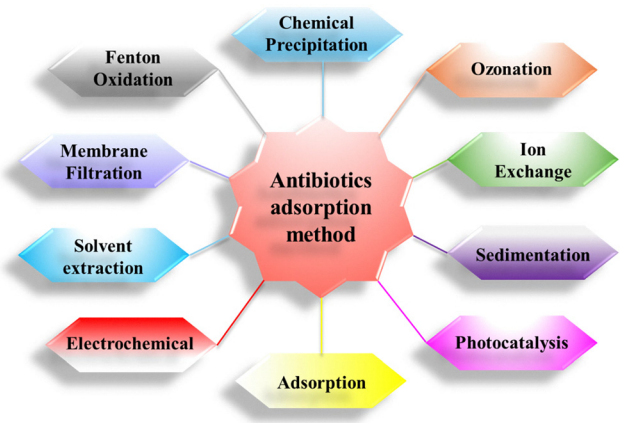

Fig. 1 Multiple techniques for the treatment of antibiotics.

© 2025 The Author(s). Published by the Royal Society of Chemistry

Open Access Article. Published on 06 10 2025. Downloaded on 2026-05-13 12:47:34.
This article is licensed under a Creative Commons Attribution-NonCommercial 3.0 Unported Licence.

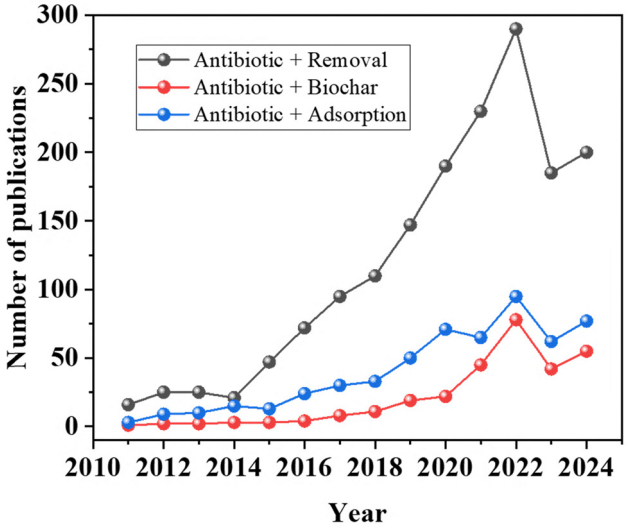

Fig. 2 Number of articles published from 2011 to 2024 with the keywords "Antibiotic + Removal", "Antibiotic + Adsorption" and "Antibiotic + Biochar" on the Web of Science.

and the risk of secondary pollution. Techniques such as electrodialysis, ion exchange, and membrane separation tend to achieve high selectivity and efficiency, but their reliance on complex equipment and high energy consumption makes them costly solutions. Unlike many complicated approaches, adsorption is a straightforward method that relies on physical or chemical interactions to capture pollutants on the surface of an adsorbent, offering both high removal efficiency and environmental compatibility.[60–62] From a cost perspective, adsorption remains a much more economical option, with expenses under $200 per million liters of treated water and considerably lower than methods like electrodialysis or ion exchange, which can cost up to $450.[63] Consequently, adsorption continues to be regarded as a promising approach for eliminating antibiotics from aqueous environments. The global research trend related to biochar, adsorption and treatment of antibiotics in aquatic environments is also increasing markedly over the years, as shown in Fig. 2.

In the context of increasing environmental pressures and the accumulation of organic pollutants including antibiotics, biochar has emerged as an environmentally friendly and cost-effective material. However, most current research remains primarily focused on heavy metal treatment,[64–66] while the application of biochar for elimination of antibiotics, a group of highly toxic pollutants with significant potential to induce antimicrobial resistance, has not yet been fully explored. Furthermore, biochar is not only enhanced by traditional chemical modification methods but is also being studied for performance improvement through advanced techniques such as electrochemical modification,[67,68] plasma treatment,[68] or integration with novel nanomaterials like MXenes and MOFs. These approaches significantly increase the material's removal capacity and selectivity toward challenging organic pollutants, including antibiotics. In addition to experimental studies, recent years have seen a growing trend in utilizing computational models, such as density functional theory (DFT), to elucidate adsorption mechanisms on biochar at the atomic level. This approach generates novel insights into the nature of interactions between biochar and pollutants, including antibiotics, which are challenging to observe through conventional experimental methods.

Unlike many reviews that focus solely on material aspects such as biomass origin, synthesis methods, and conventional biochar modification, this paper offers a more integrated perspective by connecting material development with practical insights into pollutant adsorption. Beyond detailing feedstocks and fabrication methods like pyrolysis and HTC, it highlights advanced surface engineering strategies including nanomaterial incorporation and novel activation techniques that enhance adsorption performance. A key feature of this work is its focused analysis of the elimination of antibiotics from wastewater, supported not only by experimental evidence but also by computational modeling. Specifically, density functional theory (DFT) is employed to elucidate adsorption mechanisms at the atomic level, offering insights into interactions that conventional methods often overlook. This comprehensive approach bridges material innovation with real-world applications, contributing to the development of next-generation, sustainable water purification technologies.

2. Biochar: precursors, preparation approaches, and structural features

Biochar is a carbon-dense substance that typically makes up 60 to 90% of the material's composition.[69] It could also comprise elements like oxygen, inorganic ash, and hydrogen, which depends on the biomass source.[70] Producing biochar is seen as more environmentally sustainable than burning coal, as biomass is naturally carbon neutral. Its surface area is generally large, often surpassing 100 $m^2\ g^{-1}$, which is effected by both the synthesis conditions and crude materials.[71] This property makes biochar useful in various non-fuel applications, including chemical adsorption[72] for water purification and long-term carbon storage.[70] It has also been explored and applied as a soil amendment to enhance fertility.[73]

2.1. Precursors for biochar preparation

Biomass refers to an organic substance sourced from living or once-living organisms, with the potential for regeneration and widespread application in environmental and energy-related fields. It may be utilized to generate electricity and heat and produce organic fertilizers, biofuels, pharmaceuticals, chemicals, and biological materials such as biochar. Virtually all types of organic matter including bark, seed coats, agricultural residues, and manure can be converted into biochar using appropriate processing equipment.[74–76] The original source of biomass may come from plant, animal, or human waste, including domestic and industrial wastewater.[77,78] Contingent on the specific biomass chosen, the resulting biochar will

Open Access Article. Published on 06 10 2025. Downloaded on 2026-05-13 12:47:34.
This article is licensed under a Creative Commons Attribution-NonCommercial 3.0 Unported Licence.

exhibit different physical and chemical characteristics, enabling the flexible application of carbon materials for various specific purposes.

Biomass feedstocks are commonly categorized into two main types: non-woody and woody biomass.[79] The study conducted by Shrivastava *et al.* focused on rubberwood sawdust (RWS) as a representative of woody biomass and oil palm fronds (OPF) as a representative of non-woody biomass.[80] The initial assessment of these materials covering moisture content, fixed carbon, volatile matter, and ash shows that woody biomass typically contains 75.97% volatile matter, 15.22% fixed carbon, 7.14% moisture, and 1.69% ash (by weight), while the corresponding values for non-woody biomass are 72.31, 15.68, 6.44, and 5.34%, respectively. Similarly, ultimate analysis reveals that woody biomass comprises approximately 47.65% carbon, 6.12% hydrogen, 0.33% nitrogen, 45.90% oxygen, and 0.03% sulfur compared to 44.96, 5.79, 0.41, 48.72, and 0.07% in non-woody biomass. Woody biomass mainly originates from forest residues and wood processing waste, which is characterized by minimal moisture and ash content while demonstrating elevated energy content, significant mass per unit volume, and limited pore space.[79] Conversely, non-woody biomass sources such as farm residues, bioenergy crops, animal manure, and household refuse or industrial solid waste typically have higher moisture and ash content, lower heating values, lower bulk densities, and greater porosity.[79] These significant differences underscore the importance of selecting appropriate raw materials when producing biochar for specific environmental applications.

Biomass includes living or previously living organic matter, which is a versatile renewable resource with applications in environmental and energy sectors such as heat or electricity generation. It also serves as a raw material for producing organic fertilizers, biofuels, chemicals, pharmaceuticals, and biomaterials like biochar. The characteristics of biochar-based materials vary depending on the precursor, enabling tailored use of carbonaceous materials for specific purposes. This primary resource can originate from plant, animal, or human waste, including sewage sludge, food wastes, forestry waste (*e.g.*, wood chips), farm waste (*e.g.*, animal manure), and industrial byproducts.[77,78] Nearly any organic material such as seed coats, bark, crop residues, or manure can be converted into biochar using suitable processing methods.[74,81] Fig. 3 lists the most common feedstocks for biochar fabrication, which range from plant matter to industrial byproducts.

In recent years, various raw materials including animal tissue, algae, manure, and food waste have been explored for the generation of biochar.[82–84] These investigations have produced notable findings regarding both the physicochemical characteristics and the potential uses of the resulting biochar. Although biochar is primarily derived from plant-based waste, commonly referred to as cellulosic biomass such as firewood or rice husks, not all organic-rich materials are suitable for its synthesis. Municipal solid waste (MSW) and wastewater, despite their high biomass content, often contain

Fig. 3 Widely utilized raw materials for biochar synthesis.

contaminants that may decrease the performance of biochar in soil and water remediation applications.[2]

2.2. Approaches to synthesizing biochar

2.2.1. Traditional pyrolysis. The pyrolysis method and its resulting products are illustrated in Fig. 4, which highlights the diversity of biomass precursors utilized in biochar fabrication. Pyrolysis generally refers to the heat-driven breakdown of biomass in an oxygen-limited environment, typically at elevated temperatures spanning from 300 to 900 °C.[85] These conditions result in the fragmentation of hemicellulose, lignin, and cellulose as well as depolymerization and cross-linking reactions, leading to the formation of biomass-derived products. Furthermore, pyrolysis produces liquid, solid, and gaseous products, named as bio-oil, biochar, and biogas, respectively. The physicochemical properties and yields of these products may vary depending on the type of pyrolysis applied. Based on the

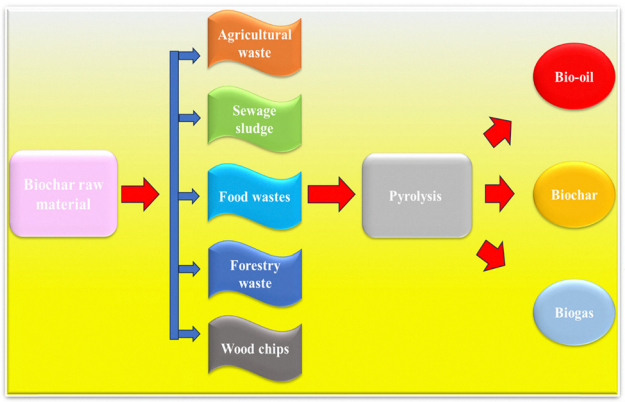

Fig. 4 Schematic diagram of biochar fabrication from multiple biomass sources through pyrolysis.

© 2025 The Author(s). Published by the Royal Society of Chemistry

Open Access Article. Published on 06 10 2025. Downloaded on 2026-05-13 12:47:34.
This article is licensed under a Creative Commons Attribution-NonCommercial 3.0 Unported Licence.

heating rate and residence duration, pyrolysis could be classified into two fundamental modes like fast and slow pyrolysis. Fast pyrolysis is primarily employed to produce high concentrations of liquid products (such as biofuels) with superior physicochemical properties including lower volatile organic compound (VOC) concentration and a higher content of long-chain hydrocarbons.[86] It usually requires brief residence times of below 10 seconds and rapid heating rates of above 200 °C min^{-1}.[15] Nonetheless, fast pyrolysis typically produces biochar with reduced yields and smaller surface areas, which may be due to tar-like substances becoming lodged within the pores.[87] In addition, fast pyrolysis tends to produce biochar with hydroxyl and carboxylic acid groups as the dominant functional groups, whereas slow pyrolysis generates biochar rich in aromatic C–H groups.[88] Slow pyrolysis typically involves extended durations for material retention during the process (more than 1 h) and lower heating rates (3–10 °C min^{-1}). While it produces a larger amount of biochar, it also yields gases and liquids with lower concentrations but containing significant amounts of VOCs, which are considered pollutants.[89]

High treatment temperatures during pyrolysis not only promote transformation reactions but also generate the activation energy necessary to facilitate the generation of carbonaceous frameworks with a higher order degree.[90] Increasing the treatment temperature significantly enhances pore development on the surface of biochar, a key factor in improving specific surface area. For example, a work conducted by Lua *et al.*[91] revealed that enhancing the temperature of the pyrolysis from 250 to 500 °C raised the surface area from 170 to 480 m^2 g^{-1}. This increase was attributed to the intense development of volatiles in pistachio shells, which contributed to the generation of a porous framework with a high pore volume of 0.469 cm^3 g^{-1} at 500 °C, more than double the value of 0.192 cm^3 g^{-1} observed at 250 °C.

In general, higher processing temperatures have a more pronounced effect on the physicochemical properties of the resulting products. Therefore, to obtain high-efficiency and high-quality biochar, the pyrolysis process should be conducted within the temperature range of 400–800 °C.[92,93] The changes in the size and arrangement of carbon structures that occur during biomass pyrolysis are key contributors to the enhancement of the physicochemical parameters of the ultimate products.[94]

2.2.2. Gasification. Gasification is an advanced thermal treatment method, typically occurring at elevated temperatures around 800 °C in the presence of reactive gases like air and oxygen,[6] where carbon-rich materials are transformed into gaseous, liquid, and solid samples. This process involves four fundamental stages such as pyrolysis, partial oxidation, reduction, and drying. Among the resulting products are carbon monoxide, carbon dioxide, nitrogen, hydrogen, tar, ash, and charcoal. Charcoal, which represents a solid output, typically makes up only approximately 10% of the initial precursor weight.[95,96]

While the original purpose of gasification was to enhance energy recovery by generating large volumes of synthesis gas, increasing interest has recently been directed toward the charcoal produced during the process. This carbon-rich material, typically identified as biochar, is now recognized as a valuable secondary product. However, balancing the dual objectives of maximizing energy recovery and increasing biochar yield presents a technical challenge. This requires careful adjustment of operational parameters including temperature, pressure, and the nature of the input gas mixture.[95] Additionally, the chemical–physical profile of input feedstocks are fundamentally important to the overall efficiency, as well as to both the amount and characteristics of the resulting biochar produced by gasification techniques.

2.2.3. Hydrothermal carbonization (HTC). Hydrothermal carbonization (HTC) refers to a thermochemical technique utilized to efficiently treat high-moisture biomass in an aqueous environment under high temperature and pressure conditions.[12] The process, also known as wet roasting, occurs within a sealed environment at temperature ranges between 120 and 260 °C and under pressures between 2 and 10 MPa without the need for pre-drying of the precursor.[97] HTC typically takes place over a period of 30 min to 8 h under either autogenous or externally applied pressure and could be employed for diverse feedstock sources such as crop byproducts, industrial wastes, sewage sludge, and aquatic biomass.[98–100]

HTC primarily produces hydrochar as its end product, a carbon-rich form of biochar formed in the solid phase. In addition to hydrochar, the process also produces an aqueous phase rich in organic matter and nutrients as well as a small mass of gas, mainly consisting of carbon dioxide.[101] Compared to biochar obtained through other thermochemical methods, hydrochar typically has lower fixed carbon and ash contents along with a smaller pore volume and S_{BET} surface area.[102] However, hydrochar possesses large energy density, making it a promising fuel for applications in energy sectors.[103]

A key benefit of HTC lies in its capacity to directly process wet biomass without the need for energy-intensive drying stages, which are commonly required in pyrolysis or other high-temperature technologies.[16,104] This process not only enhances carbon recovery efficiency but also improves product quality compared to conventional technologies. In addition, HTC helps limit the formation of toxic compounds and micropollutants that often arise under the harsh conditions of pyrolysis.[105] However, the performance of the HTC process depends largely on the properties of the precursors, size of particles, and residence time in the reactor. Particle sizes larger than 2 cm or reaction times shorter than 30 minutes can reduce the efficiency of heat and mass transfer.[16] Therefore, to achieve uniform heat distribution and optimize conversion efficiency, careful control of particle size and feedstock homogeneity is necessary. In the case of sludge treatment, dewatering steps including filtration or centrifugation are also required to facilitate the conversion reaction. Depending on the intended end use, hydrochar can serve as a coal substitute, a feedstock for gasification processes, a soil amendment to enrich nutrients or a feedstock to fabricate adsorbents and activated carbon.[106]

Open Access Article. Published on 06 10 2025. Downloaded on 2026-05-13 12:47:34.
This article is licensed under a Creative Commons Attribution-NonCommercial 3.0 Unported Licence.

The selection of appropriate feedstocks and operating conditions will determine the efficiency, quality, and potential applications of the products derived from the HTC process.

2.2.4. Torrefaction. Torrefaction occurs at relatively low temperatures (200–300 °C) under oxygen-free conditions, primarily yielding biochar, a material with inferior physicochemical properties compared to pyrolysis-derived products.[84,107,108] While both torrefaction and pyrolysis are thermochemical conversion techniques that transform biomass into value-added outputs (*e.g.*, biooil, biogas, and biochar),[70] they exhibit distinct differences in processing parameters and end products.

2.3. Approaches to biochar activation and functionalization

2.3.1. Physical activation. Biochar experiences both increased pore development on its surface and chemical property changes when subjected to physical activation (*e.g.*, hydrophobicity, polarity, and surface functional groups). At temperatures ranging from 700 to 1100 °C,[109] gas/steam expands and develops the porous structure of carbonaceous materials, thereby creating materials with high porosity and large surface areas. Conversely, research findings have demonstrated the ability of biochar activated by gas/steam to remove heavy metals and antibiotics. Research conducted by Rong *et al.*[110] demonstrated that biochar produced from sludge through pyrolysis and physical activation with steam has excellent SMX uptake capacity. Specifically, the specific surface area reached 1583.07 $m^2\ g^{-1}$ after activation while the SMX adsorption capacity increased to 204.07 mg g^{-1} in 90 min. The maximum Cu^{2+} adsorption efficiency (93%) was only achieved when biochar was activated at an appropriate steam flow rate, according to Lima and Marshall.[111] In addition, Mondal *et al.*[112] utilized biochar derived from mung bean hulls, which is activated by superheated steam to adsorb ranitidine hydrochloride in a fixed-bed column. The data revealed that the adsorption efficiency reached 99.16% at an inlet content of 100 mg L^{-1}, demonstrating the effectiveness of steam-activated biochar for the elimination of pharmaceuticals from aqueous environments. High temperature (>500 °C) combined with oxidants (ozone, steam, air, or CO_2)[113] when treating biochar will create two effects: (1) gasification of carbon atoms and (2) expansion of the previously inaccessible pore system.[114] This activation method not only increases the biochar surface area but also significantly adds surface oxygen functional groups, which are considered effective adsorption centers for pollutant treatment.[114]

Another uncomplicated but productive physical approach involves the use of ball milling (Fig. 5). The procedure harnesses the momentum of oscillating grinding elements to fracture chemical linkages, transform particle morphology, and synthesize nanomaterials.[115] As a result, biochar obtained after ball milling exhibits many superior properties, including increased pore volume, large specific surface area (SSA), low surface charge (negative), the presence of oxygen functional groups, and superior adsorption capacity.[36] Biochar from bagasse after ball milling has demonstrated superior removal

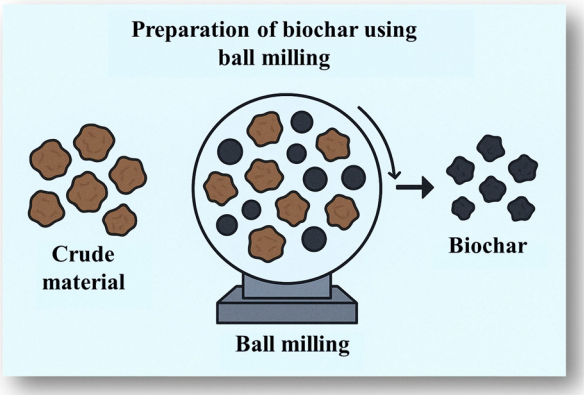

Fig. 5 Ball milling synthesis of biochar.

of Ni^{2+} and methylene blue (MB) from water compared to conventional biochar.[116] The reason is that the ball milling technique increases the surface area (both internal and external) while exposing the graphitic structure and oxygen functional groups on the carbon's surface.[117] Additionally, Peterson and colleagues demonstrated that optimizing the grinding conditions using a ball mill could increase the surface area of corn stover biochar up to 194 $m^2\ g^{-1}$, which is 60 times larger than that of the original material.[118] A notable drawback involves the high water dispersibility of ball-milled biochar, potentially causing environmental contamination.

2.3.2. Chemical activation

2.3.2.1. Utilization of acids, bases, and inorganic salts for activation. Chemical treatment techniques including acid treatment (HNO_3, H_2SO_4, HCl, *etc.*), alkali treatment (NaOH, KOH, *etc.*), oxidation ($KMnO_4$ and H_2O_2), metal salts ($FeCl_3$ and $MgCl_2$), inorganic–organic polymers (clay and chitosan), amines, cationic surfactants (*e.g.*, cetyltrimethylammonium bromide), and ethylenediaminetetraacetic acid (EDTA) are utilized to modify the chemical properties and surface structure of biochar.[119,120] Depending on their chemical nature, these agents impart distinct characteristics such as pore development, increased surface area, enhanced cation exchange capacity, and the introduction of functional groups. For example, oxidation with HNO_3 increases the mass of acidic functional groups and improves hydrophilicity but may also degrade the structure and reduce surface area.[121]

In contrast, alkaline treatment typically yields a larger surface area than acid treatment.[122] KOH modifies the porous structure, as demonstrated in a work by Han *et al.*[123] on peanut shell-derived biochar, which achieved a BET surface area of 640.57 $m^2\ g^{-1}$. Similarly, NaOH enhances thermal stability and antibiotic adsorption capacity,[124] while 30% H_2SO_4 boosts sulfadiazine adsorption efficiency.[125] In oxidation treatments, $KMnO_4$ combined with KOH increases the specific surface area (SSA), improving tetracycline (TC) adsorption,[126] whereas H_2O_2 introduces oxygen-containing functional groups, enhancing heavy metal removal.[127] Additionally, the choice of decontamination agents depends on factors including low decomposition

© 2025 The Author(s). Published by the Royal Society of Chemistry

Open Access Article. Published on 06 10 2025. Downloaded on 2026-05-13 12:47:34.
This article is licensed under a Creative Commons Attribution-NonCommercial 3.0 Unported Licence.

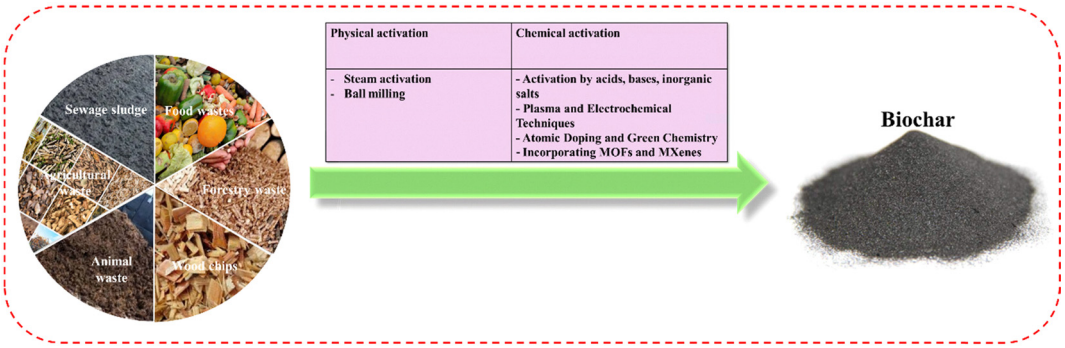

Fig. 6 Strategy for converting biomass into biochar.

temperature, short carbonization time, or the ability to form a mesoporous structure.[128] Common techniques are illustrated in Fig. 6.

2.3.2.2. Plasma and electrochemical techniques. In the current scientific climate, the issue of antibiotic contamination in aquatic environments has become a global concern. Traditional treatment methods often prove ineffective due to the complex nature of antibiotic molecules. In this context, advanced plasma and electrochemical biochar modification techniques have emerged as promising solutions, offering significant advantages over conventional chemical methods. Plasma treatment is considered a breakthrough technology in the surface modification of materials, particularly in the formation of specific functional groups. Cold plasma at atmospheric pressure can be applied within a short period (5–30 min), yet induces remarkable structural transformations. The main mechanisms include: (1) surface activation through collisions with high-energy particles, (2) oxidation to form functional groups including –COOH, –OH, and C═O, and (3) microstructural modification of the surface, increasing pore volume and surface area.

A work by Zhang *et al.*[129] employed a cold plasma system using NH_3 gas to treat corn straw biochar (CS-300), demonstrating that CIP removal efficiency increased from 31.8 to 85.7%. This improvement was attributed to the dense formation of amine and amide groups on the biochar's interface. These nitrogen-containing functional groups not only enhanced the π electron density within the conjugated system of the biochar, thereby promoting π–π stacking interactions with the aromatic ring of CIP but also contributed to strong ionic and hydrogen bonding interactions at high-energy sites (above 10 kJ mol^{-1}). Similarly, Lou *et al.* (2021) combined seaweed-derived biochar (from *Enteromorpha prolifera*) with a dielectric barrier discharge (DBD) plasma system.[130] They discovered an enhancement in biochar surface area from 415.84 to 486.32 m^2 g^{-1} after treatment. The concentration of oxygen-based functional moieties such as hydroxyl (–OH) and carboxyl groups was significantly enhanced, which results in a tetracycline hydrochloride (TCH) removal efficiency of 89.36% in just 5 min. This approach not only yielded high elimination efficiency but also improved energy efficiency, reaching 6.21 g kWh^{-1}, significantly higher than that of the plasma-only system.

Recent developments in electrochemical techniques have also advanced the modification of adsorbent materials, particularly biochar. A notable example is the work by Benis *et al.*,[131] in which an electrochemical process involving an iron anode was used to modify biochar derived from rapeseed straw. This method produced goethite (α-FeOOH) coatings on the material surface without the need for external chemical agents. The modified biochar achieved a nearly 37-fold increase in arsenic (As(v)) adsorption capacity (from 25 to 922 μg g^{-1}) under optimized conditions such as pH 3, drying temperature 60 °C, and 20 min of electric current application. The elimination mechanism involved multilayer heterogeneous adsorption and chemical bonding, with iron-containing functional groups playing a key role in creating selective active sites. A review by Tian *et al.*[132] further confirmed that electroactive functional groups including –C═O, –COOH, –OH, and persistent free radicals (PFRs) function as electron donors or acceptors in redox processes. Electrochemical modification of biochar can optimize the density of these groups, thereby enhancing its capacity to eliminate a wide range of organic and inorganic contaminants. In particular, activation with KOH, treatment with HNO_3, and heteroatom doping with elements like nitrogen and sulfur significantly improve electron transport capacity and create selective uptake sites on the biochar surface. A comparison of the two techniques reveals that each has distinct advantages. Plasma treatment is characterized by a short processing time (usually under one hour), the absence of toxic chemicals, and feasibility for pilot-scale applications. Meanwhile, electrochemical techniques offer precise control over the degree of modification *via* adjustable electrochemical parameters and the simultaneous generation of diverse functional groups. However, both methods face challenges, including high initial investment costs, the need for specialized equipment, and the necessity for further research into material reusability.

2.3.2.3. Atomic doping and green chemistry. A summary of the investigations is presented in Table 1. Biochar modified *via* atomic doping has proven to be an effective strategy for enhancing elimination performance by introducing additional active functional groups, modifying surface charge, and

Open Access Article. Published on 06 10 2025. Downloaded on 2026-05-13 12:47:34.
This article is licensed under a Creative Commons Attribution-NonCommercial 3.0 Unported Licence.

Table 1 Atomic doping strategies at the biochar interface

Feedstock	Dopant(s)	Synthesis conditions	Contaminant (efficiency)	Adsorption mechanism	Ref.
Coconut husk	B (H_3BO_3)	Microwave-assisted pyrolysis, 600–1000 °C, 1 h, N_2 atmosphere	TC (413.22 mg g^{-1})	π–π EDA interaction, H-bonding, –BCO_2 active sites	133
Rice straw	P (H_3PO_4)	Pyrolysis at 600 °C, 2 h, solid–liquid ratio 1 : 2, N_2 atmosphere	SMX (148.62 mg g^{-1})	H-bonding (C_3–P–O), electrostatic, π–π EDA	134
Maize straw	Fe/N ($FeCl_3$ + urea)	Pyrolysis at 700 °C, 2 h, 1-step mixing process	MOR (107.5 mg g^{-1}), CIP (85.1 mg g^{-1})	π–π interaction, electrostatic, surface complexation	137
Coconut shell	Fe/B ($FeSO_4$ + $NaBH_4$)	Microwave pre-treatment 5 min + pyrolysis at 1000 °C, 1 h, N_2 atmosphere	TC (107.32 mg g^{-1})	π–π interaction, electrostatic, H-bonding	139
Wood chips	Fe/Ti	Co-pyrolysis at 600 °C, 2 h, N_2 atmosphere	CIP (88.4%), NOR (88.0%)	π–π interactions, polar interactions	140
Rice husk	Cu	Hydrothermal carbonization at 180 °C, 8 h	Congo red dye (437.40 mg g^{-1})	π–π interaction, electrostatic attraction, hydrogen bonding	141
Rape straw	Fe/N	Pyrolysis at 600 °C, 2 h, N_2 atmosphere	CIP (46.45 mg g^{-1}), Cu^{2+} (30.77 mg g^{-1})	Electrostatic interaction, π–π interaction, H-bonding	142
Loofah waste	Mn/N	One-step pyrolysis with $NaHCO_3$ activation	BPA (351 mg g^{-1})	Pore filling, hydrophobicity, π–π EDA interaction	143
Maize straw	$FeCl_3$	Pyrolysis at 500–900 °C, 2 h, N_2 atmosphere	Extended-chain PFAS (per- and polyfluoroalkyl substances) (>95%)	Complexation and electrostatic interactions	144
Corn stalk	N	Pyrolysis at 600 °C, 1 h, N_2 atmosphere, 5° min^{-1}	NOR (46.27 mg g^{-1})	Pore-filling, H-bond, π–π electron donor–acceptor	145
Tea residue biochar	S/N	Carbonization at 220 °C, 6 h	TC (140.76 mg g^{-1})	Electrostatic interactions	146

increasing surface area. A representative example is boron (B)-doped biochar synthesized through microwave pyrolysis using H_3BO_3, which achieved a surface area of 933.39 m^2 g^{-1} and a TC uptake capacity of up to 413.22 mg g^{-1}.[133] This capacity surpasses that of many commercial and previously studied biochars such as straw-derived biochar modified with H_3PO_4 (267 mg g^{-1}) or peat-derived biochar (94 mg g^{-1}). Mechanistic investigations revealed that the –BCO_2 functional group, formed from B doping and served as the primary adsorption site through π–π electron interactions. Similarly, phosphorus (P)-doped biochar prepared by pyrolyzing H_3PO_4-impregnated straw at 600 °C, formed C_3–P–O functional groups, which exerted the greatest effect in the adsorption of SMX, achieving a capacity of 148.62 mg g^{-1}.[134] This performance exceeds that of commercial materials such as activated carbon (27–94 mg g^{-1}) or sludge-derived carbon. Furthermore, P-doped biochar demonstrated operational stability in continuous flow columns and showed good agreement with practical models such as the Thomas and BDST models, indicating strong potential for industrial-scale applications.[134] In the case of nitrogen (N)-doped biochar, N species including pyridinic, pyrrolic, and graphitic nitrogen were found to increase local electron density, facilitating the generation of active functional groups and enhancing the adsorption of persistent pollutants including bisphenol A (BPA), norfloxacin (NOR), and CIP.[135,136] Lian *et al.*[137] revealed that N-doped biochar derived from straw exhibited excellent adsorption capacity for phenolic pesticides. Particularly, Fe/N co-doped biochar revealed outstanding performance owing to the synergistic effect and resonance between the doped atoms. For example, Fe/N-doped biochar synthesized from sawdust achieved a NOR uptake capacity of 107.5 mg g^{-1}, significantly higher than that of the pristine biochar (35.3 mg g^{-1}) and Fe-doped biochar (58.2 mg g^{-1}).[137] Ahmad *et al.* (2022) further confirmed that Fe/N biochar exhibited a faster adsorption rate and markedly enhanced efficiency compared to other carbon-based adsorbents in treating micropollutant-containing wastewater.[138]

Additionally, Fe/B co-doped biochar synthesized using $NaBH_4$ as the B source exhibited uniform distribution of B and Fe atoms within the carbon matrix. This configuration enhanced TC adsorption *via* π–π interactions and hydrogen bonding.[139] The literature also highlights that atomically doped biochars outperform conventional materials like carbon nanotubes or activated carbon. For instance, in the work by Ma *et al.*,[147] a sludge biochar–carbon nanotube composite achieved only ~70 mg g^{-1} for SMX whereas P-doped biochar reached over 140 mg g^{-1}. In summary, whether doped with single elements such as B, P, N, or with combinations such as Fe/N and Fe/B, biochar has demonstrated substantial improvements in adsorption efficiency, stability, and practical applicability, surpassing both unmodified biochar and many commercial adsorbents reported in the literature.

A sustainable approach that continues to draw interest from researchers in wastewater treatment is the application of green chemistry techniques in both the fabrication and activation of biochar. In particular, the use of plant extracts to reduce metal precursors has proven to be an effective method for generating metal nanoparticles (NPs). These nanoparticles can be dispersed and immobilized within plant-derived biochar (BC) matrices, resulting in environmentally friendly, low-cost, and chemically non-toxic BC–NP composites.[148] Numerous studies have demonstrated the synthesis and characterization of NPs through biological methods involving either microorganisms or plant-based extracts. These include a range of metal nanoparticles (Al, Ag, Au, Pd, Fe, and Cu),[149] metal oxides (ZnO, CeO_2, CuO, TiO_2, and Fe_3O_4),[150] and metal sulfides (PbS and

© 2025 The Author(s). Published by the Royal Society of Chemistry

Open Access Article. Published on 06 10 2025. Downloaded on 2026-05-13 12:47:34.
This article is licensed under a Creative Commons Attribution-NonCommercial 3.0 Unported Licence.

CdS).[151] Inorganic salts such as $AgNO_3$ and $FeSO_4$ are commonly reduced using plant extracts to synthesize isolated nanoparticles[152] or to co-synthesize NPs *in situ* within biochar frameworks, forming composite materials.[153] For example, silver nanoparticles have been generated *via* the decrease of $AgNO_3$ using plant extracts derived from pine, rose, ginkgo, magnolia, and platanus, with applications in biomedicine and antimicrobial treatments.[152]

Additionally, the incorporation of physical attributes such as magnetism into biosorbents has been reported.[153] A representative case is the preparation of magnetic bioadsorbents through the use of rosemary leaf extract to generate Fe_3O_4 nanoparticles. In this method, rosemary leaves were initially activated with phosphoric acid (H_3PO_4) and subjected to thermal treatment at 220 °C to yield acid-modified biochar. This modified biochar was then mixed with rosemary extract, followed by the dropwise addition of $FeSO_4$ solution, facilitating the *in situ* formation of Fe_3O_4 nanoparticles within the biochar matrix. The integration of magnetic properties into such bioadsorbents enhances pollutant separation from aqueous media and promotes their reusability and practical waste management at scale.

The use of plant-derived reducing agents in nanoparticle synthesis further contributes to lowering the toxicity of the final materials, enhancing their safety and environmental compatibility. Kumar *et al.* presented a green synthesis route for biochar using seeds of *Abelmoschus esculentus* (AESB) to eliminate Direct Blue 86 dye.[154] The dried seeds were chemically activated with 88% H_3PO_4 at 100 °C for 90 min, leading to the development of mesoporous and microporous structures on the surface *via* pyrolytic degradation mechanisms.[155] Subsequent pyrolysis at 600 °C in a nitrogen environment facilitated the formation of additional functional pores, significantly increasing the material's active surface area.[156] The high-temperature thermal decomposition of lignin, cellulose, and hemicellulose is considered pivotal in generating a porous structure with enhanced adsorption efficiency.[157]

More recently, the focus of biochar research has shifted from terrestrial biomass to marine algal biomass, which offers advantages such as rapid growth and ease of harvesting. Algal species including *U. ohnoi* (Chlorophyta), *S. hemiphyllum* (Phaeophyceae), and *A. subulata* (Rhodophyta) have been explored as promising precursors for green biochar synthesis aimed at wastewater decontamination.[158–161] In *U. ohnoi*, functional groups like carboxyl and sulfate present in cell wall polysaccharides are known to assist in alkali-mediated modification of BC using agents like NaOH or KOH.[162] The biomass of *A. subulata* contains a variety of bioactive compounds including fibers, carotenoids, lipids, and proteins,[163] whereas *S. hemiphyllum* possesses functional constituents including fucoxanthin, phlorotannins, polyphenols, and sulfoglycolipids, which provide chemically active sites for further modification.[161] An additional example is the study by Mosaffa *et al.*, who developed a highly porous green sorbent by integrating hydrogel and biochar derived from *Borassus flabellifer*. Using a carbonization temperature control approach (350–700 °C), they achieved a BET of 80.34 $m^2\ g^{-1}$.[164] The resulting material demonstrated remarkable adsorption capacities for both cationic (malachite green −10 596 mg g^{-1} at pH ∼ 10) and anionic (Congo red −7095.43 mg g^{-1} at pH ∼ 6) dyes. Beyond water treatment, green-synthesized nanoparticles have been further investigated for biomedical applications including contrast imaging, magnetic hyperthermia therapy, and targeted drug delivery.[165] In summary, adopting green synthesis strategies for the development of bioadsorbent materials not only enhances water purification performance but also supports the overarching goal of global environmental sustainability.

2.4. Hybrid biochar architectures incorporating MOFs and MXenes

In recent years, hybrid biochar architectures combined with metal–organic frameworks (MOFs) and MXenes have attracted great attention in the materials science community due to their ability to significantly improve the adsorption performance of organic pollutants, especially antibiotics in wastewater. These composite structures take advantage of the unique properties of each component, in which biochar has high adsorption capacity and low cost; MOFs stand out with super large surface area, tunable porosity and high selectivity, and MXenes possess superior conductivity along with strong surface interaction and many active functional groups. MOFs are a diverse group of metal–organic frameworks comprising various substructures such as MILs, ZIFs, and other hybrid systems, which are designed with the outstanding characteristics of large surface areas, tunable porosity, and highly selective interactions with target molecules. Therefore, the integration of MOFs into biochar has opened up a promising approach for wastewater treatment, especially for organic pollutants.

One of the prominent trends is to integrate MOFs onto the biochar surface to effectively utilize both material phases. For example, Hanane Chakhtouna and co-workers successfully synthesized an MIL-53(Fe)/biochar adsorbent from date palm rachis and achieved simultaneous elimination of CIP and ofloxacin (OFL) up to 218.29 and 223.89 mg g^{-1}.[166] The primary mechanisms were identified as π–π resonance, electrostatic interactions, and hydrogen bond formation, while MIL-53(Fe) increased the density of mesopores for faster molecular diffusion. Similarly, Samar M. Mahgoub and co-workers developed a Zn-MOF/biochar composite derived from date palm seeds for the treatment of CIP in polluted water.[167] The data discovered that this material achieved a highest adsorption amount of 194.3 mg g^{-1}. A notable breakthrough came in 2020, when Chanaka M. Navarathna's group synthesized a magnetic MIL-53-Fe MOF/biochar composite incorporating magnetite. This innovative material boasted an extensive surface area (∼350 $m^2\ g^{-1}$) and demonstrated exceptional Rhodamine B (RhB) adsorption (55 mg g^{-1} at pH 6 and room temperature).[168] Beyond its high efficiency, the composite exhibited outstanding reusability, retaining over 80% adsorption capacity after multiple cycles, highlighting its stability and promise for treating dye-laden wastewater. In contrast, Liu *et al.* developed an

Open Access Article. Published on 06 10 2025. Downloaded on 2026-05-13 12:47:34.
This article is licensed under a Creative Commons Attribution-NonCommercial 3.0 Unported Licence.

Table 2 Adsorption of multiple antibiotics using a biochar/MOF-based adsorbent

Adsorbent	Antibiotics	Efficiency	Mechanism	Ref.
MIL-53(Fe)/biochar	– CIP	– OFL 223.89 mg g^{-1}	π–π resonance, electrostatic interactions, and hydrogen bonding	151
	– Ofloxacin	– CIP 218.29 mg g^{-1}		
Zn-MOF/biochar	– CIP	194.3 mg g^{-1}		152
Magnetic MIL-53-Fe MOF/biochar	– RhB	55 mg g^{-1}		153
Lignin-doped biochar/MIL-101-NH_2(Fe)	– TC	760.36 mg g^{-1}		154
Fe–Co MOF/$CoFe_2O_4$ modified biochar	– TC	909 mg g^{-1}	Chemisorption (non-electrostatic interactions including hydrophobic interactions, hydrogen bond formation, surface coordination mechanisms, and π–π stacking)	171
Hybrid (MIL-53(Al)@RH)	– Glyphosate (GLY)	GLY: 162 mg g^{-1}	Chemical bonding, electrostatic interactions	172
	– Diclofenac (DCL)	OTC: 139 mg g^{-1}		
	– OTC	DCL: 93 mg g^{-1}		
HKUST/biochar based adsorbent	– TC	396 mg g^{-1}	– Metal-organic complexation – Hydrogen bond formation – Electrostatic force – π–π interaction	173
MIL-101(Fe)-PMA-biochar	– RhB	RhB: 96%	– Electrostatic interactions	174
	– Methyl orange (MO)	MO: 93%	– Hydrogen bonding	
MIL-53(Al)@RH biochar	– GLY	297 mg g^{-1}	– π–π stacking interactions – Hydrogen bonding – Complexation	175
MPN/NH_2-MIL-101 (Fe)	– TC	– TC: 109 mg g^{-1}	– Hydrogen bonding	176
	– 2,4-Dichlorophenoxyacetic acid (2,4-D)	– 2,4-D: 79 mg g^{-1}	– Electrostatic complexation – π–π mechanisms	
Ti-MOF/TiO_2@WMPB/CTH	DOX	DOX: 95%	Pseudo-second Order Langmuir Isotherm (monolayer adsorption)	177
Biochar/ZIF-8	TC	288.85 mg g^{-1}	Hydrogen bonding, – π–π interaction	178

innovative lignin-grafted MIL-101-NH_2(Fe)/biochar composite for TC adsorption.[169] Remarkably, this material exhibited outstanding adsorption performance across a broad pH range, achieving a maximum amount of 760.36 mg g^{-1} at pH 4.19, doubling the adsorption efficiency of Carbon-MIL-101-NH_2. A summary of typical studies on ZIF/biochar and MOF/biochar composite materials for antibiotic adsorption has been presented in detail in Table 2 to provide a comprehensive view of the potential and development trends of this advanced material line. Fig. 7 illustrates the typical antibiotic adsorption mechanism of MOF/biochar composite materials through the interactions: (1) hydrogen bond formation between functional groups on the biochar surface and antibiotic molecules, (2) pore adsorption from the MOF structure, and (3) ion exchange,. . ..

MXenes constitute an innovative class within the broader field of two-dimensional materials with the general formula $M_{n+1}X_nT_x$, in which M refers to a transition metal (*e.g.*, Ti, V, and Nb), X represents nitrogen or carbon, and T_x refers to surface functional groups such as –O, –F, and –OH.[179] These substances are generated *via* the etching of A-layers from the MAX structure (*e.g.*, Ti_3AlC_2), resulting in thin sheets of material with large surface areas, high electrical conductivity, and flexible functionalization.[180] Thanks to these properties, MXenes have been widely explored in fields including sensors, energy storage, and especially water remediation as potential adsorbent materials. The combination of MXenes with biochar, a porous carbon material obtained from biomass pyrolysis, has produced composites with superior adsorption capacity due to the synergy between the electrical conductivity and ion exchange capacity of MXenes and the functional group-rich active surface of biochar. Fig. 8 shows the fabrication process of a biochar/MXene based adsorbent. Typical evidence is the investigation by Bukhari *et al.* (2024), in which the Fe_2O_3/biochar/MXene composite showed high adsorption efficiency for lead ions (Pb^{2+}) and MB dye, achieving more than 99% removal of Pb^{2+} and MB.[181] The adsorption mechanism is believed to be owing to the combination of functional groups including O^-, OH^-, and F^- from MXenes and CO, CN, and OH groups from biochar, creating many adsorption sites for metal ions and dye molecules.[181]

Another work discovered by Liu *et al.* (2023) successfully developed a biochar/MXene composite material using a coconut shell as a raw material, which combined with polydopamine (PDA) and polyethyleneimine (PEI) coating that forms Ti_3C_2Tx@biochar-PDA/PEI material through the charge self-assembly method.[182] The results showed that this material possesses a porous structure with many active functional

© 2025 The Author(s). Published by the Royal Society of Chemistry

Open Access Article. Published on 06 10 2025. Downloaded on 2026-05-13 12:47:34.
This article is licensed under a Creative Commons Attribution-NonCommercial 3.0 Unported Licence.

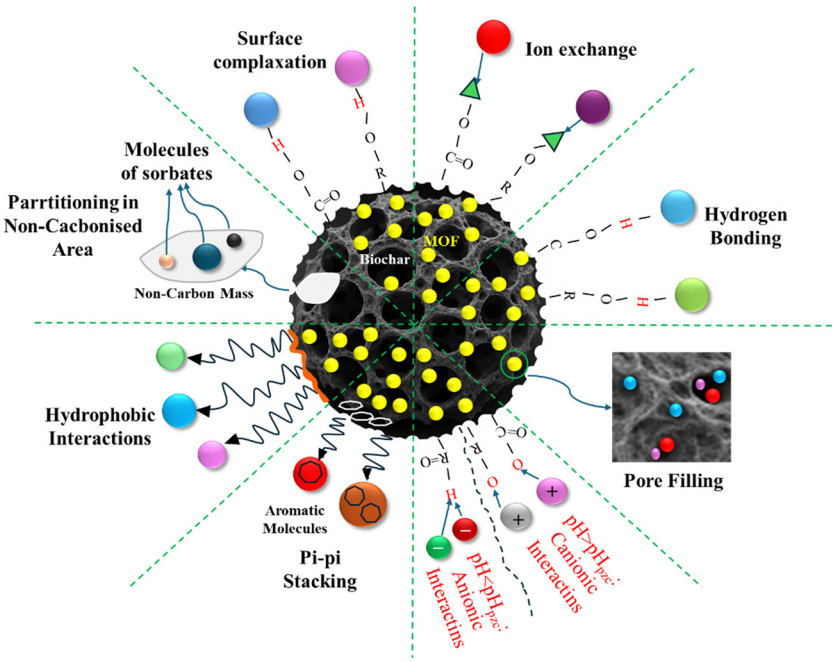

Fig. 7 Mechanism of pollutant capture by biochar/MOF (reproduced from ref. 170 – open access article under CC-BY license).

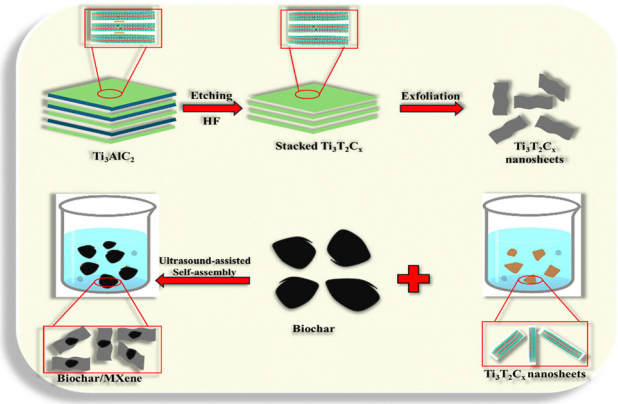

Fig. 8 Biochar/MXene fabrication strategy.

groups including –OH, $–NH_2$, and Ti–OH, which enhances the adsorption capacity of radioactive ions U(VI) and Cs(I). Batch sorption experiments showed that the elimination performance of U(VI)/Cs(I) followed second-order kinetics and the Langmuir isotherm model, discovering a monolayer sorption mechanism controlled by chemisorption. In particular, this material achieved extremely high adsorption efficiency, with a maximum removal capacity of up to 239.7 mg g^{-1} for U(VI) and 40.3 mg g^{-1} for Cs(I).[182] Even in an environment containing many competing ions, the material still maintained its superior adsorption efficiency, demonstrating the good selectivity of this composite. In addition, the reusability of the adsorbent was also examined and after three adsorption–desorption cycles, the material still maintained more than 80% of its initial efficiency. Mechanism analysis through FTIR spectroscopy, XPS, and DFT simulations discovered that the main mechanisms include ion exchange, electrostatic forces, and chelate complexation between functional groups on the material surface and the target metal ion.

Complementing the above results, the study by Kumar *et al.* (2025) successfully synthesized $Ti_3C_2T_x$ MXene@biochar (MB) composite materials *via* an ultrasonic self-assembly method with different ratios between MXene and biochar (1 : 9, 3 : 7, and 5 : 5), aiming to simultaneously treat inorganic pollutants coexisting in wastewater including metal species (Cd, Cu, Cr, and Pb), ammonium (NH_4^+), and phosphate (PO_4^{3-}).[183] The results showed high adsorption efficiencies for Cu, Pb, and Fe when all reached >98% under optimal conditions. Notably, the MB-1 : 9 material (high biochar ratio) exhibited a Cu removal efficiency of up to 99.89% at a dose of 12 mg while MB-3 : 7 was more suitable for NH_4^+ adsorption, achieving an efficiency of 97.83%. The biosorption models were accurately depicted by the Freundlich model, revealing the possibility of multilayer uptake on the heterogeneous interface. Meanwhile, the kinetics followed a second-order kinetic, indicating the crucial role of the chemical sorption mechanism. The adsorption mechanism was determined to be a combination of several interactions such as electrostatic forces that occur between metal species and the MXene surface's functional groups (–OH, –O, and –F), ion exchange *via* Ti–OH groups, chelation complexation *via* –COOH groups as well as physical adsorption in the porous structure of biochar. Furthermore, thermodynamic studies confirmed that the uptake process was endothermic ($\Delta H > 0$) and spontaneous ($\Delta G < 0$) with Zn adsorption exhibiting a strong temperature dependence (ΔH up to 61.7 kJ mol^{-1} for MB-5 : 5).[183] The MB material also demonstrated good

Open Access Article. Published on 06 10 2025. Downloaded on 2026-05-13 12:47:34.
This article is licensed under a Creative Commons Attribution-NonCommercial 3.0 Unported Licence.

reusability after multiple adsorption–desorption cycles, especially for heavy metals and PO_4^{3-}, showing great potential in practical applications. In addition, MXene/biochar composites have also been tested in the field of wastewater decontamination and energy recovery, showing effective elimination of organic pollutants in food wastewater and enhanced hydrogen recovery efficiency due to the excellent catalytic and electron transfer properties of MXenes.[184]

However, it is worth noting that up to now, there has been no published study on the direct application of biochar/MXene composite materials in the adsorption of antibiotics, an emerging group of pollutants that are causing concern in the aquatic environment. This creates an important research gap as the ideal properties of MXenes (electrostatic interactions, flexible functional groups) and biochar (diversified adsorption capacity and stability) can be combined to effectively treat antibiotic molecules such as CIP, TC, or SMX, which have been successfully treated by individual biochar or MXene forms. Therefore, future research can be directed toward the synthesis and optimization of biochar/MXene composite materials specifically for antibiotic adsorption, while studying the molecular interaction mechanism between the materials and specific antibiotic groups. The development of this new material line not only fills the current gap but also promises to bring sustainable solutions for the treatment of medical and agricultural wastewater, where antibiotic residues are an urgent problem.

2.5. Techniques for characterizing biochar

The ability of biochar to eliminate substances is improved by chemical, thermal, and mechanical modifications, which provide significant benefits to this material. The changes in the structure and biochar's properties depend on various factors including pyrolysis temperature, precursor type, particle size, and modification agent. These changes can be evaluated by various characterization techniques. In many experimental studies, the adsorption properties and efficiencies of modified biochar are further characterized through qualitative methods. Further modified forms of biochar including nano-sized adsorbents, magnetic materials, and other complex derivatives are often characterized by a variety of modern instruments such as TEM, SEM, XPS, EDS, VSM, ICP, FT-IR, and particle size analyzers.[152] Specifically, TEM and SEM are commonly employed to analyse the structure of nano-materials while EDS supports the confirmation of atomic composition. The magnetic characteristics of the biochar are evaluated by measuring the vibrational magnetic moment using a VSM. In addition, particle size analysis allows determining the influence of mechanical modification. SEM and TEM demonstrate the effect of thermal modification while EDX and FTIR techniques mainly serve to evaluate the effectiveness of chemical modification. Compared to raw biochar, the efficiency of modification or activation is better demonstrated through additional analytical methods. These methods are specifically illustrated in the following sections.

3. Biochar for adsorption of antibiotics

3.1. Key variables impacting biochar adsorption performance

In heterogeneous adsorption systems, pollutant removal efficiency depends not only on the properties of the material but also on environmental conditions and operating parameters. Factors such as solution pH, initial contaminant amount, temperature, duration time and material content influence more than just the adsorption kinetics or equilibrium; they also play a crucial role in governing interaction mechanisms at the molecular level. For instance, pH exerts a dual effect: it controls the ionization state and charge distribution of functional groups on the biochar interface while simultaneously influencing the chemical form and electronic activity of the pollutant in solution. These changes directly impact the generation of electrostatic attraction, hydrogen bonding and EDA complexes. Meanwhile, the initial concentration and temperature relate to the thermodynamic driving force, the ability to overcome energy barriers and the surface selectivity of the composite. Thus, understanding the role of each variable provides not only deeper insight into the adsorption process but also a rational basis for optimizing performance and designing biochar materials in a mechanism-driven framework.

3.1.1. pH. During the biochar treatment of antibiotics, the pH of the reaction working plays an important role because it influences both the surface charge of the adsorbent and the electrochemical structure of the antibiotic molecule.[56,185–187] This is particularly important for acid–base dissociating molecules such as TC, where pH changes lead to different ionization states that determine both the molecular form and its ability to interact with the adsorbent. A typical example is TC, an antibiotic with three acid dissociation constants, recorded with $\log K_a$ values of approximately −9.7, −7.7, and −3.3.[188] These values divide the pH range into four distinct regions, each dominated by a specific ionic form. At high pH levels, well above the first dissociation constant, the HTC_2^- form becomes dominant with a strong negative charge. At low pH and below the third dissociation constant, the molecule exists mainly in the positively charged H_4TC^+ form. Between these extremes, the molecule gradually transitions from H_2TC^- to neutral H_3TC depending on the acidity or alkalinity of the medium. Each ionic form has unique electrochemical characteristics, leading to significant differences in its interaction with the adsorbent surface, especially when that surface contains polarized groups or regions with delocalized electrons.[189] In addition to altering the structure of the antibiotic molecule, pH directly affects the biochar's surface charge through protonation and deprotonation. Once the environmental pH is lower compared to the material's pH_{pzc}, the carbon surface tends to carry a positive charge, promoting attraction with negatively charged ions. In contrast, as the pH exceeds pH_{pzc}, the surface becomes negatively charged, which can lead to electrostatic repulsion with antibiotic anions.[190] Experimental results show that under neutral to slightly acidic conditions and typically between pH 2 and 7, the removal efficiency of antibiotics is significantly

© 2025 The Author(s). Published by the Royal Society of Chemistry

Open Access Article. Published on 06 10 2025. Downloaded on 2026-05-13 12:47:34.
This article is licensed under a Creative Commons Attribution-NonCommercial 3.0 Unported Licence.

higher compared to alkaline conditions.[191,192] In basic environments, strong deprotonation reduces adsorption due to increased repulsion and weaker hydrogen bonding. Furthermore, pH regulates the charge density and polarity of surface functional groups such as OH, COOH, and NH_2.[193] These factors influence the formation of hydrogen bonds, electron donor–acceptor complexes, and π–π interactions. However, such interactions tend to weaken when the pH becomes too alkaline, as protonation decreases and changes occur in the energy levels of the involved molecular orbitals. From the above discussion, it is clear that maintaining pH within an optimal range not only preserves effective adsorption but also improves selectivity for different antibiotics, thereby enhancing both the accuracy and overall efficiency of water treatment using biochar.

In addition to the aforementioned factors, pH is also influenced by the intrinsic characteristics of the biochar, which are ascertained by the input materials and the pyrolysis conditions used during its production. Higher pyrolysis temperatures tend to rise the ash amount, thereby enhancing the alkalinity and elevating the surface pH of the biochar, which directly impacts its interaction with various charge carriers.[194] Variations in pH also influence the suspension properties of the system, including colloidal stability and dispersion, thus regulating adsorption efficiency under real environmental conditions.[195] Moreover, several studies have discovered that the antibiotic removal efficiency of biochar typically fluctuates with the pH of the solution often increasing from acidic to neutral conditions and then declining as the pH becomes more alkaline.[196] This trend is attributed to shifts in the relative charges between the biochar surface and the antibiotic molecules, leading to changes in electrostatic interactions as well as the potential for hydrogen bonding or ion exchange mechanisms.

3.1.2. Duration time. In wastewater treatment using adsorption, the duration time between the material and the contaminant such as biochar plays a crucial role in determining removal efficiency.[197] Unlike instantaneous reactions, adsorption follows a complex kinetic pathway where antibiotic molecules require sufficient time to migrate and bind to the vacant sites on the material's interface. As this interaction progresses, it gradually leads to a phase of equilibrium when the rate of uptake equals the rate of desorption. In wastewater environments with high levels of organic matter, pollutant concentrations typically decrease over time until this steady state, known as adsorption equilibrium, is reached.[198] Accurately determining the time required to reach equilibrium is essential for effective system design and operation. If the contact time is too short, the adsorption process remains incomplete but too long can lead to unnecessary energy and resource consumption. This parameter is strongly affected by the microstructural and chemical characteristics of the biochar, which include porosity, pore size, specific surface area, and surface functional groups. It is also influenced by operating levels including pH, the initial concentration of pollutants, and temperature.[199] An illustrative example of the importance of contact time can be found in a study by Fan and colleagues, who investigated MB adsorption using two types of biochar. One was derived from municipal sewage sludge, while the other was produced from a combination of sewage sludge and tea waste. Their results revealed a substantial difference in the time needed to reach equilibrium when the first biochar required 24 h,[200] whereas the second attained equilibrium in as little as 8 h.[201] This outcome indicates that the origin and structural properties of the biochar have a direct impact on the adsorption kinetics. To gain deeper insight into the influence of duration time and other influencing factors, the researchers employed Design Expert software along with the Box-Behnken response surface methodology to optimize the process. Simulation results demonstrated that, under optimal conditions, the pollutant removal efficiency could reach 99.9%, underscoring the critical role of operational parameters, including contact time, in overall treatment performance.[202] Additionally, physical characteristics such as material permeability and electrostatic interactions that occur between the material and pollutant molecules are acknowledged as major contributors to the uptake rate and the underlying mechanism throughout the process.[198] Therefore, precise control of the contact time is not only vital for maximizing treatment efficiency but also serves as an important indicator for evaluating the practical feasibility of biochar-based systems in the removal of antibiotics from wastewater.

3.1.3. Biochar dosage. Biochar dosage is an important factor that directly affects the adsorption efficiency of pollutants, particularly antibiotics. Once the amount of biochar in the medium increases, the number of available vacant sites on the sorbent's surface also increases, improving the sorbent's capacity to isolate and remove pollutant molecules.[203,204] For instance, David Adu-Poku *et al.* (2024) observed that TC removal efficiency improved from 90 to 98.9% as the mass of biochar was raised from 0.05 to 0.1 g.[205] However, this efficiency does not rise indefinitely but instead reaches an optimal threshold. Beyond this point, biochar particles may begin to overlap, causing adsorption layers to merge and obscuring active sites, which reduces overall treatment efficiency.[196] Similarly, one study demonstrated that a biochar dosage of 1 g L^{-1} could remove over 70% and even achieve 100% removal for TC, erythromycin, and clarithromycin.[206] Yet excessive dosage can diminish adsorption efficiency due to overlapping adsorption layers and active site saturation. Duc Thang Nguyen *et al.* (2025) found that improving the amount of biochar from 0.1 to 0.25 g raised CIP elimination efficiency from 40 to ~95% before reaching saturation.[207] Additionally, if the adsorbent quantity is too high relative to the initial pollutant concentration, insufficient antibiotic molecules remain to occupy all empty sites, which leads to a relative decline in adsorption efficiency.[195] Conversely, well-controlled dosage conditions can significantly accelerate the initial adsorption rate by enhancing the number of empty sites on the material surface.[208] This also shortens the time required to achieve equilibrium in the treatment system.[209] Thus, determining the optimal biochar dosage is vital to ensure both high removal efficiency and cost-effectiveness for large-scale wastewater treatment. An

Open Access Article. Published on 06 10 2025. Downloaded on 2026-05-13 12:47:34.
This article is licensed under a Creative Commons Attribution-NonCommercial 3.0 Unported Licence.

appropriate dosage maximizes resource utilization, prevents material waste, and reduces production costs in potential industrial biochar applications.

3.1.4. Contaminant concentrations. Initial levels of antibiotics are recognized as a critical factor influencing the adsorption efficiency in treatment systems that use biochar or composite materials. At the beginning, the concentration difference between the solution and the adsorption interface promotes rapid diffusion and strong interactions between antibiotic molecules and the active sites on the material. However, as the concentration continues to rise, the adsorption sites become progressively occupied, resulting in a decline in elimination performance owing to surface saturation. Experimental evidence from various studies supports this pattern. Yan *et al.* (2020)[210] reported that TC molecules quickly bonded to Zn-modified biochar (ZnBC) at the early stage. Yet, when the TC concentration exceeded 80 mg L^{-1}, the adsorption efficiency showed no further significant increase, suggesting that the material had reached saturation. Sayin *et al.*[211] also observed that CIP removal efficiency dropped from 99.9 to 97.3% as the amount of sorbate increased from 50 to 150 mg L^{-1} and fell sharply to 48.2% at 500 mg L^{-1}. This indicates that when the antibiotic concentration surpasses the capacity of the adsorption sites, treatment performance is substantially reduced. Fu *et al.*[212] further found a rising trend in DNA adsorption with increasing initial concentration when using biochar modified with quaternary phosphonium salts, but the trend plateaued beyond a certain point. Simultaneously, Wu *et al.*[213] observed that the uptake rate declined as the amount of initial antibiotic rose, which reflected competition among target molecules for the remaining active sites. Recent studies have reported similar findings. Zheng *et al.* (2021)[214] demonstrated that iron-doped biochar made from agricultural waste increased sulfamethylimidine adsorption capacity from 0.3 to over 4.0 mg g^{-1} as the concentration grew from 2 to 35 mg L^{-1}, though the efficiency eventually stabilized and no longer increased proportionally. Likewise, a study by Ouyang *et al.* (2024)[215] using bamboo biochar showed that elimination capacities for MFX, CIP, and OFLX enhanced notably from 30.71, 35.20, and 36.80 mg g^{-1} at 10 mg L^{-1} to 83.58, 102.91, and 102.77 mg g^{-1} at 50 mg L^{-1} but the efficiency declined once the concentration surpassed the optimal level. These findings suggest that although raising the initial antibiotic concentration can enhance the uptake amount of biochar up to a point, exceeding that threshold may reduce efficiency due to active site saturation. Therefore, identifying an appropriate initial antibiotic concentration is essential to optimize the wastewater treatment process using biochar.

3.1.5. Temperature. Temperature variation during adsorption can significantly affect the removal efficiency of pollutants, especially antibiotics. This is because temperature influences both the reaction rate and the interactions that occur between the interface of material and pollutant molecules. Most water treatment studies conduct experiments at around 25 °C to simulate typical environmental conditions.[216] However, many results show that temperature changes can cause significant differences in antibiotic removal efficiency, depending on the adsorbent characteristics and pollutant type. For example, when removing TC using biochar from grapefruit peel, rising the temperature from 25 to 40 °C raised the isolation efficiency from 9.89 to 26.27%. This increase occurred because higher molecular kinetic energy improved the diffusion of TC to adsorption sites.[217] The same tendency was discovered by Cheng *et al.*,[218] in which isolation performance enhanced with a temperature rise from 15 to 35 °C. The above effect is explained by the endothermic nature of the adsorption.[219] In addition, higher temperatures can raise the collision frequency between reactive molecules and SMX, promoting more efficient adsorption.[220] Liu *et al.*[221] reported a similar trend for *p*-nitrophenol removal utilizing pine sawdust biochar, as did Lonappan *et al.*[222] with diclofenac on pine wood biochar. In both cases, adsorption increased with temperature. The observed phenomenon may relate to increased molecular motion, which raises the chance of contact between antibiotics and active sites. It may also result from improvements in the biochar surface structure, owing to the development of aromatic carbon phases that enhance adsorption interactions.[223] However, it should be noted that not all adsorption processes are endothermic. In exothermic systems, higher temperature may reduce efficiency because it reduces the interaction strength between the pollutant and the sorbent.

3.1.6. Effect of other pollutants. In natural water and wastewater environments, the presence of inorganic salts is unavoidable, and they can influence the antibiotic adsorption efficiency of biochar. Liang *et al.*[224] reported that a certain concentration of sodium can enhance antibiotic adsorption on the surface of treated biochar. However, other studies have presented contrasting findings. Tang *et al.*[225] and Nguyen *et al.*[226] observed that the presence of cations in solution reduces adsorption efficiency because of their competition with antibiotic molecules for active sites. Nguyen *et al.*[226] further emphasized that both cations and anions contribute to the inhibition of the adsorption process. Apart from monovalent ions, the impact of divalent ions on the antibiotic removal capacity of biochar has also attracted attention and remains a subject of debate. Tan *et al.*[227] found that Mg^{2+} ions exert a stronger inhibitory effect than Na^{+} ions. Nevertheless, some studies have highlighted potential benefits associated with divalent ions. Nguyen *et al.*,[226] for instance, found that Ca^{2+} can form complexes with antibiotic molecules such as TC, thereby improving the TC removal efficiency in solution. As a Lewis base, TC can bond with cations like Ca^{2+} and Mg^{2+}, which act as Lewis acids, forming stable complexes that support the adsorption process (eqn (4)–(8)). In contrast, other studies including Hu *et al.*[188] and Liang *et al.*[224] suggested that divalent cations generally reduce adsorption efficiency due to stronger competition at the material surface.

$$Mg^{2+} + HTC^{-} \rightarrow MgHTC^{+} \quad (1)$$

$$Mg^{2+} + TC^{2-} \rightarrow MgTC \quad (2)$$

$$Ca^{2+} + HTC^{-} \rightarrow CaHTC^{+} \quad (3)$$

$$Ca^{2+} + TC^{2-} \rightarrow CaTC \quad (4)$$

© 2025 The Author(s). Published by the Royal Society of Chemistry

Open Access Article. Published on 06 10 2025. Downloaded on 2026-05-13 12:47:34.
This article is licensed under a Creative Commons Attribution-NonCommercial 3.0 Unported Licence.

The presence of cations in solution can influence the adsorption efficiency of negatively charged antibiotic molecules onto the surface of biochar. The extent of this effect depends significantly on the type of ion. For example, Fu *et al.* (2021) found that divalent ions tend to enhance the adsorption efficiency of antibiotics more effectively than monovalent ions, owing to their higher surface charge density and stronger interactions with biochar.[212] Calderón-Franco *et al.*[228] investigated the effects of Na^+, Ca^{2+}, and Mg^{2+} on the adsorption of several common antibiotics. The results indicated that Mg^{2+} improved adsorption efficiency by approximately 33%, whereas Na^+ and Ca^{2+} did not cause any significant changes. These findings contrast somewhat with those of Wang *et al.*,[229] who demonstrated that Ca^{2+} can form stronger ionic bridges than Mg^{2+} and may also create complexes with the functional groups of antibiotics, resulting in more compact molecular structures that fit more effectively into the micropores of biochar. Humic acids (HA) have also been shown to play an important role in promoting antibiotic adsorption. Calderón-Franco *et al.*[228] reported that HA not only directly adsorbs antibiotics but also adheres to the biochar surface, acting as an intermediate bridge layer that facilitates adsorption. Beyond these studies, several recent works have provided further insights into the role and mechanisms of cations in the adsorption process. Qiong Lu *et al.*,[230] for instance, emphasized that alkaline earth metal ions such as Mg^{2+} and Ca^{2+} not only enhance charge coupling between biochar and antibiotic molecules but also contribute to the structural stability of the material under variable pH conditions, particularly in neutral to alkaline environments. The adsorption mechanism involves more than just ionic bridging. It also includes π–π interactions, hydrogen bonding, and electrostatic forces, all of which are influenced by the type of cations present in the solution.[231] Notably, some studies have shown that incorporating metal oxides like $MgFe_2O_4$ into biochar can improve the adsorption efficiency of SMX and TC by combining several mechanisms including π–π interactions, Ca^{2+} ion bridging, and surface-mediated functional group binding.[232] In parallel, research on seaweed-derived biochar has demonstrated high antibiotic adsorption efficiency at elevated temperatures. This is primarily achieved through π–π interactions, pore filling, and hydrogen bonding, suggesting effective strategies for optimizing adsorbent materials under favorable thermodynamic conditions. Finally, the effects of aged biochar have also been documented. In the presence of Na^+ and Ca^{2+} ions, aged biochar exhibited reduced adsorption capacity for NOR.[230] In contrast, humic acid enhanced adsorption at acidic pH but had a diminishing effect at neutral pH. These observations underscore the importance of considering coexisting substances in the environment when assessing the performance of biochar in antibiotic removal.

3.2. Quantum chemical insights *via* density functional theory (DFT) calculations

Density functional theory (DFT) has emerged as a pivotal tool for investigating the sorption mechanisms of organic pollutants on carbon-based adsorbents particularly biochar. This computational approach enables detailed examination of interactions between antibiotic molecules and biochar surfaces at the electronic level providing insights into fundamental processes such as π–π interactions, hydrogen bond formation and chemical bonding while offering valuable guidance for designing biochar with optimized structures. Current applications of DFT in simulating antibiotic adsorption predominantly employ computational software packages such as Gaussian Materials Studio or Dmol^3 utilizing exchange-correlation functionals like B3LYP PBE or ωB97X-D combined with basis sets such as 6-31++G(d,p) and DNP. In recent years, many studies have expanded this approach by integrating experimental methods with DFT to elucidate the mechanism of antibiotic adsorption on biochar at the electronic level. Representative examples include the work of Badshah *et al.* (2024),[233] which investigated the stepwise mechanism of antibiotic removal using activated carbon, Zhang *et al.* (2024),[234] who standardized and analyzed the micromechanism of tetracycline adsorption on biochar, and Bai *et al.* (2023),[235] who employed magnetite-functionalized biochar to clarify the adsorption mechanism of four sulfonamide antibiotics. More recent contributions include Ezzahi *et al.* (2025),[236] who examined activated biochar derived from lignocellulosic biomass for fluoroquinolone removal, Ren *et al.* (2025),[237] who validated the adsorption mechanism of metronidazole on CO_2-activated biochar, and Jiang and Hu (2025),[238] who analyzed the synergistic effect between biochar and microplastics in tetracycline adsorption. Collectively, these studies demonstrate that combining experimental data with DFT simulations provides valuable insights into the roles of surface functional groups, metal ion bridging, π–π interactions, and pore filling. Such advances highlight the ongoing shift from purely experimental investigations to quantitative analyses at the electronic level and contribute to establishing a stronger scientific foundation for the design of next-generation biochar materials. This section comprehensively reviews representative studies that employed DFT to analyze antibiotic adsorption on biochar, representing a significant advancement from purely experimental investigations to quantum mechanical and electron-level understanding.

Among the pioneering works, Chen *et al.*[239] conducted a combined experimental and DFT modeling study examining sulfamethazine (SMT) adsorption onto porous cellulose biochar (MCB). Their computational approach utilized Materials Studio 2017 R2 software implementing the GGA-PBE exchange–correlation functional with the DNP 4.4 basis set and incorporating van der Waals corrections through Grimme's DFT-D method. The biochar model was constructed as a planar graphene sheet comprising seven aromatic rings with a 20 Å vacuum layer along the *z*-axis and employing a 4 × 4 × 1 *k*-point grid. Simulations were performed at 298 K in an aqueous environment simulated using the COSMO model (ε = 78.54). Following geometric optimization the SMT molecule was positioned on the biochar surface in multiple configurations. The adsorption energy (E_{ads}) was calculated using the standard expression:

$$E_{ads} = E_{complex} - (E_{biochar} + E_{SMT}) \quad (5)$$

Open Access Article. Published on 06 10 2025. Downloaded on 2026-05-13 12:47:34.
This article is licensed under a Creative Commons Attribution-NonCommercial 3.0 Unported Licence.

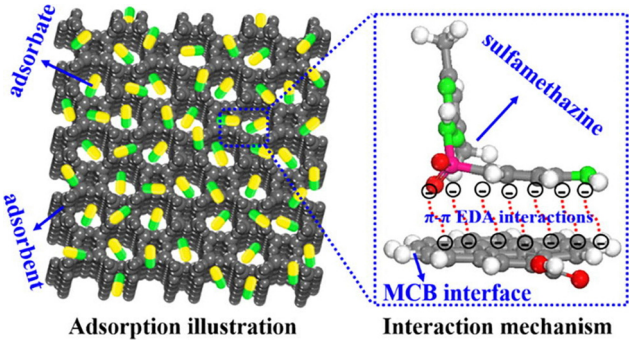

Fig. 9 Illustration of the interaction between the adsorbent and the antibiotic (reproduced from ref. 239 with permission from Elsevier, copyright 2019).

where $E_{complex}$ represents the total system energy, $E_{biochar}$ denotes the energy of the biochar model and E_{SMT} corresponds to the energy of the antibiotic molecule. Results (in Fig. 9) demonstrated that the most thermodynamically favorable adsorption configuration occurred when SMT adopted a parallel orientation relative to the graphene surface facilitating π–π stacking and electron donor–acceptor (EDA) interactions particularly at pyrrole group sites characterized by high π-electron density.

Complemented by in-depth analysis using DFT simulations, the projected density of states (PDOS) and charge density distribution calculations clearly demonstrate that the adsorption of SMT onto biochar occurs through π–π interactions, accompanied by strong electron transfer between molecular orbital regions (Fig. 10). The most stable adsorption configuration is observed when SMT adopts a V-shaped conformation, which optimizes the overlap between the π orbitals of the aromatic rings in SMT and those on the biochar surface. Moreover, the PDOS spectrum reveals a significant redistribution of the electronic density of states after adsorption, particularly in the region near the Fermi level. A notable enhancement in both the number and intensity of peaks in the p-orbital spectrum, compared to the s-orbital, confirms the dominant role of p electrons in the interaction process.

In systems such as OH-substituted MCB, NH_2-substituted MCB, and pyrrole-substituted MCB, the PDOS peaks originally located in the high-energy region corresponding to the HOMO were attenuated and reappeared at lower energy levels after adsorption, indicating electron transfer from the biochar to SMT. In contrast, for systems containing strong electron-withdrawing groups including NO_2 and COOH, several characteristic SMT peaks that appeared in the negative energy range before adsorption (from −3 to 0 eV) shifted to the positive energy range (from 1.5 to 4.5 eV) after adsorption, reflecting a reverse electron transfer direction from SMT to biochar. These findings align with the π–π electron donor–acceptor (EDA) interaction model, where both the direction and magnitude of electron transfer are governed by the polarity of the functional group. Among all functional groups studied, the pyrrole group had the most pronounced effect. It significantly increased the electronic density of states and created a distinct overlap between the PDOS peaks of SMT and biochar after adsorption, resulting in the most negative adsorption energy value. This highlights the critical role of pyrrole in enhancing the π–π EDA interaction and improving the selective uptake efficiency of SMT. Additional analyses including electrostatic potential (ESP) mapping and density of states (DOS) calculations revealed significant electron redistribution upon adsorption confirming the chemical nature of these interactions. The authors concluded that strategic enhancement of π-donor functional groups such as pyrrole moieties on biochar surfaces represents a promising approach for developing materials with superior selective adsorption capabilities.

Expanding upon the π-rich adsorption mechanism identified in the aforementioned study, Liu *et al.*[240] implemented a more sophisticated electronic analysis approach using biochar derived from durian peel and activated with KOH (KBC) for CIP adsorption. Their DFT simulations performed with Gaussian 09 software employed the hybrid B3LYP functional and

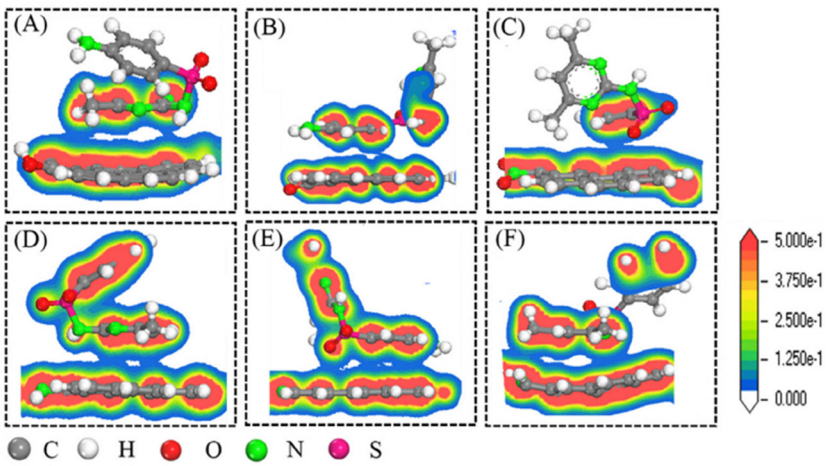

Fig. 10 Charge density images showing SMT adsorption on functionalized MCB surfaces: (A) MCB-OH, (B) MCB-COOH, (C) MCB-NO_2, (D) MCB-NH_2, (E) C_5H_5N-MCB, and (F) C_4H_5N-MCB (reproduced from ref. 239 with permission from Elsevier, copyright 2019).

© 2025 The Author(s). Published by the Royal Society of Chemistry

Open Access Article. Published on 06 10 2025. Downloaded on 2026-05-13 12:47:34.
This article is licensed under a Creative Commons Attribution-NonCommercial 3.0 Unported Licence.

6-31++G(d,p) basis set enabling simultaneous investigation of π–π stacking interactions, hydrogen bonding effects and functional group influences. Following geometric optimization of the CIP molecule the researchers calculated frontier molecular orbital energies including HOMO (−5.83 eV), LUMO (−1.41 eV) and the resulting band gap (ΔE = 4.42 eV), which collectively indicated pronounced electron-accepting characteristics. Electrostatic potential (ESP) mapping and molecular orbital calculations revealed that the oxygen-containing functional groups on the biochar surface, particularly the carboxyl and carbonyl groups with strong negative charge distributions, serve as preferential vacant sites for interactions with the locally positively charged regions of the CIP molecule (Fig. 11). The optimized adsorption profiles indicated that CIP can bind strongly to the biochar surface through both hydrogen bond formation and coplanar π–π interactions. Notably, adsorption energy analysis for each functional group highlighted the dominant role of the carboxyl (−8.06 eV) and carbonyl (−7.89 eV) groups, in contrast to the lower activity of groups like C═C (−4.08 eV) and OH (−2.72 eV). These findings confirm that oxygen-containing groups not only enhance hydrogen bonding but also function as key π donors in electron donor–acceptor π–π interactions. In addition, the relatively small HOMO–LUMO energy gap of CIP (4.42 eV) suggests a strong electron-accepting ability, which supports the formation of stable donor–acceptor complexes with the electron-rich biochar surface.

Surface charge distribution analysis was conducted using VMD software identified regions of strong negative charge localization particularly at –O–C═O and –C═O functional groups. Systematic calculations of adsorption energies across different functional group sites employing the conventional energy difference formula revealed the following trend: –O–C═O (−8.06 eV) > C═O (−7.89 eV) > C═C (−4.08 eV) > –OH (−2.72 eV). These findings not only established the predominance of oxygen-containing functional groups in uptake processes but also validated the predictive utility of ESP analysis for identifying preferential adsorption sites. Consequently the research team proposed that biochar materials enriched with carboxyl and carbonyl groups would represent an optimal design strategy for efficient fluoroquinolone (FQ) removal.

Although Liu *et al.*[240] provided comprehensive insights into the role of electron-rich functional groups in enhancing antibiotic removal *via* hydrogen bond formation and π–π stacking interactions, their investigation primarily focused on specific molecular systems and highly tailored material models. This limitation prompted an important scientific question regarding the existence of generalizable principles governing interactions between polycyclic aromatic antibiotics and carbonaceous materials such as biochar or graphene. To address this fundamental question Peng *et al.*[241] developed an innovative combined experimental and DFT simulation approach specifically designed to evaluate the influence of the aromatic ring count in antibiotic structures on their adsorption behavior toward π-rich materials including graphene and biochar. In their investigation, the authors employed DFT modeling to systematically evaluate adsorption energies for a series of π-ring compounds with progressively increasing aromatic ring counts (ranging from benzene to pentacene) on graphene flake surfaces. The computational simulations utilized Gaussian 09 software with the ωB97X-D exchange-correlation functional – a hybrid functional incorporating van der Waals dispersion corrections – paired with the 6-31+G(d,p) basis set, which offers superior accuracy for modeling π-conjugated systems. Following ground-state optimization of all molecular structures, adsorption energies (E_{ads}) were determined using the conventional formula:

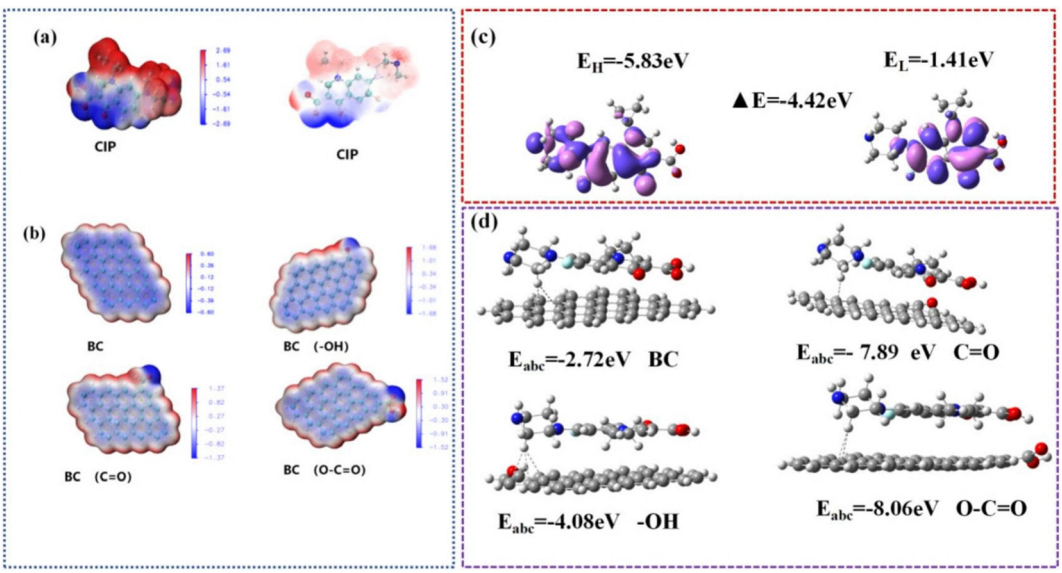

Fig. 11 (a) ESP distribution of CIP, (b) ESP distributions of BC and its functionalized forms (–OH, C═O, and O–C═O), (c) HOMO and LUMO frontier molecular orbitals, and (d) optimized sorption energies and configurations of CIP on biochar with varying oxygen-containing groups (reproduced from ref. 240 with permission from Elsevier, copyright 2025).

Open Access Article. Published on 06 10 2025. Downloaded on 2026-05-13 12:47:34.
This article is licensed under a Creative Commons Attribution-NonCommercial 3.0 Unported Licence.

$$E_{ads} = E_{system} - (E_{adsorbent} + E_{adsorbate}) \quad (6)$$

where E_{system} represents the total post-adsorption energy, $E_{adsorbent}$ denotes the graphene energy, and $E_{adsorbate}$ corresponds to the isolated π-ring molecule energy. Computational results demonstrated a progressive enhancement in E_{ads} values with increasing aromatic ring count: from −14.97 kcal mol^{-1} for benzene to −49.69 kcal mol^{-1} for pentacene. These elevated E_{ads} values signify stronger, more stable adsorption bonds, unequivocally demonstrating the direct proportionality between aromatic ring number and adsorption capacity on π-electron-rich surfaces, thereby highlighting the fundamental importance of π–π stacking interactions. Notably, the benzene E_{ads} value equates to approximately $25k_BT$ at 300 K (roughly triple the hydrogen bond energy between water molecules), confirming that even in the simplest aromatic system, π–π interactions provide sufficient strength to maintain stable adsorption structures under ambient conditions.

Complementing the theoretical modeling, the study conducted parallel experimental adsorption tests using seven antibiotics featuring varying aromatic ring counts (TC, OFL, AMX, SMZ, SDZ, CIP, and SMX). Experimental observations revealed that TC and OFL (both containing four aromatic rings) exhibited the most rapid adsorption kinetics, while SMX and CIP (each with one aromatic ring) showed the slowest uptake rates – findings that precisely mirrored the trends predicted by DFT simulations. Additional confirmation came from fluorescence microscopy imaging, which demonstrated nearly complete FITC model compound quenching on graphene surfaces within 30 min, further corroborating the predominance of π–π adsorption mechanisms. A particularly significant discovery involved the adsorption strength being sufficient to induce localized ''dehydration'' effects, whereby aromatic rings could effectively displace weakly bound water molecules, thereby enhancing both adsorption selectivity and stability in aqueous environments. Through comprehensive analysis of both experimental data and theoretical calculations, the study established that adsorption efficiency depends not only on antibiotic aromatic ring density but also critically on carbon material surface characteristics. High-temperature carbonized biochar (*e.g.*, processed at 1000 °C) with greater aromatic ring density demonstrated markedly enhanced π–π interaction capabilities. Consequently, strategic optimization of pyrolysis temperature and precise control over graphitization degree emerge as crucial parameters for designing biochars with superior selectivity toward conjugated antibiotics. This research exemplifies how DFT modeling can transcend single-interaction simulations to establish quantitative structure-activity relationships between molecular architecture and adsorption performance – achievements that remain challenging to accomplish through purely experimental approaches.

In contrast to the theoretical clarity achieved with ideal materials like graphene, real-world biochars exhibit far greater structural complexity, frequently featuring abundant surface defects, mixed functionalities, and potential for chemical transformation. To bridge the gap between modeling assumptions and actual material behavior, Hu *et al.*[242] explored a more application-relevant system: iron-activated beechwood biochar (Fe-BC-800) for adsorbing sulfonamide antibiotics such as sulfamethazine (SMZ) and sulfamerazine (SMR). Their computational approach employed Materials Studio with the Dmol^3 module, an all-electron quantum simulator particularly suitable for inorganic materials and metal-doped carbon surfaces. The simulations used the GGA-PBE exchange-correlation functional with the DNP basis set and incorporated spin-polarized settings to accurately model unpaired electron states at iron sites. A 20 Å vacuum layer along the *z*-axis eliminated interlayer interactions in the vacuum-state system. After optimizing SMZ and SMR structures *via* the BFGS algorithm, the researchers evaluated adsorption energies using the equation:

$$E_{ads} = E_{SMZ@biochar} - (E_{biochar} + E_{SMZ}) \quad (7)$$

where $E_{SMZ@biochar}$ represents the total adsorption energy, $E_{biochar}$ denotes the functionalized biochar energy, and E_{SMZ} corresponds to the optimized antibiotic energy. Results revealed maximum adsorption energies at –Fe–O (−35.8 kcal mol^{-1}) and –OH (−32.1 kcal mol^{-1}) sites, where SMZ/SMR amino groups acted as proton acceptors forming strong hydrogen bonds with oxygen atoms while aromatic rings maintained parallel orientation to the biochar's π-plane, establishing π–π stacking interactions. The study's key innovation involved density of states (DOS) calculations showing new energy levels near the HOMO region post-adsorption, confirming electron redistribution and chemisorption characteristics. Electrostatic potential (ESP) mapping further identified electron-rich regions at oxygen and iron functional groups, which served as electron traps for positively charged antibiotic moieties. These analyses demonstrated iron's dual role as both an oxidation catalyst and a surface polarization enhancer, strengthening biochar's interaction with charged antibiotic functional groups. Beyond proving Fe-functionalized biochar's efficacy for sulfonamide adsorption, this work established DFT's utility for simulating electron density changes at functionalized sites – a crucial factor determining real-world material performance. This approach proves particularly valuable for complex wastewater treatment scenarios where adsorption mechanisms transition from purely physical to electronically activated processes requiring quantum-level understanding.

While existing research has demonstrated the potential of designed and functionalized biochar for optimizing aromatic antibiotic adsorption through hydrogen bond formation and π–π stacking mechanisms, a critical gap remains in understanding how environmental conditions – particularly pH – influence the electronic nature of adsorption processes. In real wastewater systems, pH variations simultaneously alter antibiotic ionization states and biochar surface protonation levels, dramatically modifying electronic interaction capacities. Addressing this knowledge gap, Li *et al.*[243] employed DFT modeling to examine how different functional groups (–COOH, –OH, and π-ring) on corncob biochar influence SMX adsorption under alkaline conditions where SMX primarily exists in anionic form, favoring ionic/π-bond formation with electropositive

© 2025 The Author(s). Published by the Royal Society of Chemistry

Open Access Article. Published on 06 10 2025. Downloaded on 2026-05-13 12:47:34.
This article is licensed under a Creative Commons Attribution-NonCommercial 3.0 Unported Licence.

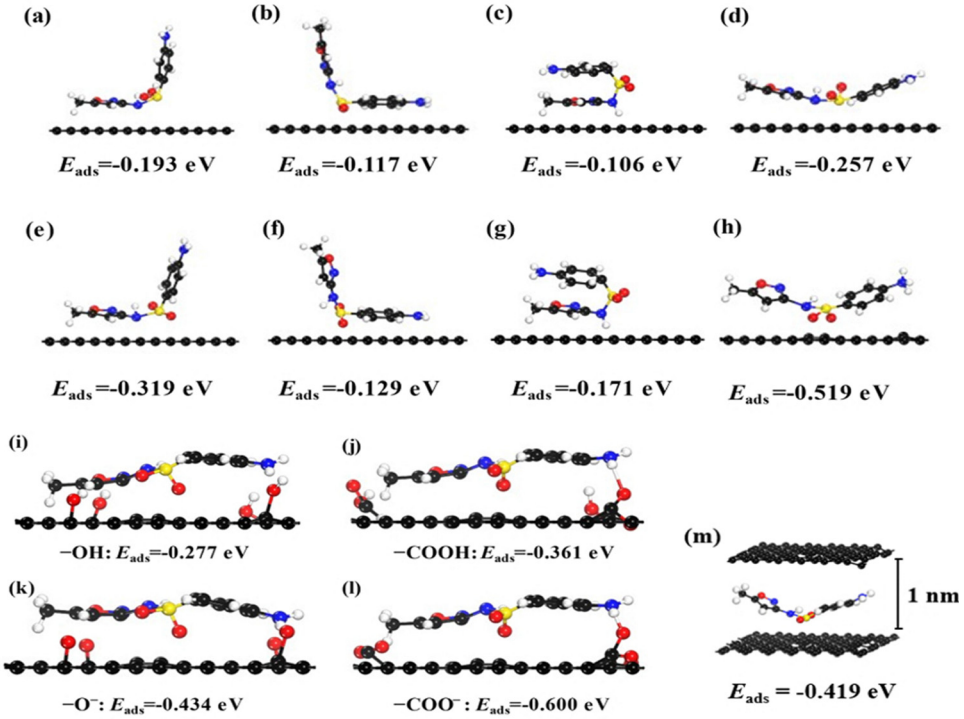

Fig. 12 Equilibrium adsorption structures and corresponding elimination energies of SMX on biochar. (a)–(d) Different adsorption configurations between neutral SMX and biochar; (e)–(h) various binding modes of the protonated SMX^+ with biochar; (i)–(l) interactions of deprotonated SMX^- with –OH/–COOH functionalized biochar; (m) a sandwich-like configuration involving biochar–SMX–biochar assembly (reproduced from ref. 243 with permission from Elsevier, copyright 2023).

surface sites (Fig. 12). Their simplified yet chemically representative model featured common functional groups on a monolayer graphene substrate. Calculations were performed using Gaussian 09 with the B3LYP functional and 6-31+G(d,p) basis set. Following geometric optimization of SMX-biochar interaction structures, adsorption energies were measured utilizing standard formulations:

$$E_{ads} = E_{SMX@biochar} - (E_{biochar} + E_{SMX}) \quad (8)$$

Results revealed that at pH ∼ 9.5, the $–COO^-$ group exhibited the strongest adsorption influence (−34.2 kcal mol^{-1}), significantly outperforming −OH (−18.6 kcal mol^{-1}) and neutral π-ring (−21.9 kcal mol^{-1}) groups. This phenomenon stems from dual proton loss: SMX loses sulfonamide amine protons to become anionic while biochar's –COOH groups deprotonate to form $–COO^-$, increasing surface negative charge density. The DFT results further support the above finding, showing that the uptake energy (E_{ads}) of $–COO^-$ reaches −0.600 eV, significantly higher than that of –OH (−0.277 eV) or –COOH (−0.361 eV). This indicates that the $–COO^-$ group not only acts as a strong negative charge center but also forms strong coordination hydrogen bonds with electron-rich regions on SMX, particularly the isoxazole cyclic amine group. Remarkably, adsorption still proceeds *via* coordinated electronic mechanisms, primarily *via* π–π EDA interactions and hydrogen bond formation at biochar's electron-rich regions. Multiwfn-generated electrostatic surface potential (ESP) maps clearly visualized this charge redistribution, showing strong polarization at $–COO^-$ and π-electron regions that serve as dominant adsorption sites for SMX's positively charged moieties, particularly the isoxazole ring amine group. The differential charge density map in the DFT simulation further elucidates the electron donor–acceptor forces that occur between SMX and biochar. Yellow regions on SMX indicate electron-accepting sites, whereas blue regions on biochar correspond to electron-donating areas, underscoring the critical role of π–π EDA interactions in the elimination process. Notably, among the tested configurations, the planar arrangement of SMX, where the two aromatic rings are aligned, exhibits a significantly higher adsorption energy compared to orthogonal or V-shaped configurations. Specifically, the planar configuration yields an E_{ads} value of −0.257 eV, demonstrating that optimal alignment for π–π interactions is the key determinant of adsorption efficiency. The study further demonstrated pH's profound impact on the system's frontier molecular orbitals. Under acidic conditions, a large HOMO–LUMO gap between SMX and biochar corresponded to weak interactions. Alkaline conditions caused SMX's HOMO to shift upward and biochar's LUMO downward, reducing ΔE and enhancing electron donor–acceptor capabilities – the key driver of improved EDA-mediated adsorption. The theoretical basis also demonstrates that at high pH levels, the anionic state of SMX and biochar leads to an improvement in the HOMO of SMX and a decline in the LUMO of biochar. This arrangement reduces ΔE

Open Access Article. Published on 06 10 2025. Downloaded on 2026-05-13 12:47:34.
This article is licensed under a Creative Commons Attribution-NonCommercial 3.0 Unported Licence.

and enhances the likelihood of electron exchange, explaining why adsorption is more effective under alkaline conditions. This pH-dependent electronic structure modulation suggests that wastewater treatment optimization could be achieved through operational pH adjustment rather than relying solely on material properties. These DFT-derived insights not only elucidate biochar functional group roles but also establish that electronic interaction capacities are environmentally dependent, particularly on pH. Moreover, a slit-like pore biochar model composed of two parallel graphene layers (~1 nm spacing) was employed to simulate the 'pore-filling' effect. The model exhibited an adsorption energy of −0.419 eV, surpassing that of neutral π–π interactions but remaining weaker than π^{+}–π or (C)AHB interactions. These findings highlight the significant role of pores in the adsorption mechanism, particularly under neutral pH conditions or in systems with limited active functional groups. Consequently, optimal antibiotic adsorption requires simultaneous consideration of material design and physicochemical operating conditions – significantly expanding practical application potential. This work powerfully illustrates DFT's dual utility as both a fundamental interaction probe and a predictive tool for adsorption behavior under variable conditions, offering insights beyond the reach of purely experimental approaches.

Research by Li *et al.* demonstrates that environmental factors such as pH can alter charge redistribution during antibiotic adsorption on biochar. However, real-world wastewater from hospitals, agriculture, and industry presents a more complex challenge, as it typically contains mixtures of antibiotics, heavy metals, and other pollutants. These complex systems can alter pollutant molecular structures through ligand effects and also affect the electronic characteristics of the material. Within this framework, the study by Zhao *et al.*[244] provides a critical connection between single-compound adsorption research and real-world environments by using DFT modeling to investigate the simultaneous adsorption of antibiotics such as oxytetracycline, sulfamethazine and amoxicillin with metal ions like Zn^{2+} and Cu^{2+} on biochar derived from rice straw activated at 700 to 800 °C. The authors used DFT to examine the role of functional groups with oxygen atoms on biochar, including carboxyl, carbonyl, and hdroxyl groups, in forming ligand bonds with both antibiotic and metal species (Fig. 13). Calculations were carried out in Gaussian 16 software using the B3LYP functional, which offers a balance between accuracy and computational cost, along with the 6-31+G(d,p) basis set for light atoms and LANL2DZ for metals. The model system consisted of a biochar cluster bearing optimized functional groups, which were allowed to interact with antibiotics in the presence or absence of metal ions. Adsorption energy was determined using the extended equation for a three-component system:

$$E_{ads} = E_{complex} - (E_{biochar} + E_{antibiotic} + E_{metal\ ion}) \quad (9)$$

where $E_{complex}$ is the total energy of the combined system and the other terms represent individual component energies. The results indicated that adding Zn^{2+} or Cu^{2+} significantly enhanced adsorption energy compared to metal-free systems. For example, the adsorption energy of sulfamethazine on –COOH modified biochar was −28.4 kcal mol^{-1} and increased to 42.7 kcal mol^{-1} in the presence of Cu^{2+}. This enhancement is attributed to a dual-site ligand mechanism in which the metal ion bridges the carboxyl group on biochar and the amino or phenolic site on the antibiotic, forming a stable five or six-membered chelate ring. Additionally, HOMO and LUMO

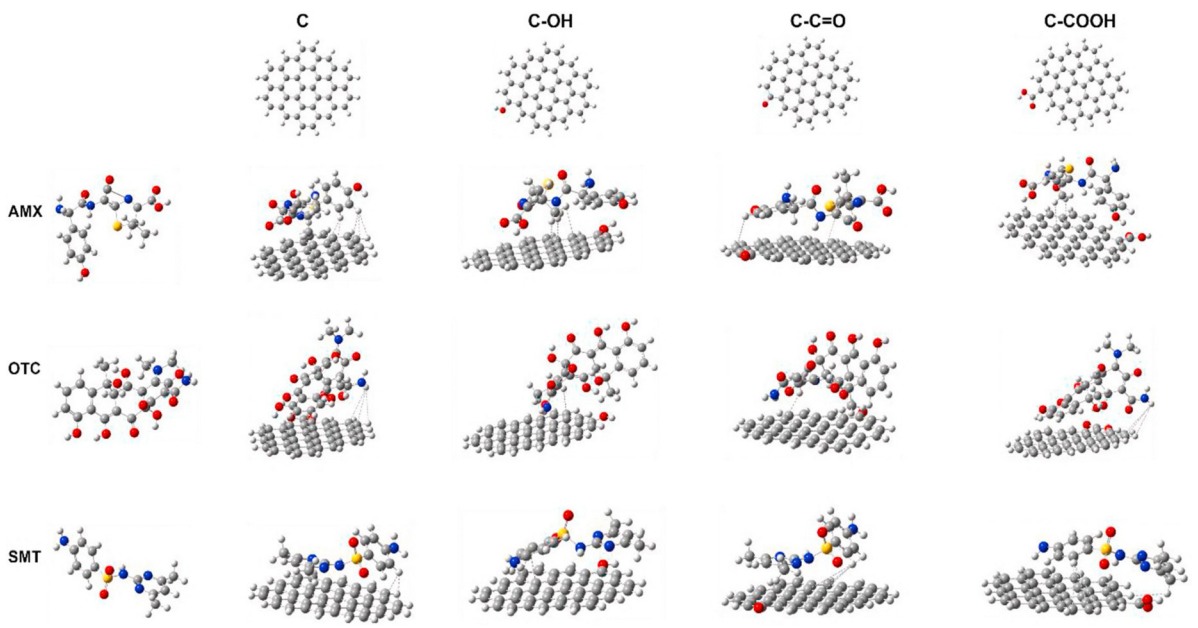

Fig. 13 The interaction geometries between antibiotics (such as AMX, OTC, and SMT) and biochar (reproduced from ref. 244 with permission from Elsevier, copyright 2023).

© 2025 The Author(s). Published by the Royal Society of Chemistry

Open Access Article. Published on 06 10 2025. Downloaded on 2026-05-13 12:47:34.
This article is licensed under a Creative Commons Attribution-NonCommercial 3.0 Unported Licence.

simulations revealed that the HOMO energy level of the antibiotic shifted closer to the LUMO of biochar after ligand formation, suggesting favorable electron transfer from the antibiotic to the adsorbent.

When metal ions were introduced, the LUMO level of the system decreased further, reflecting enhanced electron-accepting capacity consistent with the role of Zn^{2+} and Cu^{2+} as central acceptors in coordinate bonding. The electrostatic potential map showed negative charge localization around carboxylate and carbonyl oxygen atoms on biochar while Zn^{2+} held a positive charge at the center, which strengthened electrostatic attraction and ligand coordination. One important result of this investigation is the comparison of different functional groups on biochar. DFT results demonstrated that the carboxyl group formed the strongest interaction with both the antibiotic and the metal ion, followed by hydroxyl and then non-activated carbonyl groups. These theoretical results align with experimental data obtained from XPS and FTIR, confirming the dominant role of the carboxyl center in resonance-based adsorption. Moreover, all adsorption energies in the biochar–antibiotic–metal ion complexes exceeded -40 kcal mol^{-1}, surpassing the threshold for physical adsorption and indicating a stable chemisorption process. Zhao *et al.*'s study advances the understanding of multicomponent pollutant systems and shows that interactions between antibiotics and metal ions can enhance overall adsorption performance, a phenomenon often difficult to observe through conventional experiments. DFT proves essential in modeling electron states and ligand structures as well as in quantifying binding energies, thereby offering insights with real-world significance. Therefore, DFT is no longer just a complementary method but serves as a central tool in the design and evaluation of biochar adsorbents for environmental decontamination where adsorption processes are increasingly complex.

3.3. Mechanism

Antibiotic contaminants in water attach to surfaces *via* chemical or physical interaction processes. Physical adsorption, which occurs less frequently, takes place when less polar antibiotics associate with nonpolar sorbents including carbon nanotubes or minerals. The performance of this technique depends on the adsorbent's surface area.[245] Chemical or interactive adsorption is more common because antibiotics have vacant sites including functional groups and electrostatic regions containing atoms like nitrogen, sulfur, or oxygen.[246] Several interactions including van der hydrogen bond formation, Waals forces, and electrostatic attraction contribute to the isolation of these substances.[247] Biochar facilitates the adsorption of antibiotics through mechanisms like surface complexation, hydrophobic effects, pore filling, π–π interactions, electrostatic forces, hydrogen bond formation, and ion pair formation.[248,249] Recent studies have pointed out that these mechanisms often act concurrently and are largely dependent on the type of biomass used, the pyrolysis conditions, and subsequent surface functionalization.[250,251] Notably, the combined contributions of pore filling, electrostatic attraction, and π–π interactions have been identified as the principal routes governing antibiotic adsorption onto biochar.[252]

3.3.1. Surface complexation. Antibiotics and DNA can form complexes with metal species both in solution and on the biochar's interface, which promotes uptake capacity and is considered a form of ligand exchange.[253] Multiple investigations have shown that the occurrence of metal species in solution enhances the removal of TC by forming metal ion–TC complexes.[227] In addition, metal species can bind with phosphate groups in DNA to form inner sphere complexes, which reduce electrostatic repulsive forces between DNA and make them easier to adsorb onto the surface or into the pores of biochar as compact structures.[229] Many recent studies have shown that oxygen-containing functional groups, such as carboxyl (–COOH) and hydroxyl (–OH) groups, on the biochar surface can coordinate with soluble cations (*e.g.*, Fe^{2+}, Ca^{2+}, or Zn^{2+}).[254–256] This coordination facilitates the formation of stable intragranular complexes with antibiotic molecules. For instance, Li *et al.* (2022) demonstrated that Ca^{2+} can act as a cation bridge between tetracycline molecules and the carboxyl groups of biochar, which significantly enhances adsorption efficiency through a complexation mechanism.[257] Recent reviews underscore that biochar modified with metal ions or rich in iron oxides often demonstrates enhanced antibiotic adsorption efficiency. This is primarily attributed to a strengthened complexation mechanism, which is particularly effective in slightly acidic environments where complexation with antibiotic functional groups is favored.[258] Complexation occurring on the material surface plays an important role in this process, particularly for modified biochar. Wei *et al.*[259] showed that iron-containing phases such as Fe–O and Fe–OOH in sludge-derived biochar can form complexes with TC, thereby improving treatment efficiency.

3.3.2. Electrostatic forces and charge regulation. The ionization of pollutants such as antibiotics in solution is strongly influenced by pH and the electrostatic repulsive forces between them and the material's surface. This also affects the interface properties of the material.[210,260] The pH zero charge point (pH_{pzc}) values of two biochars introduced by Qing Ge *et al.*[261] and Alsaiari *et al.*,[262] including KOH modified bamboo biochar and MOF grafted magnetic biochar, were 6.68 and 5.76, respectively. In cases where the environment has a pH value less than the pH_{pzc}, the surface of APB and PB is positively charged, which facilitates the elimination of negatively charged pollutants. For example, the CIP molecule exists primarily as a cation at pH less than 6.16, an amphoteric form between pH 6.16 and 8.74, and an anion at pH greater than 8.74.[263] DNA could also be sorbed onto biochar *via* electrostatic repulsive forces, as discovered by Wu *et al.* (2022a)[213] and Lian *et al.* (2020).[264] DNA has an isoelectric point at around pH 5.0. At pH values below this point, the functional groups on DNA are protonated, making it positively charged. In contrast, the biochar surface is generally negatively charged at pH values above 3.0. Therefore, at pH around 4.0, both DNA and biochar have a lower negative charge, reducing electrostatic repulsion and enhancing adsorption capacity.[229,265]

Open Access Article. Published on 06 10 2025. Downloaded on 2026-05-13 12:47:34.
This article is licensed under a Creative Commons Attribution-NonCommercial 3.0 Unported Licence.

In addition, the salt bridges formed *via* cations such as metal cations can act as a bridge between biochar and antibiotics. The biochar's surface features negatively charged OH and COOH groups, while the sulfonic acid groups on antibiotics are also negatively charged, resulting in electrostatic repulsion.[266] However, cations in solution can reduce this repulsion and enhance the adsorption interaction by acting as salt bridge mediators. Li *et al.* (2025) demonstrated that the presence of dissolved cations (Ca^{2+} and Zn^{2+}) can act as a cation bridge, which mitigates electrostatic repulsion and thus enhances the adsorption capacity.[267] Zhang *et al.* (2023) also pointed out that the formation of a salt bridge between the sulfonic group of antibiotics and the –COOH/–OH group on biochar *via* metal ions is an important factor in stabilizing the adsorption complex.[268] Fang *et al.*[265] demonstrated this using zeta potential and FTIR spectra. As the cation concentration increased, the zeta potential of biochar decreased significantly, reflecting the weakening of electrostatic repulsion. Simultaneously, the FTIR analysis revealed that the absorption band related to the C–OH group of biochar became broader in the presence of metal cations, confirming the formation of a salt bridge between metal cations and polar functional groups of antibiotics.

3.3.3. Ion exchange. The ion exchange mechanism in the attachment of antibiotics onto biochar and its decorated variants is a key process that contributes to enhancing the efficiency of removing trace pollutants from aquatic environments, particularly antibiotics.[269,270] Biochar materials that are generated *via* the pyrolysis of organic biomass under anaerobic conditions typically contain inorganic cations such as potassium, magnesium, sodium, and calcium as well as sometimes anions such as chloride, nitrate, or phosphate, depending on the feedstock and pyrolysis conditions.[271] These ions are mainly present as loosely bound species on the material surface or embedded within the pore network and capillary structure of the biochar, enabling them to exchange readily with other ions in the solution, including ionizable functional groups from antibiotic molecules. In modified biochar, which is functionalized with acids such as H_2SO_4 or HCl, bases such as KOH or NaOH or with materials containing specific functional groups like carboxyl, hydroxyl, sulfonic, or amine groups, the ion exchange capacity is significantly improved due to the introduction of more active sites with higher charge density and increased structural flexibility.[272] Experimental studies have confirmed this mechanism. For instance, Premarathna *et al.*[273] utilized clay minerals to decorate biochar and observed that cations located between clay layers could be readily exchanged with positively charged ions in solution, thereby enhancing the adsorption process. Likewise, Guo *et al.*[272] found that under acidic conditions, tylosin, a positively charged antibiotic molecule at pH below 7, was effectively adsorbed onto biochar modified with goethite through both cation exchange and electrostatic interactions. Another work by Li *et al.*[274] demonstrated that the positively charged piperazine rings of CIP interacted with ion exchange sites on the biochar surface, confirming the contribution of ion exchange under neutral to mildly acidic pH conditions. This ion exchange mechanism depends not only on the charge characteristics of the antibiotic and the environmental pH, but also on the buffering capacity, ionic strength, the occurrence of competing ions, and the molecular structure of both the sorbate and the adsorbent. Thus, understanding the ionic composition of biochar and the nature of charge interactions between its antibiotic molecules and functional groups provides an essential scientific foundation for designing highly efficient adsorbent materials and optimizing operating conditions for the treatment of antibiotic-contaminated water.[275]

3.3.4. Pore confinement and diffusion mechanisms. The pore confinement and diffusion mechanisms in the attachment of antibiotics onto biochar and its decorated variants are essential physical processes that control the accessibility, transport, and ultimate retention of antibiotic molecules in the pore network of the adsorbent. Biochar typically possesses a hierarchical pore structure consisting of mesopores (between 2 and 50 nm), macropores (greater than 50 nm), and micropores (less than 2 nm),[276] which are formed during the pyrolysis of organic biomass in an anaerobic or a hypoxic environment. The distribution, volume, and connectivity of this pore system are strongly influenced by the composition of the precursor, the temperature of pyrolysis, and the post-treatment modification methods.[277] In addition, metal ions (Ca^{2+} and Mg^{2+}) or charged functional groups (COO^- and NH_3^+) on the porous interface of biochar facilitate the combination of electrostatic forces and confined steric interactions, thereby enhancing the retention of appropriately sized antibiotic molecules.[278] Antibiotic molecules, depending on their size, shape, and hydration radius, can penetrate into various types of capillaries to different extents. Among these, micropores play a key role in providing large surface areas and high-energy adsorption sites, while mesopores and macropores facilitate the transport of molecules by reducing diffusion resistance and shortening the time required to reach the active sites.[279] Modified biochars, especially those that are chemically or physically activated, often exhibit larger surface areas, increased capillary volumes, and more favorable pore size distributions, which enhance the accessibility of antibiotic molecules to adsorption sites.

Molecular entrapment occurs when antibiotic molecules become confined within narrow capillaries, thereby strengthening physical interactions including hydrogen bond formation, van der Waals forces or pi–pi interactions due to the close proximity between the capillary walls and the molecules. This spatial confinement extends the retention time of antibiotics within the pore structure, thus improving the adsorption efficiency. For example, Guo *et al.*[279] discovered that CIP molecules could enter the mesoporous system of biochar derived from fish scales and were stabilized through multiple simultaneous interactions within the confined capillary space, significantly enhancing adsorption efficiency. Similarly, Feng *et al.*[280] reported that NOR was effectively adsorbed in the microporous region of loofah-derived biochar, where geometric constraints and limited diffusion played a critical role in increasing both selectivity and retention of antibiotic molecules. Furthermore, the diffusion process of antibiotics into the

© 2025 The Author(s). Published by the Royal Society of Chemistry

Open Access Article. Published on 06 10 2025. Downloaded on 2026-05-13 12:47:34.
This article is licensed under a Creative Commons Attribution-NonCommercial 3.0 Unported Licence.

biochar structure comprises several stages, including diffusion across the external film of the adsorbent, internal particle diffusion, and diffusion within the capillary system, all of which are affected by the physicochemical characteristics of both the material and the antibiotics. The interaction between pore-based molecular confinement and diffusion mechanisms becomes particularly significant at low pollutant concentrations, where steric effects and slow transport rates enhance apparent adsorption performance. However, at higher concentrations of pollutants or in the presence of competing substances, capillary blockage and limited diffusion can reduce adsorption efficiency. Therefore, understanding the pore architecture and the kinetics of diffusion is fundamental for optimizing the design of biochar-based adsorbents. This knowledge supports the development of materials with tailored pore systems and surface functionalities to maximize transport, retention, and molecular interactions with antibiotics, ultimately improving the treatment of micropolluted water.

3.3.5. π–π electron donor–acceptor interactions. π–π stacking is a non-covalent, weak intermolecular interaction that is of vital importance in the elimination mechanisms of aromatic contaminants, particularly through interactions between electron-rich and electron-deficient aromatic systems. On the surface of biochar, functional moieties such as carboxyl, nitro, and ketone groups frequently function as π-electron acceptors, facilitating π–π electron donor–acceptor (EDA) interactions with aromatic pollutants. For example, in the work by Yan *et al.*,[281] biochar fabricated from barley straw *via* phosphoric acid impregnation and microwave treatment exhibited distinct π–π and n–π interactions between its surface carboxyl groups and the aromatic rings of NOR. These interactions were evidenced through C and O K-edge X-ray absorption near-edge structure (XANES) spectroscopy, underscoring the pivotal role of EDA mechanisms in the adsorption process. Similarly, Chen *et al.*[282] demonstrated that TC can be effectively eliminated by 3D PPY/CMC aerogels, where adsorption was primarily governed by π–π EDA interactions in both sandwich and parallel-displaced configurations. This was supported by density functional theory (DFT) calculations and frontier orbital theory, revealing that these interactions contributed to high uptake performance across a broad pH range. Furthermore, Li *et al.*[283] reported that biochar activated with phosphoric acid exhibited a significant enhancement in the proportion of π–π interactions from 35 to 48% at pH 2 which was accompanied by an increase in oxygenated functional groups (notably –COOH), thereby improving SMX adsorption efficiency. Collectively, these findings highlight the positive correlation between the density of oxygen-containing functional groups on biochar surfaces and the strength of π–π EDA interactions, which in turn enhances the sorption capacity for aromatic pollutants. Moreover, physicochemical parameters such as pyrolysis temperature, carbonization degree, and surface modification strategies influence the π-electron distribution on the carbon framework. Typically, biochar prepared at temperatures below 500 °C tends to behave as a π-electron acceptor, whereas materials produced above 500 °C often exhibit π-electron donor characteristics due to the formation of more electron-rich conjugated domains.[2] Thus, the optimization of thermal processing conditions and surface chemistry is essential for tailoring the electron-donating or -accepting behavior of biochar, and ultimately for maximizing adsorption performance *via* π–π electron donor–acceptor mechanisms.

4. Comparison of various biochar-derived adsorbents

The comparison of the adsorption capacity of various biochar types for different antibiotics reveals a significant diversity in efficiency (q_{max}) (Table 3), which depends on the origin of the raw material, the modification method, and the surface structure of the biochar. Traditional biochar adsorbents such as those derived from sewage sludge, bagasse, bamboo, banana peel, or wood often exhibit low to medium adsorption capacities, typically ranging from 7.91 to 120 mg g^{-1}. For instance, biochar from sewage sludge adsorbed only 8.69 mg g^{-1} of NOR,[258] while biochar produced from bagasse adsorbed 105 mg g^{-1} CIP.[269] Some chemically activated or specially modified biochars, such as those made from cow dung, rice husks, or sunflower seed husks, revealed a clear improvement in uptake capability. As an example, H_3PO_4-activated sunflower seed husk biochar achieved an uptake amount of 429.3 mg g^{-1} for TC.[277]

A key highlight of this review is the superior performance of highly modified biochars, especially those doped with heteroatoms or nanomaterials. For example, $MnCl_2$-impregnated biochar reached 534 mg g^{-1},[279] while N,S co-doped biochar achieved an outstanding 1490.10 mg g^{-1} for TC.[286] These results suggest that the incorporation of heteroatoms such as nitrogen, sulfur, or transition metals can create highly active surface sites, while also altering the electronic structure, surface area, and functional group density, all of which play essential roles in the adsorption mechanism. Particularly, graphitic biochars such as porous graphitic biochar (1122.20 mg g^{-1})[283] and N-doped graphitic biochar (1377.83 mg g^{-1} for SMX and 1070.40 mg g^{-1} for CIP)[284] exhibit far greater adsorption efficiencies compared to conventional biochars due to their enhanced conductivity, high porosity, and strong π–π interactions with the aromatic structures of antibiotics.

Current research trends focus on developing hybrid or advanced functionalized adsorbents, including metal-doped biochars (Fe/N, Mg/Fe, K-FeO_4), biochars combined with nanomaterials (such as g-MoS_2 or hydroxyapatite), and biochars derived from unique organic sources like traditional Chinese medicine residues, dye waste, or agricultural by-products rich in functional groups. These materials not only enhance adsorption performance but also offer promising potential for reuse and practical applications. For example, biochars derived from dyeing sludge or other functionalized sources can reach adsorption capacities exceeding 1000 mg g^{-1},[281,282] making them highly attractive for treating heavily polluted wastewater.

Based on the summarized data, it becomes obvious that biochar adsorption performance depends closely on three main factors. The first is the type of antibiotic, particularly those with

Open Access Article. Published on 06 10 2025. Downloaded on 2026-05-13 12:47:34.
This article is licensed under a Creative Commons Attribution-NonCommercial 3.0 Unported Licence.

Table 3 Adsorption capabilities of various biochar-derived adsorbents

Adsorbents	Antibiotics	q_{max} (mg g^{-1})	Ref.
Fe oxide/biochar	Macrolide	7.91	284
Sludge-derived biochar	NOR	8.69	285
Chitosan–biochar composite	SMX	14.73	286
Ball milled biochar	Sulfapyridine	57.90	287
HNO_3-modifitied biochar	Sulfonamides	40.00	288
N-doped magnetic biochar	SMX	42.90	289
Bamboo biochar	FQ	45.88	290
H_3PO_4-activated cow dung biochar	CIP	53.89	291
Fe/N grafted biochar	CIP	46.45	292
Alkali-modified biochar	BPA	71.43	260
B6-upgraded biochar	TC	76.92	293
Wood biochar	TCH	84.54	294
$MgFe_2O_4$-magnetic biochar	SMX	50.75	295
	TC	120.36	
Bagasse biochar	CIP	105	296
Metal doped-sewage sludge biochar	AMX	109.89	297
	TC	123.35	
	SMX	99.01	
Banana peel-based biochar	Doxycycline (DO)	113.60	298
Coffee ground biochar	TC	113.64	226
Co-gadolinium modified biochar	TC	119.05	188
Hydroxyapatite modified biochar	Tylosin	135.13	299
Herbal medicine residue-based biochar	TC	188.70	300
	OTC	129.90	
	Chlortetracycline	200.00	
H_3PO_4 activated-biochar	SMX	191.00	283
g-MoS_2 decorated biochar	TCH	245.49	301
$NiFe_2O_4$/biochar	TC	420.41	302
Rice straw biochar	CIP	131.58	303
	DO	432.90	
H_3PO_4-activated sunflower seed husk biochar	CIP	361.6	304
	Ibuprofen	251.1	
	SMX	251.3	
	TC	429.3	
K_2FeO_4 modified biochar	CIP	434.78	305
$MnCl_2$-impregnated biochar	TC	534.00	306
Caulis spatholobi biochar	TC	830.78	307
Functionalized-biochar	TC	835.70	308
Dyeing sludge-derived biochar	TC	1081.30	309
Porous graphitic biochar	TC	1122.20	310
N-doped graphitic biochar	SMX	1377.83	311
	CIP	1070.40	
Corncob xylose residue-based biochar	SMX	1429	312
N,S co-doped biochar	TC	1480.10	313

aromatic rings or hydroxyl and amino groups that form hydrogen bonds and π–π interactions. The second involves the structure and composition of the biochar including surface area, functional group content, and the extent of modification. The third relates to the processing and activation techniques such as metal impregnation, heteroatom doping, acid or base treatment, or pyrolysis at high temperatures to increase conductivity and surface area. These insights suggest that future studies should prioritize designing multifunctional biochars with highly porous architectures, abundant heteroatoms, and regenerative features to meet the increasingly complex demands of real-world wastewater treatment.

5. Challenges and future directions for biochar-based material utilization

While biochar is increasingly recognized as a versatile material in fields ranging from soil remediation and pollution adsorption to advanced technologies, there remain considerable challenges in achieving its large-scale practical applications. One major issue lies in the heterogeneity of feedstock sources and pyrolysis conditions, which causes variations in microporous structure, chemical composition, and biomechanical properties.[314] These factors directly influence the adsorption efficiency, electrical conductivity, and mechanical strength of the final material. Recent comprehensive reviews indicate that the absence of standardized indicators for properties such as functional group content, porosity, conductivity, and H/C to O/C ratios has delayed the rational design of biochar for specific uses. Nevertheless, this gap also opens new research opportunities. Scientists are now developing molecular-level models of biochar using computer simulations based on experimental data. These models allow for the creation of materials with controlled porosity and surface chemistry, optimized for applications such as pollutant adsorption, electrical conduction, and structural performance. When integrated with

 © 2025 The Author(s). Published by the Royal Society of Chemistry

Open Access Article. Published on 06 10 2025. Downloaded on 2026-05-13 12:47:34.
This article is licensed under a Creative Commons Attribution-NonCommercial 3.0 Unported Licence.

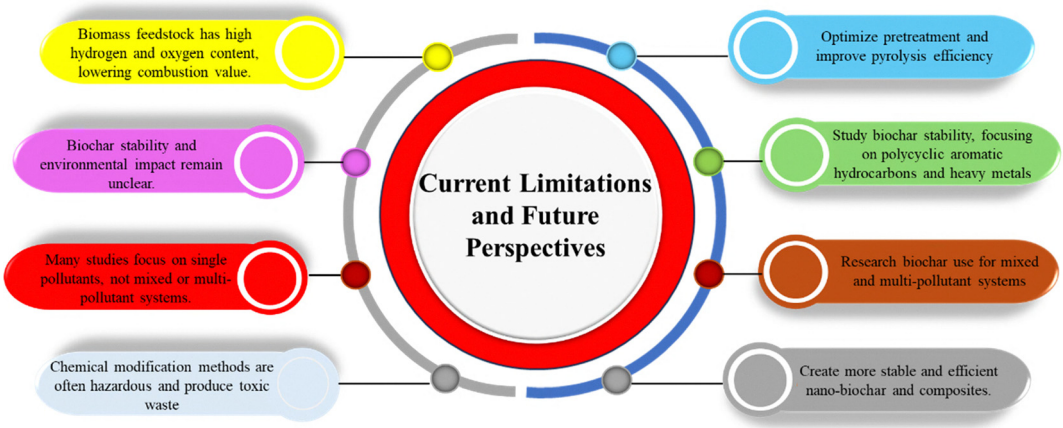

Fig. 14 Current limitations and future perspecitves of biochar.

multi-criteria decision analysis (MCDA), these models help identify optimal production conditions tailored for specific sectors, including agriculture, environmental management, construction, and energy. Another critical challenge is the potential presence of residual pollutants such as phenolic compounds, polycyclic aromatic hydrocarbons (PAHs), or metal species.[315] This risk is especially high when using untreated waste feedstocks or operating under low-temperature pyrolysis. To minimize environmental impact, it is necessary to integrate a comprehensive risk assessment process, standardize production protocols in accordance with international frameworks such as IBI, and employ pyrolysis equipment with precise control over temperature and residence time. Another commonly overlooked limitation is that chemical modification methods of biochar such as impregnation with strong acids, bases, or transition metals can enhance surface activity and adsorption capacity, yet also carry the risk of generating toxic and hard-to-manage waste. This underscores the need to develop safer, greener, and more environmentally sustainable modification approaches.

In terms of real-world applications, biochar has demonstrated broad potential (Fig. 14). It has been used in environmentally friendly concrete and construction materials to improve mechanical strength, enhance durability, and reduce cement usage. Its multi-porous structure and surface functional groups have also enabled the development of soundproofing and waterproofing solutions, as well as green electronic components like electrodes for supercapacitors and microbial fuel cells. Emerging directions include research into using biochar in CO_2-reducing cores for abandoned oil and gas wells, leveraging its long-term carbon sequestration potential and energy efficiency. Looking ahead, three essential directions should be prioritized:

• Standardization and quality control: develop a set of key indicators such as porosity, H/C–O/C ratio, particle size, and surface functionality tailored to each biochar application (*e.g.*, water treatment, soil improvement, electrodes, or building materials). Establish systems to assess performance under long-term field conditions.

• Integration of fabrication, modeling, and experimentation: use molecular simulation and MCDA to design application-specific biochar. Strengthen pilot-scale testing to evaluate real-time adsorption capacity, electrical conductivity, and interactions in systems like concrete, electronic materials or agricultural ecosystems.[316]

• Expansion into non-traditional applications: transfer biochar technologies into advanced material domains such as energy storage electrodes, biodegradable conveyor systems or corrosion-resistant carbon cores. Special attention should be given to its potential role in the circular economy through recycled composites, bio-based additives or emission-neutralizing systems in heavy industry.

6. Conclusion

In the context of increasingly severe antibiotic pollution and the limitations of conventional treatment methods, biochar has emerged as a promising adsorbent material due to its porous structure, low cost, and environmental compatibility. This review has systematically summarized the advances in biochar research, covering raw material selection, fabrication methods, and modification strategies including chemical activation, electrochemical treatment, plasma processing, and atomic doping. Notably, advanced modification techniques have greatly enhanced the efficiency of antibiotic adsorption by improving surface area, increasing the density of functional groups, and strengthening molecular interactions. The integration of quantum computational tools, particularly density functional theory (DFT), has provided insights into adsorption mechanisms at the atomic level and offered a new approach for designing optimized biochar materials. Furthermore, the combination of biochar with emerging materials such as MOFs and MXenes is identified as a promising direction, especially in improving selectivity and efficiency for the sustainable removal of antibiotic compounds. Despite these developments, several challenges remain including the practical applicability, long-term stability, and environmental safety of the spent adsorbents. Future research should therefore focus on optimizing

Open Access Article. Published on 06 10 2025. Downloaded on 2026-05-13 12:47:34.
This article is licensed under a Creative Commons Attribution-NonCommercial 3.0 Unported Licence.

material structures, expanding the use of quantum mechanical modeling, and conducting pilot-scale experiments to develop more effective and sustainable wastewater treatment solutions.

Declaration of generative AI and AI-assisted technologies in the writing process

During the preparation of this manuscript, the authors used ChatGPT to polish the English language of the manuscript, without changing the content. The authors take full responsibility for the content of the publication.

Author contributions

Van Doan Nguyen: conceptualization (supporting), formal analysis (lead), investigation (equal), writing – original draft (equal); The Anh Luu: data curation (lead), formal analysis (equal), investigation (equal), writing – original draft (equal); Guo-Ping Chang-Chien: validation (supporting), writing – review and editing (supporting); Van Giang Le: conceptualization (lead), funding acquisition (lead), project administration (lead), supervision (lead), writing – review and editing (lead).

Conflicts of interest

The authors declare that they have no known competing financial interests or personal relationships that could have appeared to influence the work reported in this paper.

Data availability

Data for this study, including figures and tables, are available within the article.

Acknowledgements

We are grateful for the insightful comments of Prof. Dr. Ruyean Doong on the manuscript. We also thank the editors and anonymous reviewers for their helpful comments and suggestions.

References

1 Y. Zhao, X. Li, Y. Li, H. Bao, J. Xing, Y. Zhu, J. Nan and G. Xu, Biochar Acts as an Emerging Soil Amendment and Its Potential Ecological Risks: A Review, *Energies*, 2023, **16**(1), 410.
2 Y. Dai, N. Zhang, C. Xing, Q. Cui and Q. Sun, The adsorption, regeneration and engineering applications of biochar for removal organic pollutants: a review, *Chemosphere*, 2019, **223**, 12–27.
3 J. S. Cha, S. H. Park, S.-C. Jung, C. Ryu, J.-K. Jeon, M.-C. Shin and Y.-K. Park, Production and utilization of biochar: a review, *J. Ind. Eng. Chem.*, 2016, **40**, 1–15.
4 Y. X. Seow, Y. H. Tan, N. M. Mubarak, J. Kansedo, M. Khalid, M. L. Ibrahim and M. Ghasemi, A review on biochar production from different biomass wastes by recent carbonization technologies and its sustainable applications, *J. Environ. Chem. Eng.*, 2022, **10**(1), 107017.
5 S. Pang, Advances in thermochemical conversion of woody biomass to energy, fuels and chemicals, *Biotechnol. Adv.*, 2019, **37**(4), 589–597.
6 M. Tripathi, J. N. Sahu and P. Ganesan, Effect of process parameters on production of biochar from biomass waste through pyrolysis: a review, *Renewable Sustainable Energy Rev.*, 2016, **55**, 467–481.
7 P. Srivatsav, B. S. Bhargav, V. Shanmugasundaram, J. Arun, K. P. Gopinath and A. Bhatnagar, Biochar as an Eco-Friendly and Economical Adsorbent for the Removal of Colorants (Dyes) from Aqueous Environment: A Review, *Water*, 2020, **12**(12), 3561.
8 K. A. Spokas, K. B. Cantrell, J. M. Novak, D. W. Archer, J. A. Ippolito, H. P. Collins, A. A. Boateng, I. M. Lima, M. C. Lamb and A. J. McAloon, Biochar: a synthesis of its agronomic impact beyond carbon sequestration, *J. Environ. Qual.*, 2012, **41**(4), 973–989.
9 H. Groot, K. Fernholz, M. Frank, J. Howe, J. Bowyer and S. Bratkovich, Biochar 101: an introduction to an ancient product offering modern opportunities, *Dovetail Partners INC*, 2016, **9**(1), 1–6.
10 B. Pandey, Y. K. Prajapati and P. N. Sheth, Recent progress in thermochemical techniques to produce hydrogen gas from biomass: a state of the art review, *Int. J. Hydrogen Energy*, 2019, **44**(47), 25384–25415.
11 Y. Wang, Y.-J. Hu, X. Hao, P. Peng, J.-Y. Shi, F. Peng and R.-C. Sun, Hydrothermal synthesis and applications of advanced carbonaceous materials from biomass: a review, *Adv. Compos. Hybrid Mater.*, 2020, **3**(3), 267–284.
12 O. Arellanoa, M. Flores, J. Guerra, A. Hidalgo, D. Rojas and A. Strubinger, Hydrothermal carbonization (HTC) of corncob and characterization of the obtained hydrochar, *Chem. Eng.*, 2016, **50**, 235–240.
13 V. Hoffmann, D. Jung, J. Zimmermann, C. Rodriguez Correa, A. Elleuch, K. Halouani and A. Kruse, Conductive Carbon Materials from the Hydrothermal Carbonization of Vineyard Residues for the Application in Electrochemical Double-Layer Capacitors (EDLCs) and Direct Carbon Fuel Cells (DCFCs), *Materials*, 2019, **12**(10), 1703.
14 Z. Liu, Z. Wang, H. Chen, T. Cai and Z. Liu, Hydrochar and pyrochar for sorption of pollutants in wastewater and exhaust gas: a critical review, *Environ. Pollut.*, 2021, **268**, 115910.
15 K. Qian, A. Kumar, H. Zhang, D. Bellmer and R. Huhnke, Recent advances in utilization of biochar, *Renewable Sustainable Energy Rev.*, 2015, **42**, 1055–1064.
16 J. Wang and S. Wang, Preparation, modification and environmental application of biochar: a review, *J. Cleaner Prod.*, 2019, **227**, 1002–1022.
17 Z. Zhang, Z. Zhu, B. Shen and L. Liu, Insights into biochar and hydrochar production and applications: a review, *Energy*, 2019, **171**, 581–598.

© 2025 The Author(s). Published by the Royal Society of Chemistry

Open Access Article. Published on 06 10 2025. Downloaded on 2026-05-13 12:47:34.
This article is licensed under a Creative Commons Attribution-NonCommercial 3.0 Unported Licence.

18 M. X. Pineda Pineda and D. C. Flórez Guarín, Evaluación del Hydrochar producido por tratamiento hidrotermal como medio adsorbente de color de un agua residual, *Ciencia Unisalle*, 2019.
19 C. Navas-Cárdenas, M. Caetano, D. Endara, R. Jiménez, A. B. Lozada, L. E. Manangón, A. Navarrete, C. Reinoso, A. E. Sommer-Márquez and Y. Villasana, The Role of Oxygenated Functional Groups on Cadmium Removal using Pyrochar and Hydrochar Derived from Guadua angustifolia Residues, *Water*, 2023, **15**(3), 525.
20 D. Angın, E. Altintig and T. E. Köse, Influence of process parameters on the surface and chemical properties of activated carbon obtained from biochar by chemical activation, *Bioresour. Technol.*, 2013, **148**, 542–549.
21 Y. Tong, P. J. McNamara and B. K. Mayer, Adsorption of organic micropollutants onto biochar: a review of relevant kinetics, mechanisms and equilibrium, *Environ. Sci.: Water Res. Technol.*, 2019, **5**(5), 821–838.
22 M. Guo, W. Song and J. Tian, Biochar-facilitated soil remediation: mechanisms and efficacy variations, *Front. Environ. Sci.*, 2020, **8**, 521512.
23 Y. Chu, M. A. Khan, S. Zhu, M. Xia, W. Lei, F. Wang and Y. Xu, Microstructural modification of organo-montmorillonite with Gemini surfactant containing four ammonium cations: molecular dynamics (MD) simulations and adsorption capacity for copper ions, *J. Chem. Technol. Biotechnol.*, 2019, **94**(11), 3585–3594.
24 J. Qu, Q. Meng, W. Peng, J. Shi, Z. Dong, Z. Li, Q. Hu, G. Zhang, L. Wang, S. Ma and Y. Zhang, Application of functionalized biochar for adsorption of organic pollutants from environmental media: synthesis strategies, removal mechanisms and outlook, *J. Cleaner Prod.*, 2023, **423**, 138690.
25 A. V. Gorovtsov, T. M. Minkina, S. S. Mandzhieva, L. V. Perelomov, G. Soja, I. V. Zamulina, V. D. Rajput, S. N. Sushkova, D. Mohan and J. Yao, The mechanisms of biochar interactions with microorganisms in soil, *Environ. Geochem. Health*, 2020, **42**(8), 2495–2518.
26 G. Fabietti, M. Biasioli, R. Barberis and F. Ajmone-Marsan, Soil contamination by organic and inorganic pollutants at the regional scale: the case of Piedmont, Italy, *J. Soils Sediments*, 2010, **10**(2), 290–300.
27 Y. Lu, K. Gu, Z. Shen, C.-S. Tang, B. Shi and Q. Zhou, Biochar implications for the engineering properties of soils: a review, *Sci. Total Environ.*, 2023, **888**, 164185.
28 B. Glaser, J. Lehmann and W. Zech, Ameliorating physical and chemical properties of highly weathered soils in the tropics with charcoal – a review, *Biol. Fertil. Soils*, 2002, **35**(4), 219–230.
29 M. Han, J. Zhang, L. Zhang and Z. Wang, Effect of biochar addition on crop yield, water and nitrogen use efficiency: a meta-analysis, *J. Cleaner Prod.*, 2023, **420**, 138425.
30 T.-B. Nguyen, K. Sherpa, X.-T. Bui, V.-T. Nguyen, T.-D.-H. Vo, H.-T.-T. Ho, C.-W. Chen and C.-D. Dong, Biochar for soil remediation: a comprehensive review of current research on pollutant removal, *Environ. Pollut.*, 2023, **337**, 122571.
31 E. N. Yargicoglu, B. Y. Sadasivam, K. R. Reddy and K. Spokas, Physical and chemical characterization of waste wood derived biochars, *Waste Manage.*, 2015, **36**, 256–268.
32 J. Tang, W. Zhu, R. Kookana and A. Katayama, Characteristics of biochar and its application in remediation of contaminated soil, *J. Biosci. Bioeng.*, 2013, **116**(6), 653–659.
33 O. Mašek, W. Buss, P. Brownsort, M. Rovere, A. Tagliaferro, L. Zhao, X. Cao and G. Xu, Potassium doping increases biochar carbon sequestration potential by 45%, facilitating decoupling of carbon sequestration from soil improvement, *Sci. Rep.*, 2019, **9**(1), 5514.
34 M. Samanta and D. Mitra, Treatment of Petroleum Hydrocarbon Pollutants in Water, in *Water Pollution and Remediation: Organic Pollutants*, ed. I. M. I. Ahamed and E. Lichtfouse, Springer International Publishing, Cham, 2021, pp. 229–275.
35 Y. Lou, S. Joseph, L. Li, E. R. Graber, X. Liu and G. Pan, Water extract from straw biochar used for plant growth promotion: an initial test, *BioResources*, 2016, **11**(1), 249–266.
36 W. Xiang, X. Zhang, J. Chen, W. Zou, F. He, X. Hu, D. C. W. Tsang, Y. S. Ok and B. Gao, Biochar technology in wastewater treatment: a critical review, *Chemosphere*, 2020, **252**, 126539.
37 D. Présiga-López, A. Rubio-Clemente and J. F. Pérez, Uso del biocarbón como material alternativo para el tratamiento de aguas residuales contaminadas, *Revista UIS Ingenierías*, 2021, **20**(1), 121–134.
38 J. E. Klaunig, L. M. Kamendulis and B. A. Hocevar, Oxidative stress and oxidative damage in carcinogenesis, *Toxicol. Pathol.*, 2010, **38**(1), 96–109.
39 S. Ho, Low-Cost Adsorbents for the Removal of Phenol/Phenolics, Pesticides, and Dyes from Wastewater Systems: A Review, *Water*, 2022, **14**(20), 3203.
40 S. Jiménez-Oyola, M.-J. García-Martínez, M. F. Ortega, E. Chavez, P. Romero, I. García-Garizabal and D. Bolonio, Ecological and probabilistic human health risk assessment of heavy metal(loid)s in river sediments affected by mining activities in Ecuador, *Environ. Geochem. Health*, 2021, **43**(11), 4459–4474.
41 N. V. Doan, V. T. Cuong, T. H. Nguyen, T. X. Do and A.-T. Vu, Preparation of novel CS/SiO_2-EDTA nanocomposite from ash of rice straw pellets for enhanced removal efficiency of heavy metal ions in aqueous medium, *J. Water Process Eng.*, 2024, **60**, 105175.
42 V. T. Tan, L. T. Vinh, N. H. Tuan, N. V. Doan, T. T. Diep and P. V. Tuan, Synthesis of α-Al_2O_3 nanosize by combustion reaction using sucrose and graphene oxide as fuel precursors, *J. Cryst. Growth*, 2025, **652**, 128048.
43 J. Li, K. Zhang and H. Zhang, Adsorption of antibiotics on microplastics, *Environ. Pollut.*, 2018, **237**, 460–467.
44 D. N. R. de Sousa, S. Insa, A. A. Mozeto, M. Petrovic, T. F. Chaves and P. S. Fadini, Equilibrium and kinetic studies of the adsorption of antibiotics from aqueous solutions onto powdered zeolites, *Chemosphere*, 2018, **205**, 137–146.

Open Access Article. Published on 06 10 2025. Downloaded on 2026-05-13 12:47:34.
This article is licensed under a Creative Commons Attribution-NonCommercial 3.0 Unported Licence.

45 M. B. Ahmed, J. L. Zhou, H. H. Ngo and W. Guo, Adsorptive removal of antibiotics from water and wastewater: progress and challenges, *Sci. Total Environ.*, 2015, **532**, 112–126.
46 C. C. Obi, M. N. Abonyi, P. E. Ohale, C. E. Onu, J. T. Nwabanne, C. A. Igwegbe, T. T. Kamuche and I. H. Ozofor, Adsorption of antibiotics from aqueous media using nanocomposites: insight into the current status and future perspectives, *Chem. Eng. J.*, 2024, **497**, 154767.
47 H. Li, D. Zhang, X. Han and B. Xing, Adsorption of antibiotic ciprofloxacin on carbon nanotubes: pH dependence and thermodynamics, *Chemosphere*, 2014, **95**, 150–155.
48 H. Kim, Y. S. Hwang and V. K. Sharma, Adsorption of antibiotics and iopromide onto single-walled and multi-walled carbon nanotubes, *Chem. Eng. J.*, 2014, **255**, 23–27.
49 T. Gangar and S. Patra, Antibiotic persistence and its impact on the environment, *3 Biotechnol.*, 2023, **13**(12), 401.
50 M. T. M. H. Hamad and M. E. El-Sesy, Adsorptive removal of levofloxacin and antibiotic resistance genes from hospital wastewater by nano-zero-valent iron and nano-copper using kinetic studies and response surface methodology, *Bioresour. Bioprocess.*, 2023, **10**(1), 1.
51 L. Thai-Hoang, T. Thong, H. T. Loc, P. T. T. Van, P. T. P. Thuy and T. L. Thuoc, Influences of anthropogenic activities on water quality in the Saigon River, Ho Chi Minh City, *J. Water Health*, 2022, **20**(3), 491–504.
52 D. Schuster, K. Axtmann, N. Holstein, C. Felder, A. Voigt, H. Färber, P. Ciorba, C. Szekat, A. Schallenberg and M. Böckmann, Antibiotic concentrations in raw hospital wastewater surpass minimal selective and minimum inhibitory concentrations of resistant Acinetobacter baylyi strains, *Environ. Microbiol.*, 2022, **24**(12), 5721–5733.
53 M. Oncel, A. Muhcu, E. Demirbas and M. Kobya, A comparative study of chemical precipitation and electrocoagulation for treatment of coal acid drainage wastewater, *J. Environ. Chem. Eng.*, 2013, **1**(4), 989–995.
54 L. Charerntanyarak, Heavy metals removal by chemical coagulation and precipitation, *Water Sci. Technol.*, 1999, **39**(10–11), 135–138.
55 V. D. Nguyen and A.-T. Vu, Synthesis of novel EDTA-modified Aluminum Oxide for Improved Removal of Heavy Metal in Contaminated Water, *Mater. Res. Bull.*, 2025, 113578.
56 T. A. Ho, V. D. Nguyen, N. B. Van, K. T. Vu, T. D. Dinh, A. T. Nguyen Duc, T. D. Do, M. K. Nguyen, S. T. Le, D. T. Le, Q. M. Pham and A.-T. Vu, Preparation of novel DTPA-Modified silica aerogel from rice husk for effective removal of Pb^{2+} ions from water, *Inorg. Chem. Commun.*, 2025, **179**, 114768.
57 U. O. Aigbe, K. E. Ukhurebor, R. B. Onyancha, O. A. Osibote, H. Darmokoesoemo and H. S. Kusuma, Fly ash-based adsorbent for adsorption of heavy metals and dyes from aqueous solution: a review, *J. Mater. Res. Technol.*, 2021, **14**, 2751–2774.
58 V. D. Nguyen, T. P. Nguyen and A.-T. Vu, Chemical modification of lettuce leaves using NaOH and EDTA: a brilliant biosorbent for the adsorption of heavy metal ions from aqueous solution, *J. Water Process Eng.*, 2025, **71**, 107202.
59 V. D. Nguyen, M. T. Nguyen and A.-T. Vu, Production of green biosorbent from chemically modified moringa leaves for enhanced removal of heavy metal in aqueous environment, *Biomass Convers. Biorefin.*, 2024, **15**(9), 13933–13953.
60 T. O. Ajiboye, O. A. Oyewo and D. C. Onwudiwe, Simultaneous removal of organics and heavy metals from industrial wastewater: a review, *Chemosphere*, 2021, **262**, 128379.
61 S. Zhuang and J. Wang, Cesium removal from radioactive wastewater by adsorption and membrane technology, *Front. Environ. Sci. Eng.*, 2023, **18**(3), 38.
62 V. D. Nguyen, A.-T. Vu and T. V. La, Fabrication of high-purity alumina particles by spray drying and surface modification with SDS for methylene blue removal, *Particuology*, 2025, **102**, 27–42.
63 N. Kasera, P. Kolar and S. G. Hall, Nitrogen-doped biochars as adsorbents for mitigation of heavy metals and organics from water: a review, *Biochar*, 2022, **4**(1), 17.
64 X. Tian, S. Chu, Y. Hu, L. Luo, X. Lin and H. Wang, Removal of heavy metals from single- and multi-metal solution by magnetic microalgae-derived biochar, *J. Water Process Eng.*, 2025, **69**, 106622.
65 M. Yang, S. An, H. Gao, Z. Du, X. Zhang, L. D. Nghiem and Q. Liu, Selective adsorption of copper by amidoxime modified low-temperature biochar: performance and mechanism, *Sci. Total Environ.*, 2025, **958**, 178072.
66 Z. Madzin, I. Zahidi, A. Talei, M. E. Raghunandan, A. A. Hermawan and D. S. Karam, Optimising spent mushroom compost biochar for heavy metal removal: mechanisms and kinetics in mine water treatment, *J. Water Process Eng.*, 2025, **69**, 106829.
67 Y. Sun, Q. Yu, T. Yang, R. Li and S. Zhao, Preparation and electrochemical properties of modified biochar, *Biomass Bioenergy*, 2025, **192**, 107496.
68 Y. Li, Y. Xin, B. Sun, C. Man, E. Mouele, L. Petrik, B. J. Bladergroen and C. Zhang, Inactivation of Cyclotella meneghiniana to prepare biochar by in-liquid pulsed discharge plasma, *Biomass Bioenergy*, 2025, **200**, 108034.
69 N. McGlashan, N. Shah, B. Caldecott and M. Workman, High-level techno-economic assessment of negative emissions technologies, *Process Saf. Environ. Prot.*, 2012, **90**(6), 501–510.
70 P. Basu, *Biomass gasification, pyrolysis and torrefaction: practical design and theory*, Academic Press, 2018.
71 S. Yusup and N. A. Rashidi, A Mini Review of Biochar Synthesis, Characterization, and Related Standardization and Legislation, in *Applications of Biochar for Environmental Safety*, ed. A. A. Abdelhafez and M. Abbas, IntechOpen, Rijeka, 2020.
72 A. Leithaeuser, M. Gerber, R. Span and S. Schwede, Comparison of pyrochar, hydrochar and lignite as additive in anaerobic digestion and NH_4^+ adsorbent, *Bioresour. Technol.*, 2022, **361**, 127674.

© 2025 The Author(s). Published by the Royal Society of Chemistry

Open Access Article. Published on 06 10 2025. Downloaded on 2026-05-13 12:47:34.
This article is licensed under a Creative Commons Attribution-NonCommercial 3.0 Unported Licence.

73 J. W. Lee, B. Hawkins, X. Li and D. M. Day, Biochar Fertilizer for Soil Amendment and Carbon Sequestration, in *Advanced Biofuels and Bioproducts*, ed. J. W. Lee, Springer New York, New York, NY, 2013, pp. 57–68.
74 K. G. Roberts, B. A. Gloy, S. Joseph, N. R. Scott and J. Lehmann, Life Cycle Assessment of Biochar Systems: Estimating the Energetic, Economic, and Climate Change Potential, *Environ. Sci. Technol.*, 2010, **44**(2), 827–833.
75 C. A. Odega, O. O. Ayodele, S. O. Ogutuga, G. T. Anguruwa, A. E. Adekunle and C. O. Fakorede, Potential application and regeneration of bamboo biochar for wastewater treatment: a review, *Adv. Bamboo Sci.*, 2023, **2**, 100012.
76 M. Hassan, Y. Liu, R. Naidu, S. J. Parikh, J. Du, F. Qi and I. R. Willett, Influences of feedstock sources and pyrolysis temperature on the properties of biochar and functionality as adsorbents: a meta-analysis, *Sci. Total Environ.*, 2020, **744**, 140714.
77 A. K. Tiwari, D. B. Pal and N. Prasad, Agricultural waste biomass utilization in waste water treatment, in *Utilization of Waste Biomass in Energy, Environment and Catalysis*, CRC Press, 2022, pp. 19–41.
78 H. I. Abdel-Shafy and M. S. M. Mansour, Solid waste issue: sources, composition, disposal, recycling, and valorization, *Egypt. J. Pet.*, 2018, **27**(4), 1275–1290.
79 N. Jafri, W. Y. Wong, V. Doshi, L. W. Yoon and K. H. Cheah, A review on production and characterization of biochars for application in direct carbon fuel cells, *Process Saf. Environ. Prot.*, 2018, **118**, 152–166.
80 P. Shrivastava, A. Kumar, P. Tekasakul, S. S. Lam and A. Palamanit, Comparative Investigation of Yield and Quality of Bio-Oil and Biochar from Pyrolysis of Woody and Non-Woody Biomasses, *Energies*, 2021, **14**(4), 1092.
81 S. P. Espíndola, M. Pronk, J. Zlopasa, S. J. Picken and M. C. M. van Loosdrecht, Nanocellulose recovery from domestic wastewater, *J. Cleaner Prod.*, 2021, **280**, 124507.
82 P. Wu, Z. Wang, H. Wang, N. S. Bolan, Y. Wang and W. Chen, Visualizing the emerging trends of biochar research and applications in 2019: a scientometric analysis and review, *Biochar*, 2020, **2**(2), 135–150.
83 M. K. Rafiq, R. T. Bachmann, M. T. Rafiq, Z. Shang, S. Joseph and R. Long, Influence of pyrolysis temperature on physico-chemical properties of corn stover (Zea mays L.) biochar and feasibility for carbon capture and energy balance, *PLoS One*, 2016, **11**(6), e0156894.
84 B. Ercan, K. Alper, S. Ucar and S. Karagoz, Comparative studies of hydrochars and biochars produced from lignocellulosic biomass via hydrothermal carbonization, torrefaction and pyrolysis, *J. Energy Inst.*, 2023, **109**, 101298.
85 R. Xiao, M. K. Awasthi, R. Li, J. Park, S. M. Pensky, Q. Wang, J. J. Wang and Z. Zhang, Recent developments in biochar utilization as an additive in organic solid waste composting: a review, *Bioresour. Technol.*, 2017, **246**, 203–213.
86 D. Mohan, A. Sarswat, Y. S. Ok and C. U. Pittman, Organic and inorganic contaminants removal from water with biochar, a renewable, low cost and sustainable adsorbent – A critical review, *Bioresour. Technol.*, 2014, **160**, 191–202.
87 E. Jakab, Analytical Techniques as a Tool to Understand the Reaction Mechanism, in *Recent Advances in Thermo-Chemical Conversion of Biomass*, ed. A. Pandey, T. Bhaskar, M. Stöcker and R. K. Sukumaran, Elsevier, Boston, 2015, ch. 3, pp. 75–108.
88 C. E. Brewer, R. Unger, K. Schmidt-Rohr and R. C. Brown, Criteria to Select Biochars for Field Studies based on Biochar Chemical Properties, *BioEnergy Res.*, 2011, **4**(4), 312–323.
89 S. Wijitkosum and P. Jiwnok, Elemental Composition of Biochar Obtained from Agricultural Waste for Soil Amendment and Carbon Sequestration, *Appl. Sci.*, 2019, **9**(19), 3980.
90 T. Zhang, W. P. Walawender, L. T. Fan, M. Fan, D. Daugaard and R. C. Brown, Preparation of activated carbon from forest and agricultural residues through CO_2 activation, *Chem. Eng. J.*, 2004, **105**(1), 53–59.
91 A. C. Lua, T. Yang and J. Guo, Effects of pyrolysis conditions on the properties of activated carbons prepared from pistachio-nut shells, *J. Anal. Appl. Pyrolysis*, 2004, **72**(2), 279–287.
92 J. Zhang, J. Liu and R. Liu, Effects of pyrolysis temperature and heating time on biochar obtained from the pyrolysis of straw and lignosulfonate, *Bioresour. Technol.*, 2015, **176**, 288–291.
93 R. Chatterjee, B. Sajjadi, W.-Y. Chen, D. L. Mattern, N. Hammer, V. Raman and A. Dorris, Effect of pyrolysis temperature on physicochemical properties and acoustic-based amination of biochar for efficient CO_2 adsorption, *Front. Energy Res.*, 2020, **8**, 85.
94 J. Lehmann, M. C. Rillig, J. Thies, C. A. Masiello, W. C. Hockaday and D. Crowley, Biochar effects on soil biota – A review, *Soil Biol. Biochem.*, 2011, **43**(9), 1812–1836.
95 S. You, Y. S. Ok, S. S. Chen, D. C. W. Tsang, E. E. Kwon, J. Lee and C.-H. Wang, A critical review on sustainable biochar system through gasification: energy and environmental applications, *Bioresour. Technol.*, 2017, **246**, 242–253.
96 C. E. Brewer, K. Schmidt-Rohr, J. A. Satrio and R. C. Brown, Characterization of biochar from fast pyrolysis and gasification systems, *Environ. Prog. Sustainable Energy*, 2009, **28**(3), 386–396.
97 K. Czerwińska, M. Śliz and M. Wilk, Hydrothermal carbonization process: Fundamentals, main parameter characteristics and possible applications including an effective method of SARS-CoV-2 mitigation in sewage sludge. a review, *Renewable Sustainable Energy Rev.*, 2022, **154**, 111873.
98 T. A. Khan, A. S. Saud, S. S. Jamari, M. H. A. Rahim, J.-W. Park and H.-J. Kim, Hydrothermal carbonization of lignocellulosic biomass for carbon rich material preparation: a review, *Biomass Bioenergy*, 2019, **130**, 105384.
99 F. Ahmad, E. L. Silva and M. B. A. Varesche, Hydrothermal processing of biomass for anaerobic digestion – A review, *Renewable Sustainable Energy Rev.*, 2018, **98**, 108–124.
100 M. P. Maniscalco, M. Volpe and A. Messineo, Hydrothermal Carbonization as a Valuable Tool for Energy and

Open Access Article. Published on 06 10 2025. Downloaded on 2026-05-13 12:47:34.
This article is licensed under a Creative Commons Attribution-NonCommercial 3.0 Unported Licence.

Environmental Applications: A Review, *Energies*, 2020, **13**(16), 4098.

101 L. Fiori, D. Basso, D. Castello and M. Baratieri, Hydrothermal carbonization of biomass: design of a batch reactor and preliminary experimental results, *Chem. Eng. Trans.*, 2014, **37**(5), 55–60.

102 Y. Sun, B. Gao, Y. Yao, J. Fang, M. Zhang, Y. Zhou, H. Chen and L. Yang, Effects of feedstock type, production method, and pyrolysis temperature on biochar and hydrochar properties, *Chem. Eng. J.*, 2014, **240**, 574–578.

103 Z. Liu, A. Quek, S. Kent Hoekman and R. Balasubramanian, Production of solid biochar fuel from waste biomass by hydrothermal carbonization, *Fuel*, 2013, **103**, 943–949.

104 E. W. Yihunu, M. Minale, S. Abebe and M. Limin, Preparation, characterization and cost analysis of activated biochar and hydrochar derived from agricultural waste: a comparative study, *SN Appl. Sci.*, 2019, **1**(8), 873.

105 B. Weiner, I. Baskyr, J. Poerschmann and F.-D. Kopinke, Potential of the hydrothermal carbonization process for the degradation of organic pollutants, *Chemosphere*, 2013, **92**(6), 674–680.

106 R. Gamgoum, A. Dutta, R. M. Santos and Y. W. Chiang, Hydrothermal Conversion of Neutral Sulfite Semi-Chemical Red Liquor into Hydrochar, *Energies*, 2016, **9**(6), 435.

107 W.-H. Chen, B.-J. Lin, Y.-Y. Lin, Y.-S. Chu, A. T. Ubando, P. L. Show, H. C. Ong, J.-S. Chang, S.-H. Ho, A. B. Culaba, A. Pétrissans and M. Pétrissans, Progress in biomass torrefaction: principles, applications and challenges, *Prog. Energy Combust. Sci.*, 2021, **82**, 100887.

108 K. Sahoo, E. Bilek, R. Bergman and S. Mani, Techno-economic analysis of producing solid biofuels and biochar from forest residues using portable systems, *Appl. Energy*, 2019, **235**, 578–590.

109 A. U. Rajapaksha, M. Vithanage, M. Ahmad, D.-C. Seo, J.-S. Cho, S.-E. Lee, S. S. Lee and Y. S. Ok, Enhanced sulfamethazine removal by steam-activated invasive plant-derived biochar, *J. Hazard. Mater.*, 2015, **290**, 43–50.

110 S. Rong, Y. He, L. Ni, Q. Gao, X. Feng, S. Liu, Y. Zhong, Y. Li and Z. Liu, Steam-activated biochar for efficient removal of sulfamethoxazole from water: activation temperature-mediated differences, *J. Water Process Eng.*, 2025, **72**, 107462.

111 I. M. Lima and W. E. Marshall, Adsorption of selected environmentally important metals by poultry manure-based granular activated carbons, *J. Chem. Technol. Biotechnol.*, 2005, **80**(9), 1054–1061.

112 S. Mondal, A. Kaustav and G. Halder, Optimization of ranitidine hydrochloride removal from simulated pharmaceutical waste by activated charcoal from mung bean husk using response surface methodology and artificial neural network, *Desalin. Water Treat.*, 2016, **57**(39), 18366–18378.

113 S. Rangabhashiyam and P. Balasubramanian, The potential of lignocellulosic biomass precursors for biochar production: performance, mechanism and wastewater application-a review, *Ind. Crops Prod.*, 2019, **128**, 405–423.

114 B. Sajjadi, W.-Y. Chen and N. O. Egiebor, A comprehensive review on physical activation of biochar for energy and environmental applications, *Rev. Chem. Eng.*, 2019, **35**(6), 735–776.

115 H. Lyu, B. Gao, F. He, C. Ding, J. Tang and J. C. Crittenden, Ball-Milled Carbon Nanomaterials for Energy and Environmental Applications, *ACS Sustainable Chem. Eng.*, 2017, **5**(11), 9568–9585.

116 H. Lyu, B. Gao, F. He, A. R. Zimmerman, C. Ding, H. Huang and J. Tang, Effects of ball milling on the physicochemical and sorptive properties of biochar: Experimental observations and governing mechanisms, *Environ. Pollut.*, 2018, **233**, 54–63.

117 H. Lyu, B. Gao, F. He, A. R. Zimmerman, C. Ding, J. Tang and J. C. Crittenden, Experimental and modeling investigations of ball-milled biochar for the removal of aqueous methylene blue, *Chem. Eng. J.*, 2018, **335**, 110–119.

118 S. C. Peterson, M. A. Jackson, S. Kim and D. E. Palmquist, Increasing biochar surface area: optimization of ball milling parameters, *Powder Technol.*, 2012, **228**, 115–120.

119 R. Ahuja, A. Kalia, R. Sikka and P. Chaitra, Nano Modifications of Biochar to Enhance Heavy Metal Adsorption from Wastewaters: A Review, *ACS Omega*, 2022, **7**(50), 45825–45836.

120 R. Wahi, N. F. Qa Zuhaidi, Y. Yusof, J. Jamel, D. Kanakaraju and Z. Ngaini, Chemically treated microwave-derived biochar: an overview, *Biomass Bioenergy*, 2017, **107**, 411–421.

121 K. Li, Y. Jiang, X. Wang, D. Bai, H. Li and Z. Zheng, Effect of nitric acid modification on the lead(II) adsorption of mesoporous biochars with different mesopore size distributions, *Clean Technol. Environ. Policy*, 2016, **18**(3), 797–805.

122 Z. Ding, X. Hu, Y. Wan, S. Wang and B. Gao, Removal of lead, copper, cadmium, zinc, and nickel from aqueous solutions by alkali-modified biochar: batch and column tests, *J. Ind. Eng. Chem.*, 2016, **33**, 239–245.

123 X. Han, L. Chu, S. Liu, T. Chen, C. Ding, J. Yan, L. Cui and G. Quan, Removal of methylene blue from aqueous solution using porous biochar obtained by KOH activation of peanut shell biochar, *BioResources*, 2015, **10**(2), 2836–2849.

124 Z. Zhou, J. Xu, L. Zou, X. Wang, Y. Chen, P. Sun, X. Zhu, L. Sheng and N. Lu, Removal of sulfonamide antibiotics by constructed wetland substrate with NaOH-modified corn straw biochar under different operating conditions, *Bioresour. Technol.*, 2024, **410**, 131274.

125 M. Vithanage, A. U. Rajapaksha, M. Zhang, S. Thiele-Bruhn, S. S. Lee and Y. S. Ok, Acid-activated biochar increased sulfamethazine retention in soils, *Environ. Sci. Pollut. Res.*, 2015, **22**(3), 2175–2186.

126 K. Yin, J. Wang, X. Tian, N. Yu, X. Zhang, Y. Zhao, Y. Liu, S. Sui, C. Wang, F. Lian, S. Zhai, X. Li and B. Xing, Effect of biochar-derived dissolved organic matter on tetracycline sorption by $KMnO_4$-modified biochar, *Chem. Eng. J.*, 2023, **474**, 145872.

© 2025 The Author(s). Published by the Royal Society of Chemistry

Open Access Article. Published on 06 10 2025. Downloaded on 2026-05-13 12:47:34.
This article is licensed under a Creative Commons Attribution-NonCommercial 3.0 Unported Licence.

127 P. Sun, Y. Li, T. Meng, R. Zhang, M. Song and J. Ren, Removal of sulfonamide antibiotics and human metabolite by biochar and biochar/H_2O_2 in synthetic urine, *Water Res.*, 2018, **147**, 91–100.

128 O. Pezoti, A. L. Cazetta, I. P. A. F. Souza, K. C. Bedin, A. C. Martins, T. L. Silva and V. C. Almeida, Adsorption studies of methylene blue onto $ZnCl_2$-activated carbon produced from buriti shells (Mauritia flexuosa L.), *J. Ind. Eng. Chem.*, 2014, **20**(6), 4401–4407.

129 X. Zhang, Y. Chu, X. Yu, C. Yan, Y. Yang, J. Liu, G. Shen, X. Wang, S. Tao and X. Wang, Introduction of N-containing moieties by ammonia plasma technique can substantially improve ciprofloxacin removal by biochar and the associated mechanisms: spectroscopic and site energy distribution analysis, *J. Hazard. Mater.*, 2022, **424**, 127438.

130 J. Lou, Y. Wei, M. Zhang, Q. Meng, J. An and M. Jia, Removal of tetracycline hydrochloride in aqueous by coupling dielectric barrier discharge plasma with biochar, *Sep. Purif. Technol.*, 2021, **266**, 118515.

131 K. Zoroufchi Benis, J. Soltan and K. N. McPhedran, Electrochemically modified adsorbents for treatment of aqueous arsenic: pore diffusion in modified biomass vs. biochar, *Chem. Eng. J.*, 2021, **423**, 130061.

132 R. Tian, H. Dong, J. Chen, R. Li, Q. Xie, L. Li, Y. Li, Z. Jin, S. Xiao and J. Xiao, Electrochemical behaviors of biochar materials during pollutant removal in wastewater: a review, *Chem. Eng. J.*, 2021, **425**, 130585.

133 L. Xu, Y. Qi, S. He, C. Wang, X. Jin, Q. Wang, K. Wang and P. Jin, Facile synthesis of boron-doped porous biochar as a metal-free adsorbent for efficient removal of aqueous tetracycline antibiotics, *J. Environ. Sci.*, 2025, **152**, 235–247.

134 Y. Cheng, J. Yang, J. Shen, P. Yan, S. Liu, J. Kang, L. Bi, B. Wang, S. Zhao and Z. Chen, Preparation of P-doped biochar and its high-efficient removal of sulfamethoxazole from water: adsorption mechanism, fixed-bed column and DFT study, *Chem. Eng. J.*, 2023, **468**, 143748.

135 Y. Li, B. Xing, X. Wang, K. Wang, L. Zhu and S. Wang, Nitrogen-Doped Hierarchical Porous Biochar Derived from Corn Stalks for Phenol-Enhanced Adsorption, *Energy Fuels*, 2019, **33**(12), 12459–12468.

136 Z. Wan, Y. Sun, D. C. W. Tsang, E. Khan, A. C. K. Yip, Y. H. Ng, J. Rinklebe and Y. S. Ok, Customised fabrication of nitrogen-doped biochar for environmental and energy applications, *Chem. Eng. J.*, 2020, **401**, 126136.

137 S. Ahmad, L. Liu, S. Zhang and J. Tang, Nitrogen-doped biochar (N-doped BC) and iron/nitrogen co-doped biochar (Fe/N co-doped BC) for removal of refractory organic pollutants, *J. Hazard. Mater.*, 2023, **446**, 130727.

138 S. Ahmad, F. Gao, H. Lyu, J. Ma, B. Zhao, S. Xu, C. Ri and J. Tang, Temperature-dependent carbothermally reduced iron and nitrogen doped biochar composites for removal of hexavalent chromium and nitrobenzene, *Chem. Eng. J.*, 2022, **450**, 138006.

139 X. Zhu, L. Xu, C. Wang, Y. Qi, J. Shi, X. Jin, X. Bai, W. Yan and P. Jin, Insights into the enhanced simultaneous adsorption and catalytic removal of antibiotics by a novel Fe/B co-doped biochar, *Sep. Purif. Technol.*, 2025, **360**, 130888.

140 N. Cheng, B. Wang, M. Chen, Q. Feng, X. Zhang, S. Wang, R. Zhao and T. Jiang, Adsorption and photocatalytic degradation of quinolone antibiotics from wastewater using functionalized biochar, *Environ. Pollut.*, 2023, **336**, 122409.

141 S. Sudan, J. Kaushal and A. Khajuria, Efficient adsorption of anionic dye (congo red) using copper-carbon dots doped magnetic biochar: kinetic, isothermal, and regeneration studies, *Clean Technol. Environ. Policy*, 2024, **26**(2), 481–497.

142 B. Yao, W. Zeng, A. Núñez-Delgado and Y. Zhou, Simultaneous adsorption of ciprofloxacin and Cu(2+) using Fe and N co-doped biochar: competition and selective separation, *Waste Manage.*, 2023, **168**, 386–395.

143 W. Wu, J. Zhang, W. Zhu, S. Zhao, Y. Gao, Y. Li, L. Ding and H. Ding, Novel manganese and nitrogen co-doped biochar based on sodium bicarbonate activation for efficient removal of bisphenol A: mechanism insight and role analysis of manganese and nitrogen by combination of characterizations, experiments and density functional theory calculations, *Bioresour. Technol.*, 2024, **399**, 130608.

144 Z. Liu, P. Zhang, Z. Wei, F. Xiao, S. Liu, H. Guo, C. Qu, J. Xiong, H. Sun and W. Tan, Porous Fe-doped graphitized biochar: an innovative approach for co-removing per-/polyfluoroalkyl substances with different chain lengths from natural waters and wastewater, *Chem. Eng. J.*, 2023, **476**, 146888.

145 J. Wu, T. Wang, Y. Liu, W. Tang, S. Geng and J. Chen, Norfloxacin adsorption and subsequent degradation on ball-milling tailored N-doped biochar, *Chemosphere*, 2022, **303**, 135264.

146 D. Yu, Y. He, S. Zeng, H. Tian and Z. Ji, A novel magnetic S/N co-doped tea residue biochar applied to tetracycline adsorption in water environment, *Colloids Surf., A*, 2024, **703**, 135400.

147 Y. Ma, L. Yang, L. Wu, P. Li, X. Qi, L. He, S. Cui, Y. Ding and Z. Zhang, Carbon nanotube supported sludge biochar as an efficient adsorbent for low concentrations of sulfamethoxazole removal, *Sci. Total Environ.*, 2020, **718**, 137299.

148 I. Hussain, N. B. Singh, A. Singh, H. Singh and S. C. Singh, Green synthesis of nanoparticles and its potential application, *Biotechnol. Lett.*, 2016, **38**(4), 545–560.

149 M. M. H. Khalil, E. H. Ismail, K. Z. El-Baghdady and D. Mohamed, Green synthesis of silver nanoparticles using olive leaf extract and its antibacterial activity, *Arabian J. Chem.*, 2014, **7**(6), 1131–1139.

150 P. Ramesh, A. Rajendran and M. Meenakshisundaram, Green synthesis of zinc oxide nanoparticles using flower extract Cassia auriculata, *J. Nanosci. Nanotechnol.*, 2014, **2**(1), 41–45.

151 N. Singh and S. Naraa, Biological synthesis and characterization of lead sulfide nanoparticles using bacterial isolates from heavy metal rich sites, *Int. J. Agric. Food Sci. Technol.*, 2013, **4**, 16–23.

152 J. Y. Song and B. S. Kim, Rapid biological synthesis of silver nanoparticles using plant leaf extracts, *Bioprocess Biosyst. Eng.*, 2009, **32**(1), 79–84.

Open Access Article. Published on 06 10 2025. Downloaded on 2026-05-13 12:47:34.
This article is licensed under a Creative Commons Attribution-NonCommercial 3.0 Unported Licence.

153 P. Arabkhani, A. Asfaram and F. Sadegh, Green and low-temperature synthesis of the magnetic modified biochar under the air atmosphere for the adsorptive removal of heavy metal ions from wastewater: CCD-RSM experimental design with isotherm, kinetic, and thermodynamic studies, *Environ. Sci. Pollut. Res.*, 2023, **30**(57), 120085–120102.

154 D. Kumar and S. K. Gupta, Green synthesis of novel biochar from Abelmoschus esculentus seeds for direct blue 86 dye removal: characterization, RSM optimization, isotherms, kinetics, and fixed bed column studies, *Environ. Pollut.*, 2023, **337**, 122559.

155 T. M. Dao and T. Le Luu, Synthesis of activated carbon from macadamia nutshells activated by H_2SO_4 and K_2CO_3 for methylene blue removal in water, *Bioresour. Technol. Rep.*, 2020, **12**, 100583.

156 Y. Wang, C. Srinivasakannan, H. Wang, G. Xue, L. Wang, X. Wang and X. Duan, Preparation of novel biochar containing graphene from waste bamboo with high methylene blue adsorption capacity, *Diamond Related Mater.*, 2022, **125**, 109034.

157 M. Danish and T. Ahmad, A review on utilization of wood biomass as a sustainable precursor for activated carbon production and application, *Renewable Sustainable Energy Rev.*, 2018, **87**, 1–21.

158 K.-M. Poo, E.-B. Son, J.-S. Chang, X. Ren, Y.-J. Choi and K.-J. Chae, Biochars derived from wasted marine macroalgae (Saccharina japonica and Sargassum fusiforme) and their potential for heavy metal removal in aqueous solution, *J. Environ. Manage.*, 2018, **206**, 364–372.

159 T.-B. Nguyen, Q.-M. Truong, C.-W. Chen, W.-H. Chen and C.-D. Dong, Pyrolysis of marine algae for biochar production for adsorption of Ciprofloxacin from aqueous solutions, *Bioresour. Technol.*, 2022, **351**, 127043.

160 Y. S. Ok, A. Bhatnagar, D. Hou, T. Bhaskar and O. Mašek, Advances in algal biochar: production, characterization and applications, *Bioresour. Technol.*, 2020, **317**, 123982.

161 W. Jin, Q. Fang, D. Jiang, T. Li, B. Wei, J. Sun, W. Zhang, Z. Zhang, F. Zhang, R. J. Linhardt, H. Wang and W. Zhong, Structural characteristics and anti-complement activities of polysaccharides from Sargassum hemiphyllum, *Glycoconjugate J.*, 2020, **37**(5), 553–563.

162 E. Bastos, M. Schneider, D. P. C. de Quadros, B. Welz, M. B. Batista, P. A. Horta, L. R. Rörig and J. B. Barufi, Phytoremediation potential of Ulva ohnoi (Chlorophyta): influence of temperature and salinity on the uptake efficiency and toxicity of cadmium, *Ecotoxicol. Environ. Saf.*, 2019, **174**, 334–343.

163 Y.-H. Hsiao, Y.-H. Wang, W.-S. Lin, Y.-C. Cheng, K. Nagabhushanam, C.-T. Ho and M.-H. Pan, Molecular Mechanisms of the Anti-obesity Properties of Agardhiella subulata in Mice Fed a High-Fat Diet, *J. Agric. Food Chem.*, 2021, **69**(16), 4745–4754.

164 E. Mosaffa, A. Banerjee and H. Ghafuri, Sustainable high-efficiency removal of cationic and anionic dyes using new super adsorbent biochar: performance, isotherm, kinetic and thermodynamic evaluation, *Environ. Sci.: Water Res. Technol.*, 2023, **9**(10), 2643–2663.

165 L. Soltys, O. Olkhovyy, T. Tatarchuk and M. Naushad, Green Synthesis of Metal and Metal Oxide Nanoparticles: Principles of Green Chemistry and Raw Materials, *Magnetochemistry*, 2021, **7**(11), 145.

166 H. Chakhtouna, H. Benzeid, N. Zari, A. E. K. Qaiss and R. Bouhfid, Microwave-assisted synthesis of MIL-53(Fe)/biochar composite from date palm for ciprofloxacin and ofloxacin antibiotics removal, *Sep. Purif. Technol.*, 2023, **308**, 122850.

167 S. M. Mahgoub, A. M. Salah, A. A. Kotp, Z. E. Eldin, W. Kamal, D. Essam, E. A. Mohamed, A. M. Radalla, A. A. Allam, H. E. Alfassam and R. Mahmoud, Efficient ciprofloxacin removal from water using Zn-MOF and Date seeds-biochar composites: a comprehensive evaluation of greenness, sustainability, and environmental impact, *Int. J. Environ. Anal. Chem.*, 2025, 1–29.

168 C. M. Navarathna, N. B. Dewage, A. G. Karunanayake, E. L. Farmer, F. Perez, E. B. Hassan, T. E. Mlsna and C. U. Pittman, Rhodamine B Adsorptive Removal and Photocatalytic Degradation on MIL-53-Fe MOF/Magnetic Magnetite/Biochar Composites, *J. Inorg. Organomet. Polym. Mater.*, 2020, **30**(1), 214–229.

169 D. Liu, W. Gu, L. Zhou, J. Lei, L. Wang, J. Zhang and Y. Liu, From biochar to functions: lignin induced formation of Fe_3C in carbon/Fe composites for efficient adsorption of tetracycline from wastewater, *Sep. Purif. Technol.*, 2023, **304**, 122217.

170 S. Ghaedi, H. Rajabi, M. Hadi Mosleh and M. Sedighi, MOF biochar composites for environmental protection and pollution control, *Bioresour. Technol.*, 2025, **418**, 131982.

171 Y.-C. Jiang, M.-F. Luo, Z.-N. Niu, S.-Y. Xu, Y. Gao, Y. Gao, W.-J. Gao, J.-J. Luo and R.-L. Liu, In situ growth of bimetallic FeCo-MOF on magnetic biochar for enhanced clearance of tetracycline and fruit preservation, *Chem. Eng. J.*, 2023, **451**, 138804.

172 K. J. Fernández-Andrade, A. A. Fernández-Andrade, L. Á. Zambrano-Intriago, L. E. Arteaga-Perez, S. Alejandro-Martin, R. J. Baquerizo-Crespo, R. Luque and J. M. Rodríguez-Díaz, Microwave-assisted MOF@biomass layered nanomaterials: characterization and applications in wastewater treatment, *Chemosphere*, 2023, **314**, 137664.

173 F. Yu, J. Pan, Y. Li, Y. Yang, Z. Zhang, J. Nie and J. Ma, Batch and continuous fixed-bed column adsorption of tetracycline by biochar/MOFs derivative covered with κ-carrageenan/calcium alginate hydrogels, *J. Environ. Chem. Eng.*, 2022, **10**(3), 107996.

174 A. Mohammadi, M. Kazemeini and S. Sadjadi, Synthesis and physicochemical evaluations of a novel MIL-101(Fe)-PMA-Biochar triple composite photocatalyst activated through visible-light and utilized toward degradation of organic pollutants: optimal operations and kinetics investigations, *Photochem. Photobiol. Sci.*, 2023, **22**(6), 1357–1378.

175 L. A. Zambrano-Intriago, E. V. Daza-López, A. Fernández-Andrade, R. Luque, C. G. Amorim, A. N. Araújo,

© 2025 The Author(s). Published by the Royal Society of Chemistry

Open Access Article. Published on 06 10 2025. Downloaded on 2026-05-13 12:47:34.
This article is licensed under a Creative Commons Attribution-NonCommercial 3.0 Unported Licence.

J. M. Rodríguez-Díaz and M. C. B. S. M. Montenegro, Application of a novel hybrid MIL-53(Al)@rice husk for the adsorption of glyphosate in water: characteristics and mechanism of the process, *Chemosphere*, 2023, **327**, 138457.

176 A. A. Aryee, Y. Xiao, R. Han and L. Qu, Uptake of 2,4-dichlorophenoxyacetic acid and tetracycline in single and binary systems onto a biomass-MOF composite: adsorption and mechanism study, *Biomass Convers. Biorefin.*, 2024, **14**(16), 18747–18760.

177 M. E. Mahmoud and G. A. A. Ibrahim, Cr(VI) and doxorubicin adsorptive capture by a novel bionanocomposite of Ti-MOF@TiO_2 incorporated with watermelon biochar and chitosan hydrogel, *Int. J. Biol. Macromol.*, 2023, **253**, 126489.

178 J. Liu, Q. Zeng, Y. Chen, Z. Dai, W. Jiang, L. Yao, J. Zheng, D. Sun, Y. Wu and L. Yang, Synthesizing ZIF-8 functionalized biochar by in situ reuse of residual Zn from chemical activation for enhanced tetracycline hydrochloride adsorption removal, *J. Environ. Chem. Eng.*, 2025, **13**(3), 116729.

179 L. Wang, H. Song, L. Yuan, Z. Li, Y. Zhang, J. K. Gibson, L. Zheng, Z. Chai and W. Shi, Efficient U(VI) Reduction and Sequestration by Ti_2CT_x MXene, *Environ. Sci. Technol.*, 2018, **52**(18), 10748–10756.

180 F. Dixit, K. Zimmermann, R. Dutta, N. J. Prakash, B. Barbeau, M. Mohseni and B. Kandasubramanian, Application of MXenes for water treatment and energy-efficient desalination: a review, *J. Hazard. Mater.*, 2022, **423**, 127050.

181 A. Bukhari, I. Ijaz, A. Nazir, S. Hussain, H. Zain, E. Gilani, A. A. Lfseisi and H. Ahmad, Functionalization of Shorea faguetiana biochar using Fe(2)O(3) nanoparticles and MXene for rapid removal of methyl blue and lead from both single and binary systems, *RSC Adv.*, 2024, **14**(6), 3732–3747.

182 F. Liu, S. Wang, C. Zhao and B. Hu, Constructing coconut shell biochar/MXenes composites through self-assembly strategy to enhance U(VI) and Cs(I) immobilization capability, *Biochar*, 2023, **5**(1), 31.

183 A. Kumar, E. Singh and S.-L. Lo, Tunable 2D porous $Ti_3C_2T_x$ MXene@biochar composites synthesized via ultrasound-assisted self-assembly for simultaneous removal of co-existing wastewater contaminants, *Sep. Purif. Technol.*, 2025, **355**, 129648.

184 A. Kumar, E. Singh and S.-L. Lo, MXene/biochar composites for enhanced wastewater reclamation and bioenergy production: a kinetics and thermodynamics study, *Chemosphere*, 2024, **359**, 142268.

185 T. P. Nguyen, V. D. Nguyen, M. T. Trinh, P. L. Han, T. H. Nguyen, M. T. Nguyen and A.-T. Vu, Effective biosorptive removal of Pb^{2+} ions from wastewater using modified lettuce leaves: a novel sustainable and eco-friendly biosorbent, *J. Hazard. Mater. Adv.*, 2025, 100770.

186 N. T. M. Nguyen Van Doan, D. T. Cam Vi, N. Thu Huong, V. Tuan Cuong, L. Trung Phong, N. Thu Huyen and V. Anh Tuan, Production of Porous Silica from Rice Husk Using Cetyltrimethylammonium Bromide to Remove Dyes in Aqueous Solution, *JST: Eng. Technol. Sustainable Dev.*, 2024, **34**(4), 009–016.

187 S. Bai, S. Zhu, C. Jin, Z. Sun, L. Wang, Q. Wen and F. Ma, Sorption mechanisms of antibiotic sulfamethazine (SMT) on magnetite-coated biochar: pH-dependence and redox transformation, *Chemosphere*, 2021, **268**, 128805.

188 B. Hu, Y. Tang, X. Wang, L. Wu, J. Nong, X. Yang and J. Guo, Cobalt-gadolinium modified biochar as an adsorbent for antibiotics in single and binary systems, *Microchem. J.*, 2021, **166**, 106235.

189 V. D. Nguyen and V.-G. Le, Ultrahigh Pb^{2+} ion adsorption by EDTA-modified super-porous silica aerogel derived from rice husk ash, *Environ. Res.*, 2025, **286**, 122803.

190 Z. Xu, Y. Xiang, H. Zhou, J. Yang, Y. He, Z. Zhu and Y. Zhou, Manganese ferrite modified biochar from vinasse for enhanced adsorption of levofloxacin: effects and mechanisms, *Environ. Pollut.*, 2021, **272**, 115968.

191 P. Cai, Q. Huang and X. Zhang, Microcalorimetric studies of the effects of $MgCl_2$ concentrations and pH on the adsorption of DNA on montmorillonite, kaolinite and goethite, *Appl. Clay Sci.*, 2006, **32**(1), 147–152.

192 M. Wu, R. Kempaiah, P.-J. J. Huang, V. Maheshwari and J. Liu, Adsorption and Desorption of DNA on Graphene Oxide Studied by Fluorescently Labeled Oligonucleotides, *Langmuir*, 2011, **27**(6), 2731–2738.

193 J. Zhao and Y. Dai, Tetracycline adsorption mechanisms by NaOH-modified biochar derived from waste Auricularia auricula dregs, *Environ. Sci. Pollut. Res.*, 2022, **29**(6), 9142–9152.

194 L. Leng and H. Huang, An overview of the effect of pyrolysis process parameters on biochar stability, *Bioresour. Technol.*, 2018, **270**, 627–642.

195 Mankomal and H. Kaur, Synergistic effect of biochar impregnated with ZnO nano-flowers for effective removal of organic pollutants from wastewater, *Appl. Surf. Sci. Adv.*, 2022, **12**, 100339.

196 S. Chen, C. Qin, T. Wang, F. Chen, X. Li, H. Hou and M. Zhou, Study on the adsorption of dyestuffs with different properties by sludge-rice husk biochar: adsorption capacity, isotherm, kinetic, thermodynamics and mechanism, *J. Mol. Liq.*, 2019, **285**, 62–74.

197 T. H. Nguyen, V. D. Nguyen and A. T. Vu, Synthesis of CS-Fe_3O_4/GO nanocomposite for adsorption of heavy metal in aqueous environment, *Nanotechnology*, 2024, **35**(34), 345705.

198 B. Qiu, Q. Shao, J. Shi, C. Yang and H. Chu, Application of biochar for the adsorption of organic pollutants from wastewater: modification strategies, mechanisms and challenges, *Sep. Purif. Technol.*, 2022, **300**, 121925.

199 C. E. R. Barquilha and M. C. B. Braga, Adsorption of organic and inorganic pollutants onto biochars: challenges, operating conditions, and mechanisms, *Bioresour. Technol. Rep.*, 2021, **15**, 100728.

200 S. Fan, Y. Wang, Z. Wang, J. Tang, J. Tang and X. Li, Removal of methylene blue from aqueous solution by sewage sludge-derived biochar: adsorption kinetics,

Open Access Article. Published on 06 10 2025. Downloaded on 2026-05-13 12:47:34.
This article is licensed under a Creative Commons Attribution-NonCommercial 3.0 Unported Licence.

equilibrium, thermodynamics and mechanism, *J. Environ. Chem. Eng.*, 2017, **5**(1), 601–611.

201 S. Fan, J. Tang, Y. Wang, H. Li, H. Zhang, J. Tang, Z. Wang and X. Li, Biochar prepared from co-pyrolysis of municipal sewage sludge and tea waste for the adsorption of methylene blue from aqueous solutions: kinetics, isotherm, thermodynamic and mechanism, *J. Mol. Liq.*, 2016, **220**, 432–441.

202 S. S. A. Miri Kafi Abad, P. Javidan, M. Baghdadi and N. Mehrdadi, Green synthesis of Pd@biochar using the extract and biochar of corn-husk wastes for electrochemical Cr(VI) reduction in plating wastewater, *J. Environ. Chem. Eng.*, 2023, **11**(3), 109911.

203 F. S. Mustafa and K. H. Hama Aziz, Heterogeneous catalytic activation of persulfate for the removal of rhodamine B and diclofenac pollutants from water using iron-impregnated biochar derived from the waste of black seed pomace, *Process Saf. Environ. Prot.*, 2023, **170**, 436–448.

204 W. T. Tsai and H. R. Chen, Adsorption kinetics of herbicide paraquat in aqueous solution onto a low-cost adsorbent, swine-manure-derived biochar, *Int. J. Environ. Sci. Technol.*, 2013, **10**(6), 1349–1356.

205 D. Adu-Poku, S. A. Saah, P. O. Sakyi, C. K. Bandoh, B. Agyei-Tuffour, D. Azanu, M. Oteng-Peprah, I. Hawawu, S. Azibere and K. A. Affram, Acid-Activated Biochar for Efficient Elimination of Amoxicillin From Wastewater, *J. Chem.*, 2024, **2024**(1), 3648098.

206 M. Stylianou, A. Christou, C. Michael, A. Agapiou, P. Papanastasiou and D. Fatta-Kassinos, Adsorption and removal of seven antibiotic compounds present in water with the use of biochar derived from the pyrolysis of organic waste feedstocks, *J. Environ. Chem. Eng.*, 2021, **9**(5), 105868.

207 D. T. Nguyen, T. K. Hoang, T. D. Tran, M. H. Nguyen, K. T. Trinh, D. A. Khuong, T. Tsubota and T. D. Pham, Adsorption characteristics of individual and binary mixture of ciprofloxacin antibiotic and lead(II) on synthesized bamboo-biochar, *Environ. Res.*, 2025, **273**, 121225.

208 S. Vigneshwaran, P. Sirajudheen, M. Nikitha, K. Ramkumar and S. Meenakshi, Facile synthesis of sulfur-doped chitosan/biochar derived from tapioca peel for the removal of organic dyes: isotherm, kinetics and mechanisms, *J. Mol. Liq.*, 2021, **326**, 115303.

209 L. Du, W. Xu, S. Liu, X. Li, D. Huang, X. Tan and Y. Liu, Activation of persulfate by graphitized biochar for sulfamethoxazole removal: the roles of graphitic carbon structure and carbonyl group, *J. Colloid Interface Sci.*, 2020, **577**, 419–430.

210 L. Yan, Y. Liu, Y. Zhang, S. Liu, C. Wang, W. Chen, C. Liu, Z. Chen and Y. Zhang, $ZnCl_2$ modified biochar derived from aerobic granular sludge for developed microporosity and enhanced adsorption to tetracycline, *Bioresour. Technol.*, 2020, **297**, 122381.

211 F. Sayin, S. T. Akar and T. Akar, From green biowaste to water treatment applications: utilization of modified new biochar for the efficient removal of ciprofloxacin, *Sustainable Chem. Pharm.*, 2021, **24**, 100522.

212 Y. Fu, F. Wang, H. Sheng, F. Hu, Z. Wang, M. Xu, Y. Bian, X. Jiang and J. M. Tiedje, Removal of extracellular antibiotic resistance genes using magnetic biochar/quaternary phosphonium salt in aquatic environments: a mechanistic study, *J. Hazard. Mater.*, 2021, **411**, 125048.

213 C. Wu, L. Fu, H. Li, X. Liu and C. Wan, Using biochar to strengthen the removal of antibiotic resistance genes: performance and mechanism, *Sci. Total Environ.*, 2022, **816**, 151554.

214 Y. Zheng, P. Lv, J. Yang and G. Xu, Characterization and Adsorption Capacity of Modified Biochar for Sulfamethylimidine and Methylene Blue in Water, *ACS Omega*, 2023, **8**(33), 29966–29978.

215 E. Ouyang, R. Zhang, W. Fu, R. Zhao, H. Yang, H. Xiang and W. He, Facile Synthesis of Bamboo Biochar for Efficient Adsorption of Quinolone Antibiotics: Effects and Mechanisms, *ACS Omega*, 2024, **9**(49), 48618–48628.

216 K. Xu, C. Zhang, X. Dou, W. Ma and C. Wang, Optimizing the modification of wood waste biochar via metal oxides to remove and recover phosphate from human urine, *Environ. Geochem. Health*, 2019, **41**(4), 1767–1776.

217 H. Yu, L. Gu, L. Chen, H. Wen, D. Zhang and H. Tao, Activation of grapefruit derived biochar by its peel extracts and its performance for tetracycline removal, *Bioresour. Technol.*, 2020, **316**, 123971.

218 N. Cheng, B. Wang, P. Wu, X. Lee, Y. Xing, M. Chen and B. Gao, Adsorption of emerging contaminants from water and wastewater by modified biochar: a review, *Environ. Pollut.*, 2021, **273**, 116448.

219 K.-W. Jung, S. Y. Lee and Y. J. Lee, Hydrothermal synthesis of hierarchically structured birnessite-type MnO_2/biochar composites for the adsorptive removal of Cu(II) from aqueous media, *Bioresour. Technol.*, 2018, **260**, 204–212.

220 S. Zeng and E. Kan, $FeCl_3$-activated biochar catalyst for heterogeneous Fenton oxidation of antibiotic sulfamethoxazole in water, *Chemosphere*, 2022, **306**, 135554.

221 B.-L. Liu, M.-M. Fu, L. Xiang, N.-X. Feng, H.-M. Zhao, Y.-W. Li, Q.-Y. Cai, H. Li, C.-H. Mo and M.-H. Wong, Adsorption of microcystin contaminants by biochars derived from contrasting pyrolytic conditions: characteristics, affecting factors, and mechanisms, *Sci. Total Environ.*, 2021, **763**, 143028.

222 L. Lonappan, T. Rouissi, S. Kaur Brar, M. Verma and R. Y. Surampalli, An insight into the adsorption of diclofenac on different biochars: mechanisms, surface chemistry, and thermodynamics, *Bioresour. Technol.*, 2018, **249**, 386–394.

223 Z. Wang, L. Han, K. Sun, J. Jin, K. S. Ro, J. A. Libra, X. Liu and B. Xing, Sorption of four hydrophobic organic contaminants by biochars derived from maize straw, wood dust and swine manure at different pyrolytic temperatures, *Chemosphere*, 2016, **144**, 285–291.

224 J. Liang, Y. Fang, Y. Luo, G. Zeng, J. Deng, X. Tan, N. Tang, X. Li, X. He, C. Feng and S. Ye, Magnetic nanoferromanganese oxides modified biochar derived from pine sawdust for adsorption of tetracycline hydrochloride, *Environ. Sci. Pollut. Res.*, 2019, **26**(6), 5892–5903.

© 2025 The Author(s). Published by the Royal Society of Chemistry

Open Access Article. Published on 06 10 2025. Downloaded on 2026-05-13 12:47:34.
This article is licensed under a Creative Commons Attribution-NonCommercial 3.0 Unported Licence.

225 L. Tang, J. Yu, Y. Pang, G. Zeng, Y. Deng, J. Wang, X. Ren, S. Ye, B. Peng and H. Feng, Sustainable efficient adsorbent: alkali-acid modified magnetic biochar derived from sewage sludge for aqueous organic contaminant removal, *Chem. Eng. J.*, 2018, **336**, 160–169.

226 V.-T. Nguyen, T.-B. Nguyen, C. P. Huang, C.-W. Chen, X.-T. Bui and C.-D. Dong, Alkaline modified biochar derived from spent coffee ground for removal of tetracycline from aqueous solutions, *J. Water Process Eng.*, 2021, **40**, 101908.

227 Z. Tan, Z. Xueyang, W. Liping, G. Bin, L. Junpeng, F. Ru, Z. Weixin and N. Meng, Sorption of tetracycline on H_2O_2-modified biochar derived from rape stalk, *Environ. Pollut. Bioavailability*, 2019, **31**(1), 198–207.

228 D. Calderón-Franco, S. Apoorva, G. Medema, M. C. M. van Loosdrecht and D. G. Weissbrodt, Upgrading residues from wastewater and drinking water treatment plants as low-cost adsorbents to remove extracellular DNA and microorganisms carrying antibiotic resistance genes from treated effluents, *Sci. Total Environ.*, 2021, **778**, 146364.

229 C. Wang, T. Wang, W. Li, J. Yan, Z. Li, R. Ahmad, S. K. Herath and N. Zhu, Adsorption of deoxyribonucleic acid (DNA) by willow wood biochars produced at different pyrolysis temperatures, *Biol. Fertil. Soils*, 2014, **50**(1), 87–94.

230 Q. Lu, K. Yin, J. Wang, X. Zhang, X. Tian, X. Ma, Y. Zhao, S. Sun, H. Yuan, S. Zhai, H. Zheng and B. Xing, Characteristics of chemical aged biochars and their adsorption behaviors for norfloxacin, *J. Environ. Chem. Eng.*, 2024, **12**(5), 113638.

231 X. Liu, D. Wang, J. Tang, F. Liu and L. Wang, Effect of dissolved biochar on the transfer of antibiotic resistance genes between bacteria, *Environ. Pollut.*, 2021, **288**, 117718.

232 Y. Deng, M. Wang, Y. Yang, X. Li, W. Chen and T. Ao, Enhanced adsorption performance of sulfamethoxazole and tetracycline in aqueous solutions by $MgFe_2O_4$-magnetic biochar, *Water Sci. Technol.*, 2022, **86**(3), 568–583.

233 K. Badshah, Q. Ali, A. A. Khan, R. Ahmad and I. Ahmad, Experimental and DFT Studies of Antibiotics Removal Through Activated Carbon: A Step-by-Step Adsorption Process at Atomic Level, *ChemistrySelect*, 2024, **9**(44), e202402422.

234 X. Zhang, J. Hou, S. Zhang, T. Cai, S. Liu, W. Hu and Q. Zhang, Standardization and micromechanistic study of tetracycline adsorption by biochar, *Biochar*, 2024, **6**(1), 12.

235 S. Bai, Y. Zhou, M. Qian, J. Xia, Z. Sun, Y. Wang, X. Huang and S. Zhu, Mechanistic insights to sorptive removal of four sulfonamide antibiotics from water using magnetite-functionalized biochar, *Biochar*, 2023, **5**(1), 80.

236 K. Ezzahi, I. Rabichi, H. Befenzi, E. Record, T. Bouzid, A. Yaacoubi, A. Baçaoui, Y. Habibi and L. El Fels, Optimization, characterization, and DFT study of activated-biochar from lignocellulosic biomass for fluoroquinolone antibiotic adsorption, *Results Eng.*, 2025, **27**, 106540.

237 H. Ren, X. Ma, B. Ma, X. Bai, H. Wang, Z. Ma, S. Gu and J. Wang, DFT-Validated adsorption mechanisms of metronidazole on CO_2-activated almond shell biochar for antibiotic wastewater treatment, *Desalin. Water Treat.*, 2025, **324**, 101414.

238 H. Jiang and H. Hu, Sustainable synergistic adsorption of tetracycline in water by biochar and microplastics: exploration of the mechanism of DFT, *J. Water Process Eng.*, 2024, **66**, 105998.

239 Q. Chen, J. Zheng, J. Xu, Z. Dang and L. Zhang, Insights into sulfamethazine adsorption interfacial interaction mechanism on mesoporous cellulose biochar: coupling DFT/FOT simulations with experiments, *Chem. Eng. J.*, 2019, **356**, 341–349.

240 X. Liu, P. Huang, W. Ma, F. Jin and L. Tai, Unveiling adsorption mechanisms and regeneration challenges of durian peel biochar for ciprofloxacin removal: batch experiments and DFT study, *J. Water Process Eng.*, 2025, **75**, 107991.

241 B. Peng, L. Chen, C. Que, K. Yang, F. Deng, X. Deng, G. Shi, G. Xu and M. Wu, Adsorption of Antibiotics on Graphene and Biochar in Aqueous Solutions Induced by π–π Interactions, *Sci. Rep.*, 2016, **6**(1), 31920.

242 W. Hu, Y. Niu, T. Shen, K. Dong and D. Wang, Magnetic biochar prepared by a dry process for the removal of sulfonamides antibiotics from aqueous solution, *J. Mol. Liq.*, 2024, **400**, 124576.

243 Y. Li, B. Wang, H. Shang, Y. Cao, C. Yang, W. Hu, Y. Feng and Y. Yu, Influence of adsorption sites of biochar on its adsorption performance for sulfamethoxazole, *Chemosphere*, 2023, **326**, 138408.

244 H. Zhao, Z. Wang, Y. Liang, T. Wu, Y. Chen, J. Yan, Y. Zhu and D. Ding, Adsorptive decontamination of antibiotics from livestock wastewater by using alkaline-modified biochar, *Environ. Res.*, 2023, **226**, 115676.

245 A. Nasiri, N. Golestani, S. Rajabi and M. Hashemi, Facile and green synthesis of recyclable, environmentally friendly, chemically stable, and cost-effective magnetic nanohybrid adsorbent for tetracycline adsorption, *Heliyon*, 2024, **10**(2), e24179.

246 A. Thakur, A. Kumar and A. Singh, Adsorptive removal of heavy metals, dyes, and pharmaceuticals: carbon-based nanomaterials in focus, *Carbon*, 2024, **217**, 118621.

247 Y. Zhou, Z. Wang, W. Hu, Q. Zhou and J. Chen, Norfloxacin adsorption by urban green waste biochar: characterization, kinetics, and mechanisms, *Environ. Sci. Pollut. Res.*, 2024, **31**(20), 29088–29100.

248 F. Dilpazeer, M. Munir, M. Y. J. Baloch, I. Shafiq, J. Iqbal, M. Saeed, M. M. Abbas, S. Shafique, K. H. H. Aziz, A. Mustafa and I. Mahboob, A Comprehensive Review of the Latest Advancements in Controlling Arsenic Contaminants in Groundwater, *Water*, 2023, **15**(3), 478.

249 F. Amalina, S. Krishnan, A. W. Zularisam and M. Nasrullah, Biochar and sustainable environmental development towards adsorptive removal of pollutants: modern advancements and future insight, *Process Saf. Environ. Prot.*, 2023, **173**, 715–728.

250 X. Zhao, G. Zhu, J. Liu, J. Wang, S. Zhang, C. Wei, L. Cao, S. Zhao and S. Zhang, Efficient Removal of Tetracycline

Open Access Article. Published on 06 10 2025. Downloaded on 2026-05-13 12:47:34.
This article is licensed under a Creative Commons Attribution-NonCommercial 3.0 Unported Licence.

from Water by One-Step Pyrolytic Porous Biochar Derived from Antibiotic Fermentation Residue, *Nanomaterials*, 2024, **14**(17), 1377.

251 S. Aziz, S. Anbreen, I. Iftikhar, T. Fatima, A. Iftikhar and L. Ali, Green technology: synthesis of iron-modified biochar derived from pine cones to remove azithromycin and ciprofloxacin from water, *Front. Environ. Sci.*, 2024, **12**, 1353267.

252 U. Sen, B. Esteves, T. Aguiar and H. Pereira, Removal of Antibiotics by Biochars: A Critical Review, *Appl. Sci.*, 2023, **13**(21), 11963.

253 A. A. MacKay and D. Vasudevan, Polyfunctional Ionogenic Compound Sorption: Challenges and New Approaches To Advance Predictive Models, *Environ. Sci. Technol.*, 2012, **46**(17), 9209–9223.

254 K. Wang, R. Yao, D. Zhang, N. Peng, P. Zhao, Y. Zhong, H. Zhou, J. Huang and C. Liu, Tetracycline Adsorption Performance and Mechanism Using Calcium Hydroxide-Modified Biochars, *Toxics*, 2023, **11**(10), 841.

255 Y. Chen, J. Shi, Q. Du, H. Zhang and Y. Cui, Antibiotic removal by agricultural waste biochars with different forms of iron oxide, *RSC Adv.*, 2019, **9**(25), 14143–14153.

256 Q. Xu, Q. Zhou, M. Pan and L. Dai, Interaction between chlortetracycline and calcium-rich biochar: enhanced removal by adsorption coupled with flocculation, *Chem. Eng. J.*, 2020, **382**, 122705.

257 L. Zhang, W. Yang, Y. Chen and L. Yang, Removal of Tetracycline from Water by Biochar: Mechanisms, Challenges, and Future Perspectives, *Water*, 2025, **17**(13), 1960.

258 Y. Jia, Y. Ou, S. K. Khanal, L. Sun, W.-S. Shu and H. Lu, Biochar-Based Strategies for Antibiotics Removal: Mechanisms, Factors, and Application, *ACS ES&T Eng.*, 2024, **4**(6), 1256–1274.

259 J. Wei, Y. Liu, J. Li, Y. Zhu, H. Yu and Y. Peng, Adsorption and co-adsorption of tetracycline and doxycycline by one-step synthesized iron loaded sludge biochar, *Chemosphere*, 2019, **236**, 124254.

260 Y. Tang, Y. Li, L. Zhan, D. Wu, S. Zhang, R. Pang and B. Xie, Removal of emerging contaminants (bisphenol A and antibiotics) from kitchen wastewater by alkali-modified biochar, *Sci. Total Environ.*, 2022, **805**, 150158.

261 Q. Ge, P. Li, M. Liu, G.-M. Xiao, Z.-Q. Xiao, J.-W. Mao and X.-K. Gai, Removal of methylene blue by porous biochar obtained by KOH activation from bamboo biochar, *Bioresour. Bioprocess.*, 2023, **10**(1), 51.

262 N. S. Alsaiari, M. S. Alsaiari, F. M. Alzahrani, A. Amari and M. A. Tahoon, Synthesis, characterization, and application of the novel nanomagnet adsorbent for the removal of Cr(VI) ions, *Rev. Adv. Mater. Sci.*, 2023, **62**(1), 20230145.

263 S. Babić, M. Periša and I. Škorić, Photolytic degradation of norfloxacin, enrofloxacin and ciprofloxacin in various aqueous media, *Chemosphere*, 2013, **91**(11), 1635–1642.

264 F. Lian, W. Yu, Q. Zhou, S. Gu, Z. Wang and B. Xing, Size Matters: Nano-Biochar Triggers Decomposition and Transformation Inhibition of Antibiotic Resistance Genes in Aqueous Environments, *Environ. Sci. Technol.*, 2020, **54**(14), 8821–8829.

265 J. Fang, L. Jin, Q. Meng, D. Wang and D. Lin, Interactions of extracellular DNA with aromatized biochar and protection against degradation by DNase I, *J. Environ. Sci.*, 2021, **101**, 205–216.

266 Z. Tan, S. Yuan, M. Hong, L. Zhang and Q. Huang, Mechanism of negative surface charge formation on biochar and its effect on the fixation of soil Cd, *J. Hazard. Mater.*, 2020, **384**, 121370.

267 N. Li, X. Zhu, Y. Miao, Z. Wang, C. S. K. Lin and C. Li, Meta-analysis and empirical research on the effectiveness of biochar in remediating tetracyclines pollution in water bodies, *Bioresour. Technol.*, 2025, **435**, 132917.

268 F. Zhang, J. Wang, Y. Tian, C. Liu, S. Zhang, L. Cao, Y. Zhou and S. Zhang, Effective removal of tetracycline antibiotics from water by magnetic functionalized biochar derived from rice waste, *Environ. Pollut.*, 2023, **330**, 121681.

269 Z. Yang, R. Xing, W. Zhou and L. Zhu, Adsorption characteristics of ciprofloxacin onto g-MoS_2 coated biochar nanocomposites, *Front. Environ. Sci. Eng.*, 2020, **14**(3), 41.

270 A. U. Rajapaksha, M. Vithanage, M. Zhang, M. Ahmad, D. Mohan, S. X. Chang and Y. S. Ok, Pyrolysis condition affected sulfamethazine sorption by tea waste biochars, *Bioresour. Technol.*, 2014, **166**, 303–308.

271 M. Duan, G. Liu, B. Zhou, X. Chen, Q. Wang, H. Zhu and Z. Li, Effects of modified biochar on water and salt distribution and water-stable macro-aggregates in saline-alkaline soil, *J. Soils Sediments*, 2021, **21**(6), 2192–2202.

272 X. Guo, H. Dong, C. Yang, Q. Zhang, C. Liao, F. Zha and L. Gao, Application of goethite modified biochar for tylosin removal from aqueous solution, *Colloids Surf., A*, 2016, **502**, 81–88.

273 K. S. D. Premarathna, A. U. Rajapaksha, N. Adassoriya, B. Sarkar, N. M. S. Sirimuthu, A. Cooray, Y. S. Ok and M. Vithanage, Clay-biochar composites for sorptive removal of tetracycline antibiotic in aqueous media, *J. Environ. Manage.*, 2019, **238**, 315–322.

274 J. Li, G. Yu, L. Pan, C. Li, F. You and Y. Wang, Ciprofloxacin adsorption by biochar derived from co-pyrolysis of sewage sludge and bamboo waste, *Environ. Sci. Pollut. Res.*, 2020, **27**(18), 22806–22817.

275 P. Huang, C. Ge, D. Feng, H. Yu, J. Luo, J. Li, P. J. Strong, A. K. Sarmah, N. S. Bolan and H. Wang, Effects of metal ions and pH on ofloxacin sorption to cassava residue-derived biochar, *Sci. Total Environ.*, 2018, **616–617**, 1384–1391.

276 E. Kabir, K.-H. Kim and E. E. Kwon, Biochar as a tool for the improvement of soil and environment, *Front. Environ. Sci.*, 2023, **11**, 1324533.

277 M. Keiluweit, P. S. Nico, M. G. Johnson and M. Kleber, Dynamic Molecular Structure of Plant Biomass-Derived Black Carbon (Biochar), *Environ. Sci. Technol.*, 2010, **44**(4), 1247–1253.

278 Y. Li, D. Chi, Y. Sun, X. Wang, M. Tan, Y. Guan, Q. Wu and H. Zhou, Synthesis of struvite-enriched slow-release

 © 2025 The Author(s). Published by the Royal Society of Chemistry

Open Access Article. Published on 06 10 2025. Downloaded on 2026-05-13 12:47:34.
This article is licensed under a Creative Commons Attribution-NonCommercial 3.0 Unported Licence.

fertilizer using magnesium-modified biochar: desorption and leaching mechanisms, *Sci. Total Environ.*, 2024, **926**, 172172.

279 S. Dou, X.-X. Ke, Z.-D. Shao, L.-B. Zhong, Q.-B. Zhao and Y.-M. Zheng, Fish scale-based biochar with defined pore size and ultrahigh specific surface area for highly efficient adsorption of ciprofloxacin, *Chemosphere*, 2022, **287**, 131962.

280 Y. Feng, Q. Liu, Y. Yu, Q. Kong, L.-L. Zhou, Y.-D. Du and X.-F. Wang, Norfloxacin removal from aqueous solution using biochar derived from luffa sponge, *J. Water Supply: Res. Technol.--AQUA*, 2018, **67**(8), 703–714.

281 B. Yan, C. H. Niu and J. Wang, Kinetics, electron–donor–acceptor interactions, and site energy distribution analyses of norfloxacin adsorption on pretreated barley straw, *Chem. Eng. J.*, 2017, **330**, 1211–1221.

282 M. Chen, Z. Yan, J. Luan, X. Sun, W. Liu and X. Ke, π–π electron–donor–acceptor (EDA) interaction enhancing adsorption of tetracycline on 3D PPY/CMC aerogels, *Chem. Eng. J.*, 2023, **454**, 140300.

283 Y. Li, Z. Cheng, H. Shang, Y. Chen, S. Li, X. Wei, T. Wang, W. Zhou and Y. Yu, Design of functional groups on biochar for sulfamethoxazole adsorption from adsorption efficiency and adsorption mechanism, *J. Environ. Chem. Eng.*, 2025, **13**(3), 116874.

284 S. Pap, L. Shearer and S. W. Gibb, Sustainable remediation of macrolide antibiotic from water using a novel Fe oxide/biochar nanocomposite: adsorption behaviour and mechanistic analysis, *J. Environ. Chem. Eng.*, 2025, **13**(1), 115208.

285 Y. Zhang, Y. Gong, G. Shi, X. Liu, M. Dai and L. Ding, Removal of Quinolone Antibiotics from Wastewater by the Biochar-Based Sludge Adsorbent, *Fermentation*, 2023, **9**(8), 752.

286 V. Son Tran, H. Hao Ngo, W. Guo, T. Ha Nguyen, T. Mai Ly Luong, X. Huan Nguyen, T. Lan Anh Phan, V. Trong Le, M. Phuong Nguyen and M. Khai Nguyen, New chitosan-biochar composite derived from agricultural waste for removing sulfamethoxazole antibiotics in water, *Bioresour. Technol.*, 2023, **385**, 129384.

287 J. Huang, A. R. Zimmerman, H. Chen and B. Gao, Ball milled biochar effectively removes sulfamethoxazole and sulfapyridine antibiotics from water and wastewater, *Environ. Pollut.*, 2020, **258**, 113809.

288 X. Geng, S. Lv, J. Yang, S. Cui and Z. Zhao, Carboxyl-functionalized biochar derived from walnut shells with enhanced aqueous adsorption of sulfonamide antibiotics, *J. Environ. Manage.*, 2021, **280**, 111749.

289 Y. Diao, R. Shan, M. Li, J. Gu, H. Yuan and Y. Chen, Efficient Adsorption of a Sulfonamide Antibiotic in Aqueous Solutions with N-doped Magnetic Biochar: Performance, Mechanism, and Reusability, *ACS Omega*, 2023, **8**(1), 879–892.

290 Y. Wang, J. Lu, J. Wu, Q. Liu, H. Zhang and S. Jin, Adsorptive Removal of Fluoroquinolone Antibiotics Using Bamboo Biochar, *Sustainability*, 2015, **7**(9), 12947–12957.

291 H. Jiang, X. Li, J. Bai, W. Pan, Z. Luo and Y. Dai, Removal of ciprofloxacin lactate by phosphoric acid activated biochar: urgent consideration of new antibiotics for human health, *Chem. Eng. Sci.*, 2024, **283**, 119403.

292 B. Yao, W. Zeng, A. Núñez-Delgado and Y. Zhou, Simultaneous adsorption of ciprofloxacin and Cu^{2+} using Fe and N co-doped biochar: competition and selective separation, *Waste Manage.*, 2023, **168**, 386–395.

293 F. Saremi, M. R. Miroliaei, M. Shahabi Nejad and H. Sheibani, Adsorption of tetracycline antibiotic from aqueous solutions onto vitamin B6-upgraded biochar derived from date palm leaves, *J. Mol. Liq.*, 2020, **318**, 114126.

294 W. Xiang, Y. Wan, X. Zhang, Z. Tan, T. Xia, Y. Zheng and B. Gao, Adsorption of tetracycline hydrochloride onto ball-milled biochar: governing factors and mechanisms, *Chemosphere*, 2020, **255**, 127057.

295 Y. Deng, M. Wang, Y. Yang, X. Li, W. Chen and T. Ao, Enhanced adsorption performance of sulfamethoxazole and tetracycline in aqueous solutions by $MgFe_2O_4$-magnetic biochar, *Water Sci. Technol.*, 2022, **86**(3), 568–583.

296 V. F. Meseguer, J. F. Ortuño, M. I. Aguilar, M. Lloréns, A. B. Pérez-Marín and E. Fuentes, Ciprofloxacin Uptake from an Aqueous Solution via Adsorption with K_2CO_3-Activated Biochar Derived from Brewing Industry Bagasse, *Processes*, 2024, **12**(1), 199.

297 X. Fan, Z. Qian, J. Liu, N. Geng, J. Hou and D. Li, Investigation on the adsorption of antibiotics from water by metal loaded sewage sludge biochar, *Water Sci. Technol.*, 2020, **83**(3), 739–750.

298 V.-T. Nguyen, T.-B. Nguyen, N. D. Dat, T.-K. Q. Vo, X. C. Nguyen, V.-C. Dinh, T.-N.-C. Le, T.-G.-H. Duong, M.-H. Bui and X.-T. Bui, Preliminary study of doxycycline adsorption from aqueous solution on alkaline modified biochar derived from banana peel, *Environ. Eng. Res.*, 2024, **29**(3), 230196.

299 Z. Li, Z. Wang, X. Wu, M. Li and X. Liu, Competitive adsorption of tylosin, sulfamethoxazole and Cu(II) on nano-hydroxyapatitemodified biochar in water, *Chemosphere*, 2020, **240**, 124884.

300 H. Wang, X. Lou, Q. Hu and T. Sun, Adsorption of antibiotics from water by using Chinese herbal medicine residues derived biochar: preparation and properties studies, *J. Mol. Liq.*, 2021, **325**, 114967.

301 Z. Zeng, S. Ye, H. Wu, R. Xiao, G. Zeng, J. Liang, C. Zhang, J. Yu, Y. Fang and B. Song, Research on the sustainable efficacy of g-MoS_2 decorated biochar nanocomposites for removing tetracycline hydrochloride from antibiotic-polluted aqueous solution, *Sci. Total Environ.*, 2019, **648**, 206–217.

302 H. Liang, C. Zhu, A. Wang and F. Chen, Facile preparation of $NiFe_2O_4$/biochar composite adsorbent for efficient adsorption removal of antibiotics in water. Carbon, *Research*, 2024, **3**(1), 2.

303 Z.-W. Zeng, X.-F. Tan, Y.-G. Liu, S.-R. Tian, G.-M. Zeng, L.-H. Jiang, S.-B. Liu, J. Li, N. Liu and Z.-H. Yin, Comprehensive Adsorption Studies of Doxycycline and Ciprofloxacin

Open Access Article. Published on 06 10 2025. Downloaded on 2026-05-13 12:47:34.
This article is licensed under a Creative Commons Attribution-NonCommercial 3.0 Unported Licence.

Antibiotics by Biochars Prepared at Different Temperatures, *Front. Chem.*, 2018, **6**, 80.

304 T. K. Nguyen, T. B. Nguyen, W. H. Chen, C. W. Chen, A. Kumar Patel, X. T. Bui, L. Chen, R. R. Singhania and C. D. Dong, Phosphoric acid-activated biochar derived from sunflower seed husk: selective antibiotic adsorption behavior and mechanism, *Bioresour. Technol.*, 2023, **371**, 128593.

305 C. Zou, Q. Wu, Z. Gao, Z. Xu and F. Nie, The magnetic porous biochar prepared by K_2FeO_4-promoted oxidative pyrolysis of bagasse for adsorption of antibiotics in the aqueous solution, *Biomass Convers. Biorefin.*, 2024, **14**(13), 14189–14205.

306 X. Liao, C. Chen, Z. Liang, Z. Zhao and F. Cui, Selective adsorption of antibiotics on manganese oxide-loaded biochar and mechanism based on quantitative structure–property relationship model, *Bioresour. Technol.*, 2023, **367**, 128262.

307 Z. Fan, J. Fang, G. Zhang, L. Qin, Z. Fang and L. Jin, Improved Adsorption of Tetracycline in Water by a Modified Caulis spatholobi Residue Biochar, *ACS Omega*, 2022, **7**(34), 30543–30553.

308 Y.-K. Choi, R. Srinivasan and E. Kan, Facile and Economical Functionalized Hay Biochar with Dairy Effluent for Adsorption of Tetracycline, *ACS Omega*, 2020, **5**(27), 16521–16529.

309 J. Gao, Y. Zhou, X. Yang, Y. Yao, J. Qi, Z. Zhu, Y. Yang, D. Fang, L. Zhou and J. Li, Dyeing sludge-derived biochar for efficient removal of antibiotic from water, *Sci. Total Environ.*, 2024, **912**, 169035.

310 B. Huang, D. Huang, Q. Zheng, C. Yan, J. Feng, H. Gao, H. Fu and Y. Liao, Enhanced adsorption capacity of tetracycline on porous graphitic biochar with an ultra-large surface area, *RSC Adv.*, 2023, **13**(15), 10397–10407.

311 C. Ling, Y. Song, Y. Zhu, R. Hong, T. Dong, J. Han and Y. Feng, Highly Efficient Adsorption of Sulfamethoxazole and Ciprofloxacin by a Novel Bowl-Shaped Nitrogen-Doped Pyrolytic Carbon and the Underlying Structural-Property Mechanism, *ACS ES&T Water*, 2025, **5**(2), 871–880.

312 Y. Li, H. Shang, Y. Cao, C. Yang, Y. Feng and Y. Yu, High performance removal of sulfamethoxazole using large specific area of biochar derived from corncob xylose residue, *Biochar*, 2022, **4**(1), 11.

313 X. Ma, Y. Cao, J. Deng, J. Shao, X. Feng, W. Li, S. Li and R. Zhang, Synergistic enhancement of N, S co-modified biochar for removal of tetracycline hydrochloride from aqueous solution: tunable micro-mesoporosity and chemisorption sites, *Chem. Eng. J.*, 2024, **492**, 152189.

314 P. Luo, W. Zhang, D. Xiao, J. Hu, N. Li and J. Yang, Biochar-Based Fertilizers: Advancements, Applications, and Future Directions in Sustainable Agriculture—A Review, *Agronomy*, 2025, **15**(5), 1104.

315 M. Dong, M. Jiang, L. He, Z. Zhang, W. Gustave, M. Vithanage, N. K. Niazi, B. Chen, X. Zhang, H. Wang and F. He, Challenges in safe environmental applications of biochar: identifying risks and unintended consequence, *Biochar*, 2025, **7**(1), 12.

316 J. A. Antonangelo, X. Sun and H. D. J. Eufrade-Junior, Biochar impact on soil health and tree-based crops: a review, *Biochar*, 2025, **7**(1), 51.

© 2025 The Author(s). Published by the Royal Society of Chemistry